JULY/AUGUST 2019
VOL 30 NO 4

CVJ AFRICA

www.cvja.co.za | CardioVascular Journal of Africa (official journal for PASCAR)

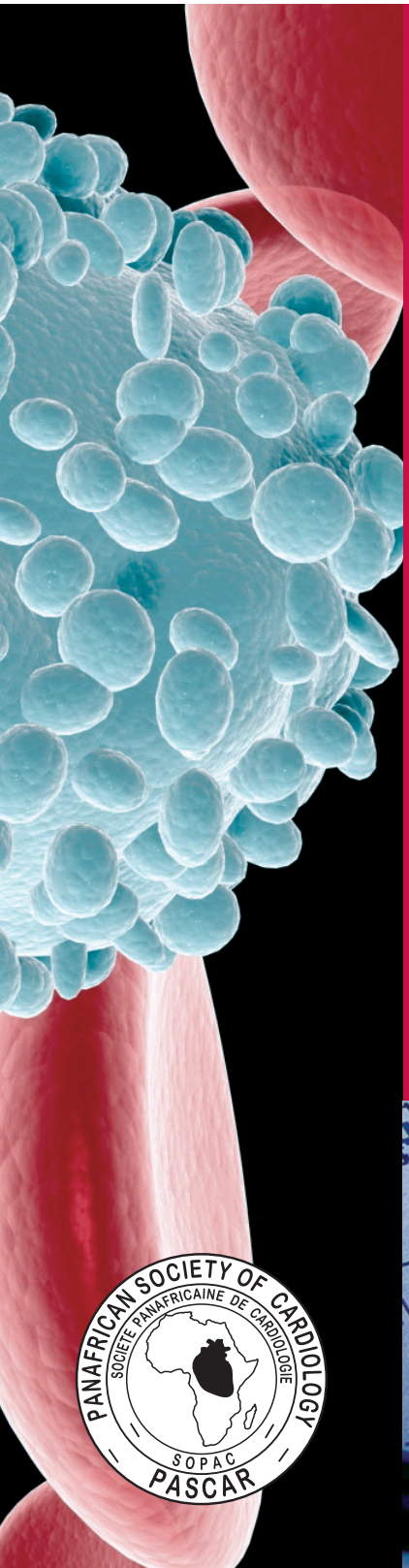

Published online

pharma dynamics
EFFECTIVE AFFORDABLE HEALTHCARE

A Lupin Group Company

HOLDS RANK
IN HYPERTENSION

Zartan
LOSARTAN POTASSIUM
50 mg | **100** mg

Zartan Co
LOSARTAN POTASSIUM **50** mg | **100** mg
HYDROCHLOROTHIAZIDE 12,5 mg | 25 mg

For further product information contact **PHARMA DYNAMICS** P O Box 30958 Tokai Cape Town 7966 **Fax** +27 21 701 5898
Email info@pharmadynamics.co.za **CUSTOMER CARE LINE** 0860 PHARMA (742 762) / +27 21 707 7000 **www.pharmadynamics.co.za**

ZARTAN 50, 100 mg. Each tablet contains 50, 100 mg losartan potassium respectively. S3 A41/7.1.3/0287, 0289. NAM NS2 08/7.1.3/0067, 0086. For full prescribing information, refer to the professional information approved by SAHPRA, 10 August 2007. **ZARTAN CO 50/12,5, 100/25.** Each tablet contains 50, 100 mg losartan potassium respectively and 12,5, 25 mg hydrochlorothiazide respectively. S3 A42/7.1.3/1068, 1069. NAM NS2 12/7.1.3/0070, 0071. For full prescribing information, refer to the professional information approved by SAHPRA, 17 February 2017. **ZNCH514/04/2019.**

ISSN 1995-1892 (print)
ISSN 1680-0745 (online)

CVJ AFRICA

Cardiovascular Journal of Africa | www.cvja.co.za

Vol 30, No 4, JULY/AUGUST 2019

CONTENTS

EDITORIAL

CARDIOVASCULAR TOPICS

INDEXED AT SCISEARCH (SCI), PUBMED, PUBMED CENTRAL AND SABINET

REVIEW ARTICLE

PUBLISHED ONLINE (Available on www.cvja.co.za and in PubMed)

CASE REPORTS

FINANCIAL & PRODUCTION CO-ORDINATOR
ELSABÉ BURMEISTER
Tel: 021 976 8129
Fax: 086 664 4202
Cell: 082 775 6808
e-mail: elsabe@clinicscardive.com

PRODUCTION EDITOR
SHAUNA GERMISHUIZEN
Tel: 021 785 7178
Cell: 083 460 8535
e-mail: shauna@clinicscardive.com

CONTENT MANAGER
MICHAEL MEADON (Design Connection)
Tel: 021 976 8129
Fax: 0866 557 149
e-mail: michael@clinicscardive.com

GAUTENG CONTRIBUTOR
PETER WAGENAAR
Cell 082 413 9954
e-mail: skylark65@myconnection.co.za

The *Cardiovascular Journal of Africa*, incorporating the *Cardiovascular Journal of South Africa*, is published 10 times a year, the publication date being the third week of the designated month.

COPYRIGHT:
Clinics Cardive Publishing (Pty) Ltd.

LAYOUT:
Martingraphix

PRINTER:
Tandym Print/Castle Graphics

ONLINE PUBLISHING & CODING SERVICES:
Design Connection & Active-XML.com

All submissions to CVJA are to be made online via www.cvja.co.za

Electronic submission by means of an e-mail attachment may be considered under exceptional circumstances.

Postal address: PO Box 1013, Durbanville, RSA, 7551

Tel: 021 976 8129
Fax: 0866 644 202
Int.: +27 21 976 8129

e-mail: info@clinicscardive.com

Electronic abstracts available on Pubmed

Audited circulation

Full text articles available on: www.cvja.co.za or via www.sabinet.co.za; for access codes contact elsabe@clinicscardive.com

Subscriptions for 6 issues:
To subscribe to the journal or change your postal address, e-mail elsabe@clinicscardive.com

South Africa: R490 (incl VAT)
Overseas: $135
Online subscription: R300

Editorial

Searching the lipidome for answers to prevent and treat non-communicable diseases

Louise van den Berg, Corinna Walsh

Non-communicable diseases (NCDs), once restricted to certain affluent societies, currently represent 70% of all global mortality, and are predicted to be the leading cause of morbidity and mortality in all regions of the world by 2030.[1] Cardiovascular diseases (CVD) and diabetes count among the four NCDs that cause over 80% of all premature deaths. Finding effective ways to predict, prevent and treat these diseases is, therefore, essential to address this growing threat to global health and economic security.[1,2]

The significant drivers for NCDs, particularly CVD and diabetes, are modifiable behavioural risk factors, including unhealthy diets and physical inactivity, which cause a specific clustering of metabolic abnormalities referred to as the metabolic syndrome (MetS). The severity of these metabolic abnormalities predicts the risk for and progression to the associated NCDs.[3] The MetS is defined as the presence of at least three out of five clinical risk factors, namely abdominal obesity (defined by waist circumference above population-specific thresholds), hypertension, insulin resistance, elevated serum triglycerides and low serum high-density lipoprotein cholesterol.[4,5]

Obesity, however, is not a homogeneous condition across individuals. The MetS and associated metabolic abnormalities occur in some apparently healthy and lean individuals.[6] Moreover, 25–40% of obese individuals do not present with metabolic abnormalities associated with the MetS,[7] although recent studies do suggest that metabolically healthy obesity (HO) is transient and, over time, does transform to the MetS.[8,9] Simple anthropometric screening, therefore, does not always reflect the biological effects of excessive body fat on health. Additional molecular characterisations of lean and obese phenotypes are needed to assess the risk of developing subsequent metabolic conditions at the individual level.

One area of study for finding predictive biomarkers is the lipidome, including the adipose tissue, circulating free fatty acids, and the phospholipid bilayers that constitute cellular and sub-cellular membranes. Adipose tissue, far from just a caloric reservoir, is metabolically active. In the obese state, the enlarged adipose tissue is transformed by macrophage infiltration and enhanced inflammatory activity, causing increased levels of circulating pro-inflammatory cytokines. These cytokines include tumour necrosis factor-alpha and interleukin-6, which are associated with insulin resistance[10] and increased risk for CVD and type 2 diabetes mellitus (T2DM).[10-12]

The serum/plasma free fatty acid profile, in turn, reflects fatty acid metabolism and dietary intake, providing an objective assessment of dietary fat composition that is potentially independent of the errors associated with reliance on self-reported dietary intake. Obese individuals present with chronically elevated circulating free fatty acid levels, which may, therefore, serve as a biomarker of obesity-associated MetS and CVD.[13]

Increased risk for NCDs has been associated with higher levels of circulating and phospholipid bilayer-associated saturated fatty acids (SFAs); studies indicate that increasing membrane rigidity may be one plausible mechanism by which SFA levels are associated with the risk for T2DM and CVD.[14] Conversely, long-chain mono-unsaturated fatty acids (LCMUFAs) and long-chain poly-unsaturated fatty acids (LCPUFAs) contribute to the fluidity of the phospholipid bilayers, which could explain at least some of the protective effects against NCDs reported in many studies. Beyond membrane fluidity, n-6 and n-3 LCPUFAs in the phospholipid bilayers serve as substrates for several enzymes that produce pro- and anti-inflammatory oxylipins, rendering them potent modulators of cytokine production.[15]

The distinction between HO and the MetS was recently proposed to be related to the degree of chronic inflammation present.[16] An increase in plasma and phospholipid bilayer-associated n-6 results in a decrease of n-3 LCPUFAs in the plasma and phospholipid bilayers, and higher concentrations of plasma n-6 oxylipins;[17] therefore, an increased n-6/n-3 ratio is associated with increased inflammation in obesity.[18]

A recent meta-analysis of 21 studies[15] found that the composition of LCPUFAs in the circulation and phospholipid bilayers differed significantly between overweight and obese compared to normal-weight subjects. Obese subjects had significantly lower n-6 linolenic acid (LA) levels and significantly higher levels of dihomo-γ-linolenic acid (DGLA), compared with controls in all the investigated biomarkers. The meta-analysis also found that the activity of Δ6-desaturase, which converts GLA (which in turn, is derived from LA in the phospholipid bilayers) to DGLA, was significantly increased in the overweight and obese subjects. Conversely, the activity of Δ5-desaturase, which converts DGLA to arachidonic acid (AA), was significantly decreased in the overweight and obese subjects.[15]

Overall, this accounts for the accumulation of DGLA, which is a crucial player in the synthetic pathway for pro-inflammatory oxylipins; therefore elevated levels of this LCPUFA may

Department of Nutrition and Dietetics, University of the Free State, South Africa
Louise van den Berg, BMedSc, BMedSc Hons (Haematology), MSc (Immunology), PhD (Immunology), BSc Dietetics
Corinna Walsh, BSc Dietetics, MSc (Dietetics), PhD (Nutrition), WalshCM@ufs.ac.za

contribute to the inflammatory phenotype in obesity and the MetS.[7] Indeed, a set of four recent studies found that circulating levels of DGLA and the SFA, palmitoleic acid (PA), in particular, were predictive of the risk of developing the MSet or diabetes remission after metabolic surgery in a group of obese subjects, and were also potential markers for the inflammatory status of the subject.[7]

In this issue of the journal (page 228), Ojwang *et al*.[19] applied factor analysis to identify fatty acid patterns from 11 dietary fatty acids and 26 individual phospholipid bilayer-associated fatty acids in 711 black South African adults who participated in the South African leg of the Prospective Urban and Rural Epidemiology (PURE) study. Two patterns from dietary fatty acids and six patterns from phospholipid bilayer-associated fatty acids were identified that explained the association between fatty acid patterns with adiposity and the MetS in this population. The association for dietary fatty acid patterns was weaker than for phospholipid bilayer-associated fatty acid patterns. Phospholipid bilayer-associated fatty acid patterns, characterised by, first, high levels of SFAs and, second, high levels of n-3 very long-chain PUFAs, were positively associated with measures of adiposity and the MetS. Phospholipid bilayer-associated fatty acid patterns, characterised by, first, high levels of LCMUFAs and, second, high levels of n-3 LCPUFAs, were inversely associated with the MetS and some measures of adiposity.

In the clinical setting, identifying specific high-risk profiles of fatty acid and oxylipins in the lipidome could assist in identifying obese and possibly lean individuals who are most likely to develop diseases associated with chronic inflammation or oxidative stress.[20] Further research, including polymorphism analysis of desaturases, may provide a better understanding of the contribution of LCPUFAs to the development and consequences of obesity and the MetS.[15] In the fight against NCDs, knowledge of beneficial and harmful biomarker profiles could also assist in improving dietary guidelines for fat intake to prevent obesity and the MetS.

References

1. World Health Organization. Global Status Report on noncommunicable diseases: 2014. Geneva, Switzerland, 2014.
2. Frenk J, Gómez-Dantés O. False dichotomies in global health: the need for integrative thinking. *Lancet* 2017; **389**(10069): 667–670.
3. Guo Y, Musani SK, Sims M, Pearson TA, Deboer MD, Gurka MJ. Assessing the added predictive ability of a metabolic syndrome severity score in predicting incident cardiovascular disease and type 2 diabetes: The Atherosclerosis Risk in Communities Study and Jackson Heart Study. *Diabetol Metab Syndr* 2018; **10**: 42.
4. Alberti KGMM, Eckel RH, Grundy SM, Zimmet PZ, Cleeman JI, Donato K, *et al*. Harmonizing the metabolic syndrome: A joint interim statement of the International Diabetes Federation Task Force on Epidemiology and Prevention; National Heart, Lung, and Blood Institute; American Heart Association and the World Heart Federation. *Circulation* 2009; **120**(16): 1640–1645.
5. Paley C, Johnson M. Abdominal obesity and metabolic syndrome. *BMC Sports Sci Med Rehabil* 2018; **10**: 7.
6. Townsend DK, McGregor K, Wu E, Cialkowski K, Haub MD, Barstow TJ. Insulin resistance and metabolic syndrome criteria in lean, normoglycemic college-age subjects. *Diabetes Metab Syndr Clin Res Rev* 2018; **12**(5): 609–616.
7. Ni Y, Zhao L, Yu H, Ma X, Bao Y, Rajani C, *et al*. Circulating unsaturated fatty acids delineate the metabolic status of obese individuals. *EBioMedicine* 2015; **2**(10): 1513–1522.
8. Kouvari M, Panagiotakos DB, Yannakoulia M, Georgousopoulou E, Critselis E, Chrysohoou C, *et al*. Transition from metabolically benign to metabolically unhealthy obesity and 10-year cardiovascular disease incidence: The ATTICA cohort study. *Metabolism* 2019; **93**: 18–24.
9. Zhao L, Ni Y, Ma X, Zhao A, Bao Y, Liu J, *et al*. A panel of free fatty acid ratios to predict the development of metabolic abnormalities in healthy obese individuals. *Sci Rep* 2016; **6**: 1–9.
10. Bersch-Ferreira ÂC, Da Silva JT, Torreglosa CR, Weber B, Sampaio GR, Gehringer MO, *et al*. Association between plasma fatty acids and inflammatory markers in patients with and without insulin resistance and in secondary prevention of cardiovascular disease, a cross-sectional study. *Nutr J* 2018; **17**(1): 1–10.
11. Burhans MS, Hagman DK, Kuzma JN, Schmidt KA, Kratz M. Contribution of adipose tissue inflammation to the development of type 2 diabetes mellitus. *Compr Physiol* 2018; **9**(1): 1–58.
12. Choe SS, Huh JY, Hwang IJ, Kim JI, Kim JB. Adipose tissue remodelling: Its role in energy metabolism and metabolic disorders. *Front Endocrinol* 2016; **7**: 1–16.
13. Zhang HW, Zhao X, Guo YL, Zhu CG, Wu NQ, Sun J, *et al*. Free fatty acids and cardiovascular outcome: A Chinese cohort study on stable coronary artery disease. *Nutr Metab* 2017; **14**(1): 1–8.
14. Weijers RNM. Lipid composition of cell membranes and its relevance in type 2 diabetes mellitus. *Curr Diabetes Rev* 2012; **8**: 390–400.
15. Fekete K, Györei E, Lohner S, Verduci E, Agostoni C, Decsi T. Long-chain polyunsaturated fatty acid status in obesity: A systematic review and meta-analysis. *Obes Rev* 2015; **16**(6): 488–497.
16. Perreault M, Zulyniak MA, Badoud F, Stephenson S, Badawi A, Buchholz A, *et al*. A distinct fatty acid profile underlies the reduced inflammatory state of metabolically healthy obese individuals. *PLoS One* 2014; **9**(2).
17. Calder PC. Omega-3 fatty acids and inflammatory processes: from molecules to man. *Biochem Soc Trans* 2017; **45**(5): 1105–1115.
18. Raphael W, Sordillo LM. Dietary polyunsaturated fatty acids and inflammation: The role of phospholipid biosynthesis. *Int J Mol Sci* 2013; **14**(10): 21167–21188.
19. Ojwang AA, Kruger HS, Zec M, Ricci C, Pieters M, Kruger IM, *et al.* Plasma phospholipid fatty acid patterns are associated with adiposity and the metabolic syndrome in black South Africans: a cross-sectional study. *Cardiovasc J Afr* 2019; **30**(4): 228–238.
20. Pickens CA, Sordillo LM, Comstock SS, Harris WS, Hortos K, Kovan B, *et al*. Plasma phospholipids, non-esterified plasma polyunsaturated fatty acids and oxylipids are associated with BMI. *Prostaglandins Leukot Essent Fat Acids* 2015; **95**: 31–40.

Cardiovascular Topics

Ellisras Longitudinal Study 2017: elevated serum levels of carboxymethyl-lysine, an advanced glycation end-product, are associated with higher odds of developing endothelial dysfunction in black South African patients with type 2 diabetes mellitus (ELS 29)

Motetelo Alfred Mogale, Catherine Martha Mhlanga, Stanley Sechene Gololo, Agustine Adu

Abstract

This case–control study investigated the association between major types of serum advanced glycation end-products (AGEs) and selected serum/plasma markers of endothelial dysfunction in black patients with type 2 diabetes mellitus at Dr George Mukhari Academic Hospital. Serum AGEs were measured using either enzyme-linked immunosorbent assay (ELISA) or spectrofluoremetry. Serum markers of endothelial dysfunction were measured using either ELISA or calometry. The correlation and associations between major types of serum AGEs and markers of endothelial dysfunction were investigated using the Spearman correlation coefficient and bivariate logistic regression analysis, respectively. Although both serum total immunogenic AGEs and serum carboxymethyl-lysine (CML) were moderately and negatively associated with endothelial dysfunction, only serum CML was significantly associated with a higher odds for the development of endothelial dysfunction (low nitric oxide levels) in our diabetic subjects. It can therefore be concluded from this study that high serum levels of CML may predispose to endothelial dysfunction in black South Africans with type 2 diabetes.

Keywords: serum AGEs, endothelial dysfunction, markers of endothelial dysfunction, black South Africans, type 2 diabetes mellitus

Submitted 11/4/18, accepted 31/10/18
Published online 2/8/19
Cardiovasc J Afr 2019; **30**: 193–197 www.cvja.co.za

DOI: 10.5830/CVJA-2018-060

Department of Biochemistry, School of Science and Technology, Sefako Makgatho Health Sciences University, Pretoria, South Africa
Motetelo Alfred Mogale, MD, alfred.mogale@smu.ac.za
Catherine Martha Mhlanga, MD
Stanley Sechene Gololo, MD

Department of Internal Medicine, School of Medicine, Sefako Makgatho Health Sciences University, Pretoria, South Africa
Agustine Adu, MD

Clinical and research-based evidence indicates that both type 1 and type 2 diabetes mellitus are associated with long-term microvascular complications (nephropathy, retinopathy and neuropathy) and macrovascular complications (myocardial infarction and cerebrovascular accident).[1,2] Available evidence also suggests that the pathogenesis of these vascular complications of diabetes involve endothelial activation or dysfunction.[3] Endothelial dysfunction, defined as impaired biosynthesis of endothelium-derived nitric oxide (NO) or its reduced bioavailability, is an established mediator of the atherosclerotic process.[3,4] Indeed, most of the traditional and emerging cardiovascular risk factors are known to promote the development and progression of vascular atherosclerosis through their deleterious effect on the endothelium.[4] The development of endothelial dysfunction in diabetes mellitus is attributable, among other factors, to the formation and action of advanced glycation end-products (AGEs).[5,6]

AGEs are a heterogeneous group of compounds formed by the non-enzymatic reaction between reducing sugars such as glucose and proteins, nucleic acids and lipids.[5] The formation of AGEs is reported to be enhanced by both chronic hyperglycaemia and oxidative stress, two conditions that are closely associated with diabetes mellitus.[2,6]

Available evidence also suggests that in diabetes mellitus, AGEs may promote endothelial dysfunction via a variety of mechanisms. Firstly, collagen cross-linked AGEs in the vascular wall may trap and quench NO on its way from the endothelium to the smooth muscle layer to stimulate their relaxation.[7] Secondly, the interaction of certain serum AGEs with the receptor for advanced glycation end-products (RAGE) on vascular endothelial cells results in the activation and translocation of nuclear factor kappa B (NF-κB) into the nucleus.[8] Once in the nucleus, NF-κB up-regulates several genes whose protein and peptide products are involved in the activation of the endothelium or endothelial dysfunction.[1,7] Thirdly, serum AGE/RAGE interaction on the vascular endothelium may result in deactivation of the enzyme, endothelial nitric oxide synthase (eNOS), which synthesises NO in the endothelium.[9] Fourthly, the superoxide anion (O_2^-) generated during the formation of AGEs may react with NO to form the peroxy-nitrite ion $(ONOO)^-$, thereby reducing the bioavailability of NO.[9,10] Lastly, AGEs may

impair Ca^{2+} signalling in endothelial cells, thereby interfering with several endothelial cell processes, including the biosynthesis of NO.[11]

Racial/ethnic disparities in endothelial dysfunction have been observed in a number of studies. For example, African-Americans are reported to have reduced NO bioavailability compared to their Caucasian counterparts.[12,13] Also, Tibetan type 2 diabetes patients are reported to have less NO levels than their Chinese Han counterparts.[14] On the other hand, research evidence has also shown that both tissue and serum AGE levels may be influenced by genetics.[12,15] Taken together, this information suggests that the association between serum (and tissue) AGE levels and endothelial dysfunction may be influenced by the genetic make-up and ethnicity/race of an individual. However, with the exception of a single study that investigated the association between serum AGE levels and endothelial dysfunction among Chinese type 2 diabetes patients,[16] there is no other information in the literature regarding the association between serum levels of AGEs and endothelial dysfunction. In particular, no study has ever been conducted to investigate the association between serum AGE levels and endothelial dysfunction among type 2 diabetes patients of black African descent. Therefore, the aim of this study was to investigate the association between the different types of serum AGEs and circulating markers of endothelial dysfunction among black South African patients with type 2 diabetes mellitus.

Methods

A random sample of 138 black type 2 diabetes patients attending the diabetes clinic of Dr George Mukhari Academic Hospital (DGMAH) for medical review, and a convenient sample of 81 age-matched non-diabetic control subjects were recruited into this study. The control subjects were recruited mainly from the orthopaedic wards of DGMAH. Controls were included in the study if they had fasting blood glucose level of < 6.1 mmol/l. Both type 2 diabetes patients and control subjects were excluded from the study if they had any sign of renal impairment, history or evidence of any of the factors known to affect endothelial dysfunction, such as the traditional cardiovascular risk factors, uncontrolled hypertension, dyslipidaemia, cigarette smoking and obesity.

All type 2 diabetes patients and control subjects gave their informed consent after the purpose of the study and their rights were clearly explained to them. The study was conducted in accordance with the requirements of the research and ethics committee of the University of Limpopo (MREC/P/2013/PG).

After an overnight fast, venous blood samples for measurement of levels of the different types of serum AGEs, urea and electrolytes, as well as selected circulating markers of endothelial dysfunction were collected from all participants into blood collection tubes (BD Vacutainer®, Franklin Lakes, NJ, USA). The samples were left to clot for 30 min and then centrifuged at 4 000 rpm for 15 min at 4°C. Aliquots of the resultant serum samples were then stored at –80°C until analysed. For blood glucose and glycated haemoglobin (HbA_{1c}) measurements, blood samples were collected into citrate and EDTA blood tubes, respectively.

Serum total immunogenic AGEs (TIAGEs), Nε-carboxymethyl-lysine (CML) and Nε-carboxyethyl-lysine (CEL) were measured using STA-317, STA-316 and STA-300 Oxiselect™ ELISA kits, respectively, (2BScientific, Upper Heyford, UK), according to the manufacturer's instructions. Fluorescent serum AGEs (FAGEs) were measured according to the method described by Munch *et al.*[17] In brief, 20 µl of serum was diluted to a volume of 10 ml with 20 mM phosphate buffered saline, pH 7.4. Fluorescence of the diluted sample was then measured spectrofluorometrically (excitation at 370 nm and emission at 440 nm) using a GloMaxR multi-detection spectrofluorometer (Promega Corp, Madison, WI, USA). Fluorescent readings were expressed as arbitrary units (emission intensity/excitation intensity).

Plasminogen activator inhibitor-1 (PAI-1) was measured using ELISA kits purchased from Cell Biolabs, and NO and endothelin-1 (ET-1) were measured using colorimetric and immunometric kits, respectively, purchased from Cayman Chemical's ACE. Fasting blood glucose levels were measured using a commercially available glucose oxidase-based kit adapted to the Beckman Coulter® UniCell DXC 800 Synchron® Clinical System available in the National Laboratory Health Services (NLHS) laboratory at the DGMAH. HbA_{1c} level was measured using the immune chemiluminescent assay kit adapted to the Abbot Architect system Ci 8200 in the NLHS laboratory at DGMAH, in accordance with the manufacturer's instructions.

Statistical analysis

All analyses were performed using the Statistical Package for the Social Sciences (SPSS) software (Version 23.0), SPSS Inc, Chicago, IL, USA. Continuous variables are expressed as mean ± standard deviation (SD) while categorical variables are expressed as percentages. Means of the experimental and control groups were compared using the student's *t*-test, and $p < 0.05$ was regarded as statistically significant differences between the groups. Bivariate logistic regression and the Spearman rank correlation coefficient were used to determine the association and correlation between the major types of serum AGEs and circulating markers of endothelial dysfunction, respectively. Significance level was set at $p < 0.05$.

Results

Table 1 shows the demographic, clinical and laboratory characteristics of the type 2 diabetes patients and the non-diabetic controls. With the exception of the fasting blood glucose and HbA_{1c} levels, there were no significant differences in any other demographic, clinical or laboratory parameters between the diabetic and the non-diabetic groups.

As shown in Fig. 1, the mean serum levels of TIAGEs, CML and CEL were significantly higher in the diabetic than the non-diabetic group ($p < 0.001$, $p < 0.001$ and $p < 0.01$, respectively). On the other hand, there was no significant difference between serum FAGE levels of the diabetic and non-diabetic groups.

As shown in Fig. 2, the mean NO serum level of the diabetic patients was significantly lower than that of the non-diabetic control group ($p < 0.001$). On the other hand, the mean serum ET-1 and PAI-1 levels of the diabetic group were significantly higher than those of the control group ($p < 0.05$) (Fig. 2).

Gender and age of the study subjects, as well as the different types of serum AGEs (TIAGEs, CML, CEL and FAGEs) measured in the diabetic group were correlated with

Table 1. Demographic, clinical and laboratory characteristics of the study subjects

Characteristics	*Type 2 diabetes group (n = 120) mean ± SD*	*Non-diabetic control group (n = 83) mean ± SD*	p-*value*
Gender			
Male, *n* (%)	49 (41)	36 (44)	0.512
Female, *n* (%)	71 (59)	47 (56)	0.734
Age (years)	56.9 ± 9.4	51.1 ± 9.8	0.152
FBG (mmol/l)	11.6 ± 3.3	5.2 ± 6.3	0.012*
HbA_{1c} (%)	9.7 ± 1.2	6.1 ± 2.6	0.037*
HbA_{1c} (mmol/mol)	81 ± 0.99	43 ± 5	0.037*
BMI (kg/m²)	26.6 ± 4.7	25.8 ± 5.5	0.081
TC (mmol/l)	4.20 ± 1.80	4.03 ± 0.95	0.174
LDL (mmol/l)	2.3 ± 0.15	2.1 ± 0.2	0.511
TG (mmol/l)	1.2 ± 0.5	1.32 ± 0.4	0.712
SBP (mmHg)	127 ± 10.9	128 ± 8.7	0.141
DBP (mmHg)	81 ± 10.8	82 ± 8.4	0.091
Urea (mmol/l)	6.0 ± 2.5	5.6 ± 1.3	0.452
Creatinine (µmol/l)	94 ± 55.9	86.4 ± 21.1	0.318

FBG: fasting blood glucose; HbA_{1c}: glycated haemoglobin; BMI: body mass index; TC: total cholesterol; LDL: low-density lipoprotein; TG: triglycerides; SBP: systolic blood pressure; DBP: diastolic blood pressure; GFR: glumerular filtration rate.

the corresponding selected circulating markers of endothelial dysfunction (NO, ET-1 and PAI-1) using the Spearman rank correlation coefficient (r_s).

Results shown in Table 2 suggest a significant weak negative correlation ($p < 0.05$) between the age of the study subject and serum levels of NO, as well as a significant moderate negative correlation between serum TIAGE and NO levels ($p < 0.05$), and between serum CML and NO levels ($p < 0.05$) (Table 2). Table 2 also shows a significant weak positive correlation between serum TIAGE and ET-1 levels ($p < 0.05$), as well as between serum CML and ET-1 levels ($p < 0.05$).

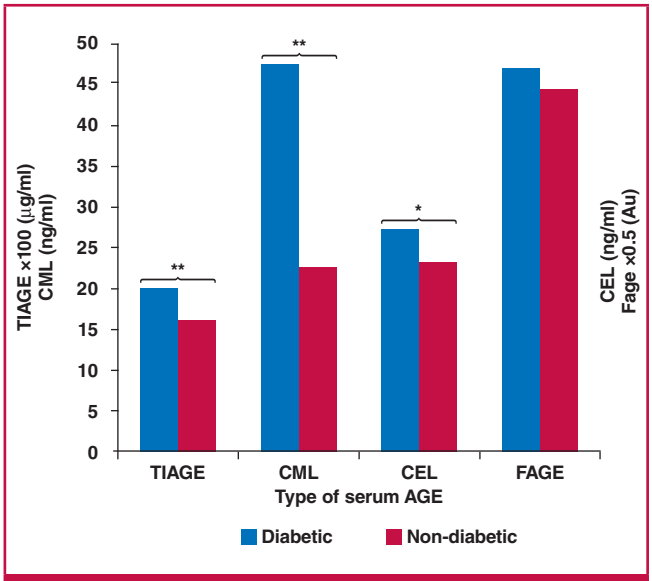

Fig. 1. Comparison of median levels of total immunogenic AGEs (TIAGEs), Nε-carboxymethyl-lysine (CML), Nε-carboxyethyl-lysine (CEL) and fluorescent AGEs (FAGEs) between the type 2 diabetes and non-diabetic control groups. *Significant at $p < 0.01$, **significant at $p < 0.001$.

Table 2. Correlations between age of the study subjects, gender, different types of serum AGEs and selected circulating markers of endothelial dysfunction

	Serum NO (pmol/l)		*Serum ET-1 (ng/ml)*		*Serum PAI-1 (ng/ml)*	
Parameters	r_s	p-*value*	r_s	p-*value*	r_s	p-*value*
Age	–0.236*	0.031	0.149	0.302	0.080	0.582
Gender	0.191	0.896	0.048	0.741	–0.230	0.109
TIAGEs (µg/ml)	–0.382*	0.026	0.279*	0.012	–0.185	0.108
CML (ng/ml)	–0.412*	0.011	0.281*	0.021	–0.228	0.112
CEL (ng/ml)	–0.015	0.920	0.150	0.297	–0.145	0.758
FAGEs (Au)	0.050	0.722	–0.036	0.802	0.175	0.224

r_s: Spearman rank correlation coefficient; TIAGEs: total immunogenic advanced glycation end-products; CML: Nε-carboxymethyl-lysine; CEL: Nε-carboxyethyl-lysine; FAGEs: fluorescent advanced glycation end-products; Au: arbitrary units; *Correlation is significant at $p < 0.05$ level.

Bivariate logistic regression analysis of the association between age and gender of the diabetic subjects, as well as serum levels of the major types of serum AGEs with endothelial dysfunction (serum NO levels less than the first quartile) revealed that only higher serum levels of CML were significantly associated with higher crude odds of endothelial dysfunction [COR (95% CI), 1.910 (0.655–0.893) ($p < 0.05$) (Table 3).

Discussion

As expected, serum levels of TIAGEs, CML and CEL were found to be significantly higher in the diabetic patient group compared with the non-diabetic control group. However, serum FAGE levels of diabetic patients were not significantly different from those of non-diabetic controls. This observation might be attributed to the nature of the control group used in the study.

High serum FAGE levels, in particular high serum levels of pentosidine, the most abundant fluorescent AGE in plasma and tissues, have been associated with the development and progression of osteoporosis in diabetic and non-diabetic

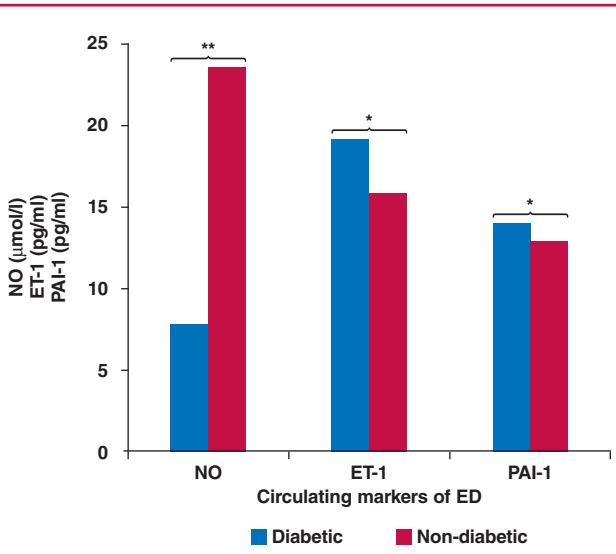

Fig. 2. Comparison of mean serum levels of nitric oxide (NO), endothelin-1 (ET-1) and plasminogen activator inhibitor (PAI-1) between the type 2 diabetes and non-diabetic control groups. *Significant at $p < 0.05$; **significant at $p < 0.01$.

Table 3. Bivariate logistic analysis of the association between gender, age and the major types of serum AGEs with endothelial dysfunction (less than the first quartile of NO levels)

Parameters	*COR*	*95% CI*	p-*value*
Age	0.600	1.372–2.62	0.460
Gender	1.040	0.996–1.12	0.296
TIAGEs (µg/ml)	0.348	0.014–8.916	0.523
CML (ng/ml)	1.910	0.655–0.893	0.013*
CEL (ng/ml)	1.172	0.963–1.638	0.112
FAGEs (Au)	0.991	0.882–1.038	0.141

COR: crude odds ratio; CI: confidence interval; TIAGEs: total immunogenic advanced glycation end-products; CML: Nε-carboxymethyl-lysine; CEL: Nε-carboxyethyl-lysine; FAGEs: fluorescent advanced glycation end-products; *Significant at $p < 0.05$.

menopausal women.[18,19] Whether the high level of pentosidine observed in the cited studies was the cause or product of osteoporosis is currently not clear. It is possible that our patient control group, which was recruited from orthopaedic wards at DGMAH, may have included non-diabetic postmenopausal women with osteoporosis-related fractures. While this likelihood was not verified in the current study, it might explain the observed high levels of FAGE in the non-diabetic control group.

Previous studies reported in the literature have used circulating levels of NO, ET-1 and PAI-1, among others, as surrogate markers of endothelial dysfunction *in vivo*.[3,4,20] According to these previous studies, serum levels of NO and its metabolites are expected to be decreased, while serum levels of both ET-1 and PAI-1 are expected to be increased in conditions associated with endothelial dysfunction, such as type 2 diabetes mellitus. Therefore the findings of significantly reduced NO levels and significantly higher serum levels of both ET-1 and PAI-1 are in perfect agreement with the results of these previous studies. However, these findings should be interpreted with caution, since these circulating markers of endothelial dysfunction may come from sources other than the vascular endothelium.[4,20]

The observation in this study that serum NO levels were negatively and significantly correlated with the age of the study subject is in agreement with the well-documented observation that endothelial function decreases with advanced age.[21,22] The findings that serum levels of both TIAGEs and CML were negatively and significantly correlated with serum NO levels and positively and significantly correlated with serum levels of ET-1 were also not unexpected, since high levels of some serum AGEs are known to promote endothelial dysfunction through their interaction with RAGE on the surface of the vascular endothelial cell.[1] The finding that serum CML level was the only parameter in this study that was significantly associated with increased odds of developing endothelial dysfunction suggests that serum CML is the major type of serum AGEs that interacts with RAGE to promote endothelial dysfunction.

Limitations

There are several limitations that should be taken into consideration when interpreting results of this study. Firstly, the sample size was small and study subjects were recruited from a single health institution, therefore the findings could not be generalised beyond the study samples. Secondly, the study was cross-sectional and therefore cause and effect relationships could not be inferred from the results. Thirdly, the possible confounding effect of exogenous dietary and smoking-related AGEs on serum AGE levels was not addressed. Fourthly, the control group selected for this study might have confounded the results, particularly those of the FAGEs. Fifthly, we did not concurrently measure serum AGE levels and circulating markers of endothelial dysfunction of other South African race groups for comparison purposes.

Despite these limitations, we believe that the results of this study are of great interest in that they are the first to describe the status of serum AGE levels among black South African patients with type 2 diabetes, as well as the association between serum AGE levels and endothelial dysfunction in black South African patients with type 2 diabetes mellitus.

Conclusions

The results of this study showed that serum AGE levels were significantly higher in type 2 diabetes patients than in non-diabetic black South Africans, and with the exception of CEL were not influenced by gender. In addition, serum FAGE levels appeared to be positively associated with increasing age of the subjects in the non-diabetic controls, but not in in the diabetic subjects. Furthermore, the findings of this part of the thesis showed that serum TIAGEs, CML, CEL, ET-1 and PAI-1 levels were significantly elevated, whereas serum levels of NO were significantly reduced in black South African patients with type 2 diabetes compared to those in non-diabetic control subjects. Moreover, the findings indicated that serum TIAGE and CML levels, but not CEL and FAGE levels were correlated with endothelial dysfunction in black South African patients with type 2 diabetes mellitus. However, only serum CML levels were associated with a higher odds of developing endothelial dysfunction in these black South African type 2 diabetes patients.

We acknowledge the contribution of the nursing and medical personnel as well as the phlebotomists at the diabetes clinic of Dr George Mukhari Academic Hospital. We are grateful for the research funding obtained from the National Research Foundation (grant no. TP1407187704).

References

1. Hegab Z, Gibbons S, Neyses L, Mamas MA. Role of advanced glycation end products in cardiovascular disease. *World J Cardiol* 2012; **4**: 90–102.
2. Stirban A, Gawlowski T, Roden M. Vascular effects of advanced glycation end-products: Clinical effects and molecular mechanisms. *Mol Met* 2014; **3**: 94–108.
3. Vita JA and Keaney JF Jr. Endothelial function: a barometer for cardiovascular risk? *Circulation* 2002; **106**: 640–642.
4. Sena CM, Pereira AM, Seiça R. Endothelial dysfuction – A major mediator of diabetic vascular disease. *Biochim et Biophys Acta* 2013; **1832**: 2216–2231.
5. Goh SY and Cooper ME. Role of AGEs in progression and complications of diabetes. *J Clin Endocrinol Metab* 2008; **93**: 1143–1152.
6. Rojas A, Morales MA. Advanced glycation end products and endothelial functions: a link towards vascular complications in diabetes. *Life Sci* 2004; **76:** 715–730.
7. Bucala R, Tracey KJ, Cerami A. Advanced glycosylation products quench nitric oxide and mediate defective endothelium-dependent vasodilatation in experimental diabetes. *J Clin Invest* 1991; **87:** 432–438.
8. Yan SF, D'Agati V, Schidt AM, Ramasamy R. Receptor for Advanced

Glycation End Products (RAGE): a formidable force in the pathogenesis of the cardiovascular complications of diabetes and aging. *Curr Mol Med* 2007; **7**: 699–710.
9. Biao XU, Yong JI, Kang YAO, Yue-Xin CAO, Ferro A. Inhibition of human endothelial cell nitric oxide synthesis by advanced glycation end-products but not glucose: relevance to diabetes. *Diabet Clin Sci* 2005; **109**: 439–446.
10. Xu B, Chibber R, Ruggerio D, Kohner E, Ritter J, Ferro A, *et al*. Impairment of vascular endothelial nitric oxide synthase activity by advanced glycation end products. *FASEB J* 2003; **17**: 1289–1291.
11. Naser N, Januszewski AS, Brown BE, Jenkins AJ, Hill MA, Murphy TV. Advanced glycation end products acutely impair Ca^{2+} signaling in bovine aortic endothelial cells. *Front Physiol* 2013; **4**: 38–45.
12. Marjonneke JM, Mohamed ME, Ahmed HT, Al-Homsi H, Al-Mahmoud KAS, Al-Obaidli A , *et al.* Ethnic and gender differences in AGEs measured by skin auto-fluorescence. *Dermatol Endocrinol* 2013; **5**: 325–330.
13. Mulukutla SR, Venkitachalam L, Bambs C, Kip KE, Aiyer A, Marroquin OC, *et al*. Black race is associated with digital artery endothelial dysfunction: results from the HEART SCORE study. *Eur Heart J* 2010; **22**: 2808–2815.
14. Tessari P, Cecchet D, Cosma A, *et al*. Nitric oxide synthesis is reduced in subjects with type 2 diabetes and nephropathy. *Diabetes* 2010; **59**(9): 2152–2159.
15. Leslie DR, Beyan H, Sawtell P, Boehm BO, Spector TD, Snieder H. Level of an advanced glycated end product is genetically determined. *Diabetes* 2003; **52**: 2441–2444.
16. Tan KCB, Chow WS, Ai VHG, Metz C, Bucala R, Lam KS. Advanced glycation end products and endothelial dysfunction in type 2 diabetes. *Diabetes Care* 2002; **25**: 1055–1059.
17. Munch G, Keis R, Wessels A, Riederer P, Bahner U, Heidland A, *et al*. Determination of advanced glycation end products in serum by fluorescence spectroscopy and competitive ELISA, *Eur J Clin Chem Clin Biochem* 1997; **35**: 669–677.
18. Yang DH, Chiang TI, Chang IC, Lin FH, Wei CC, Cheng YW. increased levels of circulating advanced glycation end-products in menopausal women with osteoporosis. *Int J Med Sci* 2014; **11**: 453–460.
19. Yamamoto M, Yamaguchi T, Yamauchi M, Yano S, Sugimoto. Serum pentosidine levels are positively associated with the presence of vertebral fractures in postmenopausal women with type 2 diabetes. *J Clin Endocrinol Metab* 2007; **93**: 1013–1019.
20. Deanfield JE, Halcox JP, Rabelink TJ. Endothelial function and dysfunction: testing and clinical relevance. *Circulation* 2007; **115**: 1285–1295.
21. Vlassara H, Uribarri J, Ferruci L. Identifying AGEs as a major source of oxidants in aging: Implications for the management and/or prevention of reduced renal function in elderly persons. *Clin Diabetes* 2009; **29**: 594–603.
22. Kanamori MJ, Selim MM, Takiddin AH, Al-Homsi H, Al-Mahmoud KA, Al-Obaidli A et al. Ethnic and gender differences in advanced glycation end products measured by skin auto-fluorescence. *Dermatotol Endocrinol* 2013; **5**(2): 325–330.

New, cheaper pill taken with statins lowers LDL cholesterol more

A small biotech company has a shot at shaking up a market roosted by giants, moving towards approval with a pill it believes can lower bad cholesterol at a discount to other medicines, reports *Stat News*. According to Esperion Therapeutics, a combination of its once-a-day treatment and a maximum dose of statin lowered LDL cholesterol 18% more than statins alone after 12 weeks.

The results come from the last of five successful trials on Esperion's drug, called bempedoic acid. The company plans to submit all of its data to the US Food and Drug Administration in the early months of 2019.

The report says the most important finding of the latest bempedoic acid trial related to safety. In the 779-patient study, Esperion's drug was indistinguishable from placebo when it came to side effects and deaths. That's important because, in an earlier trial involving more than 2 200 subjects, more patients getting bempedoic acid died than those getting placebo. The difference wasn't big enough to rule out random chance, and none of the deaths was blamed on the drug, but it was enough to stoke concern that the FDA might think twice about approving Esperion's treatment.

'From my perspective, I think the noise around those imbalances should not be overestimated in importance,' said Dr Steven Nissen, a cardiologist at the Cleveland Clinic who has served as unpaid investigator of bempedoic acid. 'I certainly don't think it's a regulatory issue at this point.'

The report says Esperion's drug is meant for patients who have had a cardiovascular event, like a heart attack or a stroke, and who are getting as large a dose of statins as they can handle. The drug is widely expected to win FDA approval and hit the market in 2020, and that's when the company will find out whether its Goldilocks plan can turn bempedoic acid into a commercial success.

As it stands, the vast majority of at-risk patients get statins, which have long since gone generic and are available for pennies a day for those with insurance. If bad LDL cholesterol levels stay high, doctors prescribe the now-generic Zetia. And in extreme cases, they reach for injected treatments from Amgen and partners Regeneron Pharmaceuticals and Sanofi, drugs that block a protein called PCSK9.

continued on page 215…

Performance of HAS-BLED and CRUSADE risk scores for the prediction of haemorrhagic events in patients with stable coronary artery disease

Ersin Yildirim, Okkes Uku, Mehmet Nail Bilen, Ozlem Secen

Abstract

We aimed to compare the power of the HAS-BLED and CRUSADE risk scores in predicting in-hospital bleeding events in patients with stable coronary artery disease undergoing elective coronary angiography. A total of 405 consecutive patients were included in the study. The mean HAS-BLED score was significantly higher ($p < 0.001$) in the in-hospital bleeding group. In patients with a HAS-BLED score ≥ 3, the in-hospital bleeding rate was significantly higher than in those with a HAS-BLED score < 3 ($p < 0.001$). Receiver operating characteristic curve analysis revealed that the HAS-BLED score was superior in predicting in-hospital bleeding events compared to the CRUSADE score [area under the curve (AUC) = 0.684 vs 0.569, respectively, $p = 0.002$]. Also in the percutaneous coronary intervention subgroup, the HAS-BLED score was superior to the CRUSADE score (AUC = 0.722 vs 0.520, respectively, $p = 0.002$). We showed that the HAS-BLED and CRUDASE scores are helpful in stable patients undergoing elective coronary angiography. Our results suggest that as a practical, easy-to-implement and more predictive scoring system, the HAS-BLED score was more useful for predicting in-hospital bleeding in patients who did not present with acute coronary syndrome.

Keywords: coronary artery disease, angiography, haemorrhage

Submitted 15/1/19, accepted 26/2/19
Published online 29/3/19
Cardiovasc J Afr 2019; **30**: 198–202 www.cvja.co.za

DOI: 10.5830/CVJA-2019-014

Bleeding is one of the most common problems in the clinic post coronary angiography. Many patients undergoing coronary angiography need antithrombotic treatment and simultaneously have other co-morbid diseases, leading to more frequent bleeding problems.[1,2] For this reason, a number of risk scores have been developed in order to predict bleeding events. One of the most important ones is the CRUSADE risk score, which has been proven effective for predicting the bleeding risk in patients presenting with non-ST segment elevation myocardial infarction (NSTEMI).[3] However, a reliable scoring system that can predict bleeding risk has not been identified yet for patients with stable coronary artery disease, which constitutes a large part of our daily practice.

Bleeding is an important cause of co-morbidity, not only in patients with coronary artery disease, but also for diseases requiring anticoagulation therapy, such as atrial fibrillation (AF). In patients with AF, the HAS-BLED bleeding risk score is one of the most useful scoring systems used to predict the risk of bleeding.[4] Several studies have previously demonstrated that the HAS-BLED risk score is an important predictor of bleeding in patients without AF.[5-7] However, a valid bleeding risk score has not been established in patients undergoing elective coronary angiography, except for those presenting with acute coronary syndrome (ACS). In this study, we aimed to determine whether significant risk scores, such as the HAS-BLED and CRUSADE, are useful in predicting the risk of in-hospital bleeding in patients undergoing elective coronary angiography.

Methods

Following ethical committee approval, 405 elective coronary angiography patients, who were treated in our coronary angiography unit, were included in the study. Patients with ST-segment elevation myocardial infarction (STEMI), NSTEMI patients, those undergoing coronary angiography after sudden cardiac events, patients with a dynamic ECG or cardiac enzyme changes, and those with unstable angina were excluded from the study. Patients with known or suspected stable coronary artery disease only were included in the study.

Data on the clinical and demographic characteristics of the patients, history of diabetes mellitus, hypertension, smoking, stroke or neurological disease, coronary artery disease, cardiac failure and medications were recorded from the patients and the patient files. Patients were divided into two groups according to whether or not bleeding occurred during in-hospital follow ups. These groups were compared in terms of demographic characteristics and risk factors.

The groups with and without bleeding were compared using the HAS-BLED and CRUSADE risk scores. When the HAS-BLED score was calculated, each of the following parameters was calculated as one point: hypertension (systolic blood pressure > 160 mmHg), abnormal renal function [defined as the presence of chronic dialysis or renal transplantation or serum creatinine > 2.3 mg/dl (203.32 mmol/l)], abnormal liver function (defined as chronic hepatic disease or biochemical

Department of Cardiology, University of Health Sciences, Istanbul Umraniye Education and Research Hospital, Istanbul, Turkey
Ersin Yildirim, MD, ersinyil44@gmail.com

Department of Cardiology, University of Health Sciences, Elazig Education and Research Hospital, Elazig, Turkey
Okkes Uku, MD
Mehmet Nail Bilen, MD
Ozlem Secen, MD

evidence of significant hepatic derangement, e.g. bilirubin more than twice the upper limit of normal, in association with AST/ALT/ALP more than three times the upper limit of normal), stroke (previous history of stroke), bleeding (major bleeding history or predisposition to bleeding), labile INRs (refers to unstable/high INRs or poor time in therapeutic range < 60%), elderly (age ≥ 65 years), drug therapy (concomitant therapy such as antiplatelet agents, NSAIDs) and alcohol intake (consuming eight or more alcoholic drinks per week).

The CRUSADE score was calculated using baseline haematocrit, glomerular filtration rate, heart rate on admission, systolic blood pressure on admission, prior vascular disease, diabetes mellitus, signs of congestive heart failure on admission and gender. The Cockcroft–Gault formula was used to calculate creatinine clearance rate.

In addition to comparing the mean of HAS-BLED and CRUSADE scores, patients were divided into groups according to HAS-BLED score ≥ 3 (high risk) or 0–2 (low risk), and CRUSADE score > 40 (high risk), > 30 (medium-high risk) and ≤ 30 (low risk). The risk groups were then assessed in terms of the incidence of bleeding. The Bleeding Academic Research Consortium (BARC) classification was used to classify bleeding. In addition, 130 patients undergoing percutaneous coronary intervention (PCI) were compared with the same tests in a subgroup analysis.

PCIs were performed via the femoral and radial route by an experienced interventional cardiologist (Siemens Axiom Artis zee Angiography System, Germany). Non-ionic low osmolality contrast medium (Omnipaque 350 MG/ml; GE Healthcare, Cork, Ireland) was used for the procedures. All stented patients were given 300 mg aspirin and a 600-mg clopidogrel loading dose during the procedure. After having visualised the arterial anatomy, 100 U/kg heparin was administered. Glycoprotein IIb/IIIa use was left to the discretion of the physician. No vascular closure device was used in any patient. After the sheath was removed, haemostasis was obtained with direct manual pressure of the fingertips over the pulse. The pressure was held for approximately 20 minutes (about three minutes for each French size) until there was no bleeding.

All patients were transferred to the intensive care unit or cardiology service after the procedure. Bed rest is generally required for six hours after a sheath is removed. Stented patients were continued on 100 mg aspirin and 75 mg clopidogrel. In patients without stenting, treatment was continued on 100 mg aspirin, but in patients with gastrointestinal intolerance to aspirin, we used 75 mg clopidogrel instead of aspirin. The decision for concurrent use of statins, angiotensin converting enzyme inhibitors, calcium channel blocker and beta-blockers was made according to the recommendations of the American College of Cardiology/American Heart Association. No patients used new oral anticoagulants. The use of non-steroidal anti-inflammatory drugs was avoided. Patients were followed up with blood samples and the femoral artery area was checked.

Statistical analysis

Statistical analysis was performed using the SPSS 15.0 for Windows evaluation version statistical package. Continuous variables are presented as mean ± standard deviation. Categorical variables are summarised as frequencies. Differences between the two groups according to continuous variables were determined by the independent samples *t*-test. Categorical variables were compared with the chi-squared or Fisher's exact test. *C*-statistics and receiver operating characteristic (ROC) curve analysis were used to assess the performance of the HAS-BLED and CRUSADE bleeding scores. Comparison of ROC curves was done using the de Long test. A *p*-value of < 0.05 was considered statistically significant.

Results

The mean age was higher in the group with in-hospital bleeding than in the group without bleeding (65.32 ± 11.40 vs 60.01 ± 13.57 years, respectively, $p = 0.003$). Diabetes mellitus was more frequent among patients in the non-bleeding group compared to the in-hospital bleeding group (33.8 vs 8%, respectively, $p = 0.001$). Potassium and haematocrit values were statistically significantly lower in the in-hospital bleeding group.

The results of the groups according to bleeding status are shown in Table 1. Bleeding was observed in 65 patients. Major bleeding (BARC type 3) was observed in four patients, in the form of gastrointestinal bleeding in one patient and from femoral artery haemorrhage in the others. Minor bleeding was observed in the remaining 61 patients (femoral artery bleeding in 57, bleeding from the nose in two, and bleeding in the gingiva in two). Erythrocyte suspension replacement was needed in only four patients with major haemorrhage. In one patient with major haemorrhage, a haematoma in the groin was evacuated and the femoral artery was sutured.

The mean HAS-BLED score of the patients with in-hospital bleeding was significantly higher than that of the group without bleeding (2.21 ± 1.15 vs 1.49 ± 0.95, $p < 0.001$). There was no significant difference between the mean CRUSADE scores of the two groups (23.69 ± 11.37 vs 21.28 ± 10.82, $p = 0.105$).

The in-hospital bleeding rate in patients with a HAS-BLED score ≥ 3 was significantly higher than in patients with a HAS-BLED score < 3 (49.2 vs 14.1%, $p < 0.001$). Similarly, the rate of in-hospital bleeding in patients with a CRUSADE score > 30 was significantly higher than in patients with a CRUSADE score ≤ 30 (36.9 vs 18%, $p = 0.001$). There was no significant difference in haemorrhage rate between patients with CRUSADE scores > 40 and ≤ 40.

In the ROC curve analysis, the HAS-BLED score was found to be superior to the CRUSADE score in predicting in-hospital bleeding risk among the whole study population who underwent elective coronary angiography (AUC = 0.684 vs 0.569, respectively, $p = 0.002$) (Fig. 1). According to the Youden index *J*-statistics, the HAS-BLED score predicted in-hospital bleeding in patients undergoing coronary angiography without ACS with a sensitivity of 59.09% and a specificity of 89.81%. In this patient group, the sensitivity of the CRUSADE score was 36.36% and the specificity was 82.69%.

When patients who underwent PCI only were examined, there was no significant difference between the groups in terms of mean CRUSADE scores, although there was a significant difference with regard to the mean HAS-BLED scores of the groups (Table 2). In the ROC curve analysis of the patient subgroup that underwent stent implantation, the HAS-BLED score was superior in predicting in-hospital bleeding events compared to the CRUSADE score (AUC = 0.722 vs 0.520, respectively, $p = 0.002$) (Fig. 2). According to the Youden index,

Table 1. Baseline characteristics and laboratory findings of the two groups

Variables	*Bleeding* (n = *65*)	*No bleeding* (n = *340*)	p-*value*
Baseline characteristics			
Age (years), mean (SD)	65.32 ± 11.40	60.01 ± 13.57	0.003*
Gender (female), *n* (%)	36 (55.4)	157 (46.2)	0.173
Current smoker, *n* (%)	13 (20)	104 (30.6)	0.084
Hypertension, *n* (%)	32 (49.23)	149 (43.8)	0.421
Vascular disease, *n* (%)	8 (12.3)	20 (5.9)	0.061
Coronary artery disease, *n* (%)	22 (33.8)	123 (36.2)	0.720
Diabetes mellitus, *n* (%)	8 (12.3)	115 (33.8)	0.001*
Congestive heart failure, *n* (%)	6 (9.2)	18 (5.3)	0.218
Cerebrovascular disease, *n* (%)	5 (7.6)	12 (3.5)	0.177
Body mass index (kg/m^2)	28.51 ± 3.69	28.43 ± 4.24	0.882
Systolic blood pressure (mmHg)	128.30 ± 14.96	130.33 ± 19.23	0.421
Diastolic blood pressure (mmHg)	76.24 ± 12.28	77.39 ± 13.19	0.517
Heart rate (beats/min)	78.26 ± 13.79	75.26 ± 10.55	0.101
Angiographic characteristics			
Stenting	22 (33.8)	108 (31.7)	0.741
Opaque amount (cm^3)	76.53 ± 55.57	70.13 ± 53.62	0.382
Duration of angiography (min)	22.36 ± 21.51	18.21 ± 12.07	0.135
Femoral artery intervention, *n* (%)	44 (67.6)	233 (68.5)	0.894
Unfractionated heparin bolus, *n* (%)	24 (36.9)	110 (32.4)	0.473
Tirofiban bolus, *n* (%)	2 (3.1%)	12 (3.5)	0.855
Laboratory findings			
Sodium (mmol/dl; SD)	139.20 ± 2.61	138.33 ± 8.63	0.424
Potassium (mmol/dl; SD)	4.28 ± 0.36	4.47 ± 0.45	< 0.001*
Creatinine (mg/dl; SD) (mmol/l)	0.75 ± 0.24 (66.3 ± 21.22)	0.82 ± 0.23 (72.49 ± 20.33)	0.059
Urea (mg/dl; SD)	37.05 ± 10.05	34.73 ± 14.76	0.226
WBC (× 10^3/µl; SD)	7.36 ± 2.02	7.84 ± 5.09	0.454
Haemoglobin (g/dl; SD)	14.27 ± 5.39	14.11 ± 1.76	0.816
Haematocrit, *n* (%; SD)	40.61 ± 4.58	42.78 ± 4.46	< 0.001*
Platelets (×10^3/µl; SD)	258.85 ± 65.24	263.16 ± 78.07	0.686
TSH (µIU/ml)	2.48 ± 4.43	1.96 ± 3.19	0.318
International normalised ratio	1.05 ± 0.10	1.03 ± 0.11	0.174
Drugs			
Clopidogrel, *n* (%)	32 (49.2)	133 (39.1)	0.128
Oral anticoagulant *n* (%)	2 (3.1)	4 (1.2)	0.245
Acetylsalicylic acid, *n* (%)	40 (61.5)	215 (63.2)	0.795
Beta-blocker, *n* (%)	26 (40)	141 (41.5)	0.825
RAAS blockers, *n* (%)	22 (33.8)	106 (31.2)	0.671
Calcium channel blockers, *n* (%)	8 (12.3)	37 (10.9)	0.738
Diuretics, *n* (%)	10 (15.4)	27 (7.9)	0.056
Nitrate	8 (12.3)	29 (8.5)	0.333

*Independent samples *t*-test, chi-squared test, Fisher's exact test; *$p < 0.05$ statistically significant. Continuous variables are reported as mean ± SD. Categorical variables are reported as *n* (%).
WBC, white blood cells; RAAS, renin–angiotensin–aldosterone system; NSAID, non-steroidal anti-inflammatory drugs; TSH, thyroid-stimulating hormone.

Table 2. Bleeding scores

Risk scores	*Bleeding*	*No bleeding*	p-*value*
Bleeding scores of all patients who underwent coronary angiography	(*n* = 65)	(*n* = 340)	
HAS-BLED	2.21 ± 1.15	1.49 ± 0.95	< 0.001*
CRUSADE	23.69 ± 11.37	21.28 ± 10.82	0.105
HAS-BLED ≥ 3, *n* (%)	32 (49.2)	48 (14.1)	< 0.001*
CRUSADE > 30, *n* (%)	24 (36.9)	60 (18)	0.001*
CRUSADE > 40, *n* (%)	2 (3.1)	18 (5.4)	0.440
Bleeding scores of stented patients	(*n* = 22)	(*n* = 108)	
HAS-BLED	2.50 ± 1.10	1.62 ± 0.81	0.001*
CRUSADE	22.27 ± 12.31	21.62 ± 11.68	0.815
HAS-BLED ≥ 3, *n* (%)	13 (59.1)	11 (10.2)	< 0.001*
CRUSADE > 30, *n* (%)	8 (36.4)	22 (21.2)	0.128
CRUSADE > 40, *n* (%)	1 (4.5)	8 (7.5)	0.616

*Independent samples *t*-test, chi-squared test;*$p < 0.05$ statistically significant. Continues variables are reported as mean ± SD. Categorical variables are reported as *n* (%).

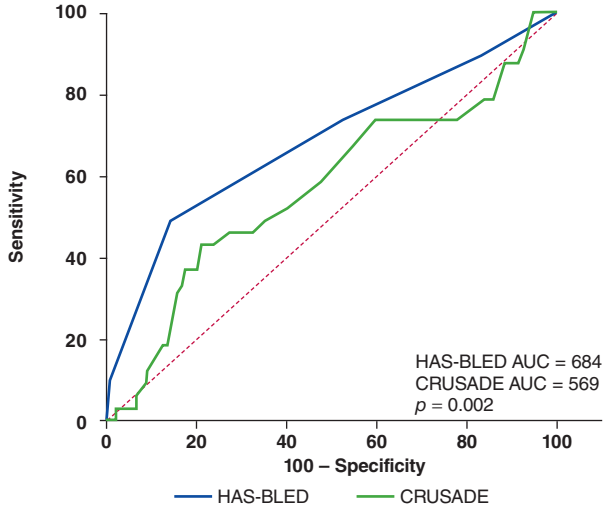

Fig. 1. Comparison of ROC curves in all patients undergoing coronary angiography.

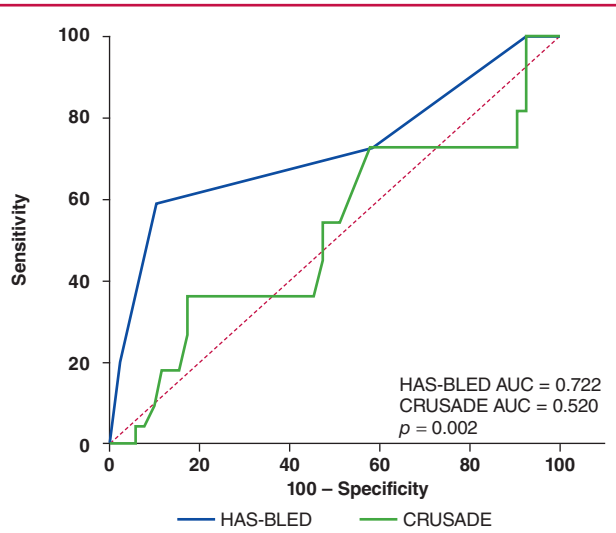

Fig. 2. Comparison of ROC curves in coronary stent implanted patients.

sensitivity of the HAS-BLED score was 59.09% and specificity was 89.81% in the subgroup with stenting.

According to the ROC curve analysis, the HAS-BLED score was found to be statistically significantly predictive of in-hospital bleeding in patients who underwent stenting due to stable coronary artery disease ($p = 0.0012$). In the same patient group, the sensitivity of the CRUSADE score was 36.36% and the specificity was 82.69%, but it was not statistically significant ($p = 0.789$).

Discussion

The main finding of this study was that patients with stable coronary artery disease undergoing elective coronary

angiography with a CRUSADE score of > 30 were under a significantly increased risk of in-hospital bleeding compared to those with a CRUSADE score ≤ 30; however the HAS-BLED score was more valuable for predicting in-hospital bleeding in these patients compared to the CRUSADE score. To the best of our knowledge, this is the first study to compare bleeding risk scores in this patient group.

One of the most important causes of co-morbidity in patients with stable coronary artery disease undergoing elective coronary angiography is haemorrhage. For this reason, avoiding bleeding is as important as treating ischaemia in the patient.[8] Since bleeding is a significant cause of morbidity and mortality in these patients, a precision risk-analysis method is needed to identify patients who are at high risk of bleeding after the invasive coronary angiography procedure.[9]

Many risk models have been used to predict this important co-morbid situation. Rao *et al*. found that bleeding complications in patients presenting with ACS increased long- and short-term mortality rates, and suggested that the GUSTO bleeding risk classification was successful in identifying short- and long-term adverse cardiac event risk among this patient population. Hence, they suggested that identifying patients with ACS with high bleeding risk and using appropriate management techniques could improve outcomes.[1] Although this study provides valuable information, it provides information only on patients presenting with ACS.

In another study, the SYNTAX score was shown to be associated with major bleeding events in patients presenting with NSTEMI who underwent PCI.[10] It is also well known that the CRUSADE score is valuable in predicting bleeding risk in NSTEMI patients.[11] However, all of these studies were performed on ACS patients. Bleeding complications are however an important problem in patients with stable coronary artery disease undergoing elective coronary angiography, as well as in ACS patients.

In this regard, Ndrepepa *et al*. included only patients with stable coronary artery disease who underwent elective PCI, and they showed that bleeding within 30 days of the procedure was associated with an increased risk of one-year mortality after PCI. These findings suggest that prevention of procedural bleeding may contribute to PCI outcomes in terms of reducing mortality rate in patients with stable coronary artery disease.[12] However, in this study, a scoring system that could predict bleeding was not used. Our study revealed the predictive value of the HAS-BLED and CRUSADE scores on the risk of in-hospital bleeding in patients with stable coronary artery disease.

Although HAS-BLED is mainly used to predict bleeding risk in AF patients,[4] some previous studies have demonstrated that it may also predict bleeding risk in patients with coronary artery disease. In a study conducted on NSTEMI patients, the HAS-BLED bleeding score was shown to be as effective as GRACE and CRUSADE, and even better than the TIMI scoring system with regard to future bleeding risk prediction.[5] In another study, the HAS-BLED score was also found to be useful in predicting in-hospital major bleeding risk in NSTEMI patients, together with the CRUSADE and ACUITY-HORIZONS scores.[6] All these studies have emphasised that the HAS-BLED score, which is as useful as other scoring systems, is more practical and easy to apply. The ease of calculating the HAS-BLED score and its ease of implementation in clinical practice further increases the importance of this bleeding risk scoring system.

The CRUSADE score has been studied several times to predict bleeding risk in patients with coronary artery disease, especially in NSTEMI patients. In other studies, the CRUSADE score has been shown to be effective in predicting major bleeding in patients undergoing PCI,[13,14] and was shown to be even more valuable than the platelet reactivity test in PCI patients.[15] It can be used to predict mortality risk, similar to the GRACE risk score in ACS patients,[16] and to predict bleeding risk in STEMI patients.[17] The prognostic accuracy of the CRUSADE score can be used to predict major or moderate bleeding events even in non-invasively treated ACS patients.[18] It is interesting that such an impressive scoring system did not give as good predictive results as the HAS-BLED scoring system in our patient group.

Costa *et al*. showed that the CRUSADE risk score predicted major bleeding events better than the HAS-BLED score in their study.[19] However their study differed from ours in that it involved only patients receiving dual antiplatelet therapy after stenting and included only major bleeding events. Similar negative results for the CRUSADE risk score have also been found in some previous studies. In a study conducted in octogenarians, it was reported that the CRUSADE score was insufficient to predict the risk of bleeding in NSTEMI patients and that new scoring systems were needed.[20] In a study by Correia *et al*., it was reported that the ACUITY scoring system was a better predictor of major bleeding in patients admitted to hospital with ACS compared to the CRUSADE score.[21]

These conflicting results suggest that we do not have an ideal scoring system to use on all patients and that new developments are needed in this regard. For this reason, in our study we examined patients with stable coronary artery disease who underwent elective coronary angiography, since there is little data on them and they were often overlooked in previous studies. We included all patients with stable coronary artery disease with or without stent implantation, and examined the HAS-BLED and CRUSADE scores, which were not previously studied in this group.

We have shown that the HAS-BLED score was more predictive in these patients, even though the results of the CRUSADE score were reasonable, and that HAS-BLED may help us to predict bleeding events and reduce co-morbidity in these patients. The ease of calculating the HAS-BLED score and its ease of implementation in clinical practice further increases the importance of this bleeding risk-scoring system. The present study provides valuable data because this group of patients is frequently encountered in the angiography laboratory in daily cardiology practice and there is no scoring system as yet to predict bleeding risk among these patients.

This study has some limitations, such as it was a single-centre study with a small sample size and did not include long-term results. Another limitation is that the femoral artery was preferred to the radial artery for coronary angiography.

Conclusion

Various scoring systems are used in the prediction of bleeding risk in patients undergoing angiography due to ACS. However, in stable angina patients without ACS, there is not enough data on this subject. This study showed that the HAS-BLED and

CRUDASE scores were useful in stable coronary artery disease patients who underwent elective coronary angiography. However, in these patients without ACS, we found that it would be more appropriate to use the HAS-BLED scoring, which is more practical, easy to calculate, easy to implement in clinical practice and more predictive for in-hospital bleeding. Although this study introduces a new approach, there is a need for larger studies to make a definite decision in this regard.

References

1. Rao SV, O'Grady K, Pieper KS, *et al*. Impact of bleeding severity on clinical outcomes among patients with acute coronary syndromes. *Am J Cardiol* 2005; **96**: 1200–1206.
2. Mauri L, Kereiakes DJ, Yeh RW, *et al*. Twelve or 30 months of dual antiplatelet therapy after drug-eluting stents. *N Engl J Med* 2014; **371**: 2155–2166.
3. Braunwald E, Antman EM, Beasley JW, *et al.* ACC/AHA 2002 guideline update for the management of patients with unstable angina and non-ST-segment elevation myocardial infarction: a report of the American College of Cardiology/American Heart Association Task Force on Practice Guidelines (Committee on Management of Patients with Unstable Angina). 2002. Available at http://www.acc.org/clinical/guidelines/unstable/unstable.pdf. Accessed Aug 19, 2007.
4. Zhu W, He W, Guo L, *et al*. The HAS-BLED score for predicting major bleeding risk in anticoagulated patients with atrial fibrillation: a systematic review and meta-analysis. *Clin Cardiol* 2015; **38**(9): 555–561.
5. Hsieh MJ, Lee CH, Chen CC, *et al*. Predictive performance of HAS-BLED risk score for long-term survival in patients with non-ST elevated myocardial infarction without atrial fibrillation. *J Cardiol* 2017; **69**(1): 136–143.
6. Hsieh MJ, Wang CC, Chen CC, *et al*. HAS-BLED score predicts risk of in-hospital major bleeding in patients with acute non-ST segment elevation myocardial infarction. *Thromb Res* 2015; **136**(4): 775–780.
7. Konishi H, Miyauchi K, Tsuboi S, *et al*. Impact of the HAS-BLED score on long-term outcomes after percutaneous coronary intervention. *Am J Cardiol* 2015; **116**(4): 527–531.
8. Vries MJ, van der Meijden PE, Henskens YM, *et al*. Assessment of bleeding risk in patients with coronary artery disease on dual antiplatelet therapy. A systematic review. *Thromb Haemost* 2016; **115**(1): 7–24.
9. Mehran R, Pocock S, Nikolsky E, *et al*. Impact of bleeding on mortality after percutaneous coronary intervention results from a patient-level pooled analysis of the REPLACE-2 (randomized evaluation of PCI linking angiomax to reduced clinical events), ACUITY (acute catheterisation and urgent intervention triage strategy), and HORIZONS-AMI (harmonizing outcomes with revascularisation and stents in acute myocardial infarction) trials. *J Am Coll Cardiol Cardiovasc Interv* 2011; **4**: 654–664.
10. Madhavan MV, Généreux P, Palmerini T. The association between the extent of coronary artery disease and major bleeding events after percutaneous coronary intervention: from the ACUITY trial. *J Invasive Cardiol* 2015; **27**(4): 203–211.
11. Abu-Assi E, Gracía-Acuña JM, Ferreira-González I, *et al*. Evaluating the performance of the Can Rapid Risk Stratification of Unstable Angina Patients Suppress Adverse Outcomes With Early Implementation of the ACC/AHA Guidelines (CRUSADE) bleeding score in a contemporary Spanish cohort of patients with non-ST-segment elevation acute myocardial infarction. *Circulation* 2010; **121**(22): 2419–2426.
12. Ndrepepa G, Stephan T, Fiedler KA, *et al*. Procedure-related bleeding in elective percutaneous coronary interventions. *Eur J Clin Invest* 2015; **45**(3): 263–273.
13. Jarrah M, Hammoudeh A, Okkeh O, *et al*. Major bleeding events in Jordanian patients undergoing percutaneous coronary intervention (PCI): Incidence, associated factors, impact on prognosis, and predictability of the CRUSADE bleeding risk score. Results from the first Jordanian PCR (PCR1). *Anatol J Cardiol* 2017; **17**(6): 445–451.
14. Liu R, Lyu SZ, Zhao GQ, *et al.* Comparison of the performance of the CRUSADE, ACUITY-HORIZONS, and ACTION bleeding scores in ACS patients undergoing PCI: insights from a cohort of 4939 patients in China. *J Geriatr Cardiol* 2017; **14**(2): 93–99.
15. Bang J, Choi SY, Kim MH, *et al*. CRUSADE score is superior to platelet function testing for prediction of bleeding in patients following coronary interventions. *EBioMedicine* 2017; **21**: 213–217.
16. Cordero A, Rodriguez-Manero M, García-Acuña JM. Additive value of the CRUSADE score to the GRACE score for mortality risk prediction in patients with acute coronary syndromes. *Int J Cardiol* 2017; **245**: 1–5.
17. Ariza-Solé A, Sánchez-Elvira G, Sánchez-Salado JC, *et al*. CRUSADE bleeding risk score validation for ST-segment-elevation myocardial infarction undergoing primary percutaneous coronary intervention. *Thromb Res* 2013; **132**(6): 652–658.
18. Kharchenko MS, Erlikh AD, Gratsianskiĭ NA. Assessment of the prognostic value of the CRUSADE score in patients with acute coronary syndromes hospitalized in a noninvasive hospital. *Kardiologiia* 2012; **52**(8): 27–32.
19. Costa F, Tijssen JG, Ariotti S, *et al*. Incremental value of the CRUSADE, ACUITY, and HAS-BLED risk scores for the prediction of hemorrhagic events after coronary stent implantation in patients undergoing long or short duration of dual antiplatelet therapy. *J Am Heart Assoc* 2015; **4**(12).
20. Faustino A, Mota P, Silva J, *et al*. Non-ST-elevation acute coronary syndromes in octogenarians: applicability of the GRACE and CRUSADE scores. *Rev Port Cardiol* 2014; **33**(10): 617–627.
21. Correia LC, Ferreira F, Kalil F, *et al*. Comparison of ACUITY and CRUSADE scores in predicting major bleeding during acute coronary syndrome. *Arq Bras Cardiol* 2015; **105**(1): 20–27.

Atherosclerotic plaque in HIV-positive patients presenting with acute coronary syndromes

Ahmed Vachiat, Keir McCutcheon, Nqoba Tsabedze, Don Zachariah, Pravin Manga

Abstract

Aim: This study aimed to characterise the atherosclerotic plaque and plaque burden in HIV-positive patients presenting with acute coronary syndromes (ACS), using intravascular ultrasound (IVUS) and virtual histology (VH).

Methods: This was a prospective study of 20 HIV-positive patients who presented with ACS. IVUS and VH were used to assess plaque burden and plaque characteristics in the culprit and non-culprit coronary arteries.

Results: HIV-positive patients with ACS had a mean age of 51.1 ± 8.1 years. There were 13 (65%) male patients. ST-segment elevation myocardial infarction was the most common presentation of ACS (75%) with the left anterior descending artery being the most common culprit artery (60%). In 60% of patients, the total plaque burden was of moderate degree (40–70% stenosis) while it was of mild degree (< 40% stenosis) in 35%, and in 5% of patients it was severe (> 70% stenosis). A severe degree of total plaque burden was more commonly found in the culprit vessel (30%) than in the non-culprit vessels (5%). Furthermore, the plaque burden was found to be located predominantly in the proximal portion of the coronary arteries. The predominant plaque morphology consisted of fibrous plaque (55.4%) and fibro-fatty plaque (26.6%), while necrotic core was present in 13.3%. Dense calcium was present in only 4.7% of the cohort.

Conclusions: IVUS and VH demonstrated a high burden of atherosclerosis in the left anterior descending artery and proximal vasculature of HIV-positive patients. The atherosclerotic plaque predominantly comprised non-calcified fibrous and fibro-fatty plaque.

Keywords: atherosclerosis, HIV, acute coronary syndromes, intravascular ultrasound, virtual histology

Submitted 2/11/18, accepted 15/3/19
Published online 4/6/19
Cardiovasc J Afr 2019; **30**: 203–207 www.cvja.co.za

DOI: 10.5830/CVJA-2019-016

Division of Cardiology, Department of Internal Medicine, Faculty of Health Sciences, University of the Witwatersrand, Johannesburg, South Africa
Ahmed Vachiat, MB BCh, FCP (SA), MMed, Cert Cardiology (SA), PhD, drvachiat@joburgheart.co.za
Keir McCutcheon, MB BCh, MSc, FCP (SA), Cert Cardiology (SA), PhD
Nqoba Tsabedze, MB BCh, FCP (SA), MMed, Cert Cardiology (SA)
Don Zachariah, MB BCh, FCP (SA), MMed, Cert Cardiology (SA)
Pravin Manga, MB BCh, FCP (SA), PhD

Department of Cardiovascular Medicine, University Hospitals Leuven, Belgium
Keir McCutcheon, MB BCh, MSc, FCP (SA), Cert Cardiology (SA), PhD

There are approximately 37 million people living with human immunodeficiency virus (HIV) infection worldwide, 70% of whom live in sub-Saharan Africa.[1,2] Studies suggest that HIV infection confers an overall 1.5- to 2.0-fold increased risk of developing ischaemic heart disease (IHD).[3-6] Combination antiretroviral therapies (cART), particularly protease inhibitors and high levels of traditional cardiovascular disease risk factors have increased the prevalence of IHD in this population.[7,8]

Based upon spectral analysis of ultrasound backscatter, intravascular ultrasound (IVUS) facilitates the characterisation of coronary plaque morphology by transforming the coronary vascular ultrasound images into a colour-coded representation, thereby creating a virtual histological (VH) assessment of the plaque. Virtual histological intravascular ultrasound (VH-IVUS) imaging uses four colour-coded spectral parameters (dark green, yellow-green, red and white) representing fibrous and fibro-fatty lesions, necrotic core and calcium, respectively.[9] This spectral analysis of coronary plaque has been well correlated with histopathology, with a predicative accuracy of 87.1, 87.1, 88.3 and 96.5% for fibrous, fibro-fatty, necrotic core and dense calcium, respectively.[10]

The characteristics of the atherosclerotic plaque in HIV-negative patients with IHD are well defined. In a study of HIV-negative patients with stable angina or troponin-positive acute coronary syndrome (ACS), VH-IVUS of non-culprit lesions has shown that fibrous and fibro-fatty plaque was present in 43.7% of patients, and calcific plaque was present in the remaining 56.3% of patients.[11]

On the other hand, coronary plaque characteristics in HIV-positive patients have not been well studied and are poorly elucidated. Autopsy studies in HIV-positive patients have described coronary lesions as eccentric atherosclerotic plaques with 80 to 90% reduction of the vascular lumen, and histopathological findings as hyperplastic endothelial cells lining a thickened intima, characterised by the proliferation of smooth muscle cells and monocyte macrophages.[12,13] Using coronary computed tomography, asymptomatic HIV-positive patients have been found to have a higher prevalence of coronary atherosclerosis, a greater degree of coronary plaque volume and a greater number of coronary segments with plaque compared to HIV-negative patients with a similar Framingham 10-year risk for myocardial infarction.[14]

To date there are no published data describing plaque characteristics and plaque burden by direct visualisation using IVUS in HIV-positive patients with ACS. The primary objective of this study was to characterise the atherosclerotic plaque and plaque burden in HIV-positive patients presenting with ACS using IVUS and VH.

Methods

The study was a cross-sectional, prospective study of HIV-positive patients with ACS conducted at a large urban public hospital

in Johannesburg, South Africa, over three years (July 2012 to July 2015). All HIV-positive patients with ACS at the time of admission were included in the study. Exclusion criteria included patients less than 18 years and those with previous ACS or known atherosclerotic vascular disease. Approval for conducting of the study was obtained from the local institutional review board (ethics clearance number M111143).

All patients underwent coronary angiography performed via the femoral route. Following left ventriculography, a 7F guiding catheter was engaged in the culprit vessel. A coronary (balanced middle-weight) guide-wire was introduced through the guiding catheter and tracked into the distal portion of the coronary vessel. IVUS imaging was initially performed in the culprit vessel prior to coronary intervention. Culprit lesions were defined by electrocardiographic criteria such as ST-segment shift or T-wave inversion and angiographic appearances such as filling defects consistent with thrombus, plaque irregularity suggestive of ulceration or point of maximal stenosis.

In patients who had complete vessel occlusion, flow was first restored and then IVUS imaging was performed. The non-culprit vessels were then assessed using IVUS. Fractional flow reserve (Volcano Corporation, Rancho, California) assessment was used for intermediate lesions.

A 20-Mhz Eagle Eye (Volcano Corporation, Rancho, California) IVUS catheter with a motorised pull-back device at 0.5 mm/s from the distal safe position to the guide catheter was used to acquire IVUS images. Data were captured and analysed offline using the image analysis software version 3.1 (Volcano Corporation). This was done independently by an experienced reader (JD), blinded to the clinical data.

Each artery was divided into proximal, mid and distal segments. The plaque burden was classified into mild disease (< 40% plaque), moderate (40–70% plaque) and severe disease (> 70% plaque). Atherosclerotic plaque characteristics as well as the total plaque burden in both the culprit and non-culprit arteries were measured. The plaque burden in each of the three coronary arteries was measured using the difference between the vessel area and the minimum lumen area. The software of the IVUS system automatically analysed the coronary vessel area and narrowest lumen area. Plaque characterisation in our patient cohort was performed using VH assessment of the IVUS images in all three major coronary arteries.

Statistical analysis

Results are presented, using descriptive statistics, as mean ± standard deviation, median ± interquartile range (IQR) or percentages, as appropriate. Mean total plaque burden at different locations was compared using the paired *t*-test. Data analysis was carried out using SAS version 9.4 for Windows. A 5% significance level was used.

Results

The mean age of the study population was 51.1 ± 8.1 years. Thirteen (65%) patients were male and 17 (85%) were black. None of the patients had known prior cardiac history. The median CD4 count of our study group was 301 cells/mm^3 (IQR 205–417). At the time of admission half of the patient cohort was on cART. The average use of cART in these patients was 24 months (IQR 5–51 months). None of the patients was on protease inhibitors. Seven (35%) patients in this group were newly diagnosed with HIV at the time of presentation with ACS.

Fifteen (75%) patients presented with STEMI (eight anterior and seven inferior MIs), three (15%) with non-STEMI and two (10%) patients presented with unstable angina. Only three (21%) of the 15 STEMI patients received thrombolysis within six hours of presentation. No patient had a known prior ACS event.

Risk factors for IHD included smoking in 11 (55%), hypertension in six (30%), diabetes in two (10%), dyslipidaemia in two (10%), and one (5%) patient had a family history of early IHD. The average body mass index was 24.4 ± 5.5 kg/m^2 with a mean waist circumference of 83.0 ± 9.6 cm (Table 1).

A typical presentation in our cohort was of a young patient with STEMI involving the left anterior descending artery, which was the most common artery involved (60%), followed by the right coronary artery (35%) and the left circumflex artery (20%). Fractional flow reserve assessment was used in only three patients to assess significance of the proximal left anterior descending coronary artery lesions and these were all found to be non-significant. Six second-generation drug-eluting stents were implanted, with an average length of 22 mm (18–26 mm).

A high thrombus burden, visualised angiographically, was present in eight patients (40%) and one patient was given an intracoronary thrombolytic, which resulted in improved perfusion. Four patients had complete occlusion of the infarct-related artery.

There were no peri-procedural complications following percutaneous coronary intervention. No patients required coronary artery bypass grafting. At six months' follow up, one patient had in-stent restenosis and another died due to sudden cardiac death at home, two weeks after intervention.

In 60% of our patients, the total plaque burden in the

Table 1. Baseline characteristics of the HIV-positive patients presenting with acute coronary syndrome

Variables	*HIV-positive patients with ACS (n = 20)*
Age	51.1 ± 8.1
Race (black), *n* (%)	17 (75)
Male, *n* (%)	13 (65)
Risk factors, *n* (%)	
Smoking	11 (55)
Hypertension	6 (30)
Diabetes	2 (10)
Dyslipidaemia	2 (10)
Family history	1 (5)
Laboratory analysis	
Haemoglobin (g/dl)	12.9
Creatinine (mg/dl)	0.84
(mmol/l)	(74.26)
Total cholesterol (mg/dl)	158.3
(mmol/l)	(4.10)
Triglycerides (mg/dl)	46.3
(mmol/l)	(0.52)
HDL-C (mg/dl)	38.6
(mmol/l)	(1.00)
LDL-C (mg/dl)	92.7
(mmol/l)	(2.40)
CD4 (cells/mm^3)	313

HDL-C: high-density lipoprotein cholesterol, LDL-C: low-density lipoprotein cholesterol.

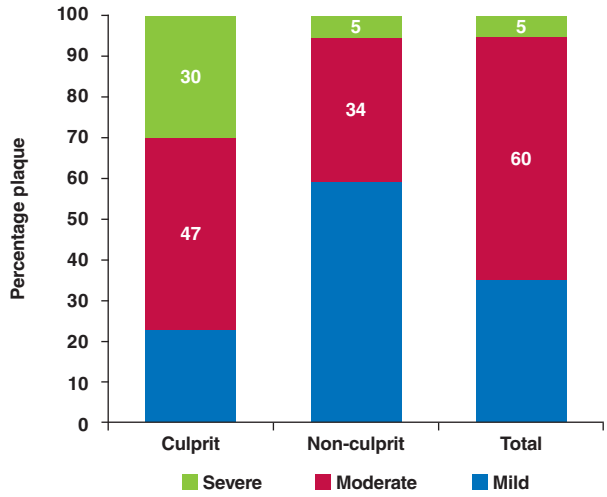

Fig. 1. Plaque burden in HIV-positive patients with acute coronary syndrome.

coronary vasculature was of moderate degree, while in 35% the total plaque burden was mild, and in a minority (5%) it was severe (Fig. 1). The atherosclerotic disease was significantly higher in the proximal coronary vasculature compared to the mid and distal segments of the coronary arteries ($p = 0.010$). Furthermore, it was significantly higher in the mid segments than in the distal segments of the coronary arteries ($p = 0.0006$). There was more severe plaque burden (30%) in the culprit vessel compared to non-culprit vessels (5%).

Assessment of the entire coronary vasculature by VH in these patients demonstrated that the predominant plaque morphology consisted of fibrous plaque (55.4%). Fibro-fatty plaque was found in 26.6% of patients, necrotic core was present in 13.3%, and dense calcium was present in only 4.7% of patients (Fig. 2). There were significant differences between the mean volumes of fibrous plaque, fibro-fatty plaque, necrotic core and dense calcium (all $p < 0.05$).

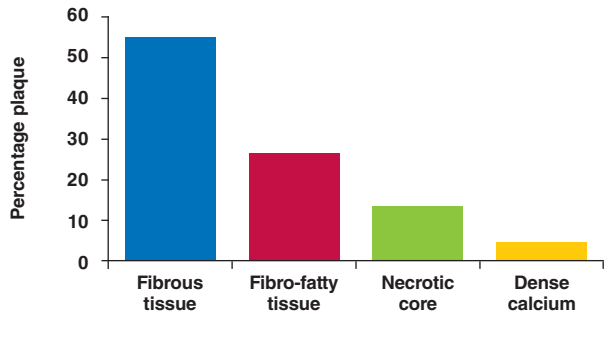

Fig. 2. Virtual histology in HIV-positive patients with acute coronary syndrome. The mean fibrous plaque volume was significantly greater than the mean fibro-fatty plaque volume, which was significantly greater than the mean necrotic core volume. This in turn was significantly greater than the mean dense calcium volume (all $p < 0.05$).

On assessing plaque morphology in the culprit coronary arteries, the major plaque morphology remained fibrous plaque (56.5%), while fibro-fatty tissue (21.2%), necrotic core (14.4%) and dense calcium (3.6%) plaque constituted the remainder (Fig. 2). In non-culprit arteries, the lesion morphology was similar, with fibrous plaque found in 55.1% of patients, fibro-fatty plaque in 29.5%, necrotic core in 8.2% and dense calcium in 4.8% of patients.

Discussion

This was a prospective study using VH-IVUS to characterise the coronary plaque morphology in HIV-positive patients presenting with ACS. First, we demonstrated that some form of atherosclerosis was present in all HIV-positive patients presenting with ACS without any prior cardiac history. Even normal vessels on angiography were found to have atherosclerosis, and in 5% of these vessels, the plaque burden was surprisingly severe. Our findings help explain the discrepancy of lower plaque volumes that have been reported in HIV-positive patients studied angiographically, as coronary angiograms are not accurate in defining minor plaque volumes.[15]

Second, our study has shown that the predominant plaque morphology in the coronary arteries of HIV-positive patients presenting with ACS consisted of fibrous tissue in just over half of all patients and fibro-fatty tissue in a further quarter of patients. Necrotic core lesions were uncommon and dense calcified lesions were rare. Hence the plaque morphology in HIV-positive patients can be described as predominantly non-calcified fibrous and fibro-fatty disease (Fig. 3).

Our findings are supported by non-invasive imaging such as coronary computer tomography angiography (CCTA), which has shown an increased prevalence of subclinical atherosclerosis in HIV-positive compared with HIV-negative patients.[16,17] A recent meta-analysis of 1 229 asymptomatic HIV-positive patients on cART demonstrated a three-fold higher prevalence

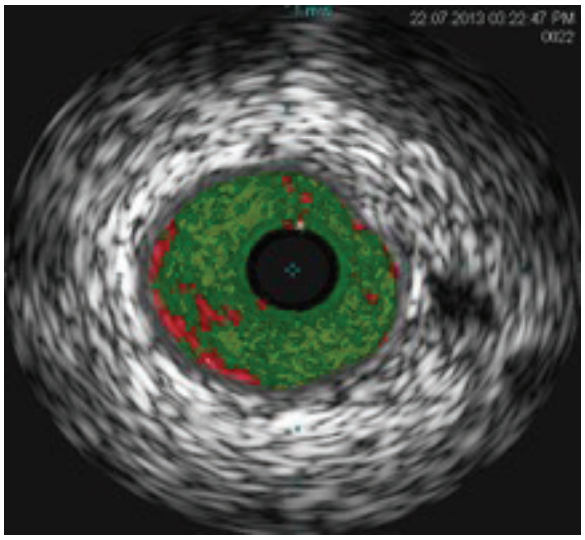

Fig. 3. Virtual histology intravascular ultrasound of non-calcified fibrous and fibro-fatty plaque from HIV-positive patients with acute coronary syndrome.

of non-calcific coronary artery plaques on CCTA, compared with HIV-negative controls.[16] HIV-infected women also showed a significantly higher percentage of non-calcified plaque on CCTA compared to HIV-negative women.[18]

Using dual-source CCTA, features of non-calcified plaque have also been found in early atherosclerosis of healthy HIV-negative populations with a family history of early onset of coronary artery disease.[19] Therefore, the plaque morphology of atherosclerosis in HIV-positive populations, as found in our study, was very similar to that found in early atherosclerosis in HIV-negative populations. Our findings suggest that the difference in atherosclerotic plaque characteristics of HIV-positive compared to HIV-negative populations is that the atherosclerosis was more extensive in HIV-positive patients and with less calcification. The reasons for these differences are unclear but are probably related to the link between HIV infection and atherosclerosis, independent of traditional cardiovascular risk factors.

Data from the Strategies for Management of Antiretroviral Therapy (SMART) study suggest that immune, inflammatory and viral factors contribute to higher prevalence of coronary artery disease in HIV-positive patients.[20] Undetectable viral loads do not equate to amelioration of ongoing inflammation and while inflammation and immune activation are diminished with cART, they are not abolished. HIV infection, even in the presence of cART, not only initiates endothelial dysfunction and immune cell activation but activates a number of cellular pathways.[21]

As HIV predominantly infects T cells and macrophages, there is induction of oxidative and endoplasmic reticulum stress, dysregulation of autophagy and inflammasome formation, all of which may contribute to HIV-associated atherosclerosis.[21] In addition, HIV-positive patients presenting with ACS have been found to have a 'thrombo-inflammatory' state caused by heightened platelet function, hypercoagulability and inflammation.[22] Mechanisms that promote thrombosis such as increased levels of soluble p-selectin, CD-40L and microparticles have been demonstrated in HIV-positive patients with ACS.[22] This inflammatory and thrombotic milieu may well be involved in the pathogenesis of the 'athero-thrombotic plaque', as was found in 40% of our patients.

Disease severity may also contribute to atherosclerosis. An association between reduced CD4 cell count and non-calcified coronary artery plaque as well as the presence of coronary stenosis greater than 50% in HIV-positive compared to HIV-negative patients have been reported.[16,23] The average CD4 count in our cohort was low (301 cells/mm^3), despite 50% being on cART at the time of presentation with ACS.

Higher rates of ACS in the general population have been reported in a number of studies to be associated with fibrous and fibro-fatty plaque, compared to mixed or calcified plaques.[14,16,23] Non-calcified plaques, as found in our cohort, represent an earlier stage of atherosclerosis and are more prone to rupture, leading to ACS.[24] Furthermore, HIV-positive patients have a larger burden of coronary atherosclerosis, particularly non-calcified plaque, compared to HIV-negative patients with similar cardiovascular risk factors.[14] Therefore the presence of more extensive non-calcific fibrous and fibro-fatty plaque and its vulnerability to rupture could explain the higher prevalence and earlier onset of ACS in HIV-positive compared with HIV-negative patients.

IHD in HIV-positive patients most commonly manifests with an acute episode of ACS. Studies to date suggest distinct demographic characteristics of ACS presentation in HIV-positive patients.[25-28] The mean age at presentation of ACS in HIV-positive patients is a decade younger (mean age 50 years) than the general population, with patients more likely to be male, current smokers and to have lower high-density lipoprotein cholesterol levels. This is similar to our cohort where the mean age was 51.1 ± 8.1 years, the majority being male (65%) and more than half (55%) current smokers.

It is also recognised that ACS in HIV-positive patients presents with different risk-factor profiles in developing compared to developed regions.[25] Traditional risk factors such as hypertension, diabetes and dyslipidaemia are more common in developed regions, whereas in the developing regions, smoking is the predominant risk factor.[25,29] Similarly, in our study few patients had hypertension, diabetes, dyslipidaemia or a family history of IHD but there was a high prevalence of smoking (55%).

The most common modes of presentation of ACS in our cohort were STEMI, a low TIMI score (TIMI 2) and single-vessel disease angiographically. These findings are consistent with other studies in HIV-positive patients.[26-28] In some regions, HIV-positive patients with ACS may present without classic atheromatous plaques but with a large burden of thrombus in the infarct-related artery.[25] In our cohort, a high thrombotic burden was present in 40% of ACS patients. Of interest is that the profile of ACS in developed countries is changing. In a recent study from six United States centres, half (50.4%) of all HIV-positive patients presenting with an ACS had type 2 MI, which occurs in the setting of supply-and-demand mismatch.[30]

In many studies, including the current study, only half of HIV-positive patients presenting with ACS were on cART. However, the expectation is that in future, many more patients will be on cART based on the findings of the SMART study, which found that patients who deferred or interrupted cART had a 70% increased hazard of cardiovascular disease events.[20] The widespread adoption of cART will hopefully translate not only to better long-term outcomes but also lead to substantially fewer cardiac events.

Limitations

This was a single-centre study with a small sample size. There was no case–control group of HIV-negative patients who had IVUS and VH imaging. There were clinical limitations, for example, repeat coronary angiography was not performed on all patients to determine in-stent restenosis. However, the focus of this study was not on long-term outcomes but coronary artery plaque characteristics at ACS presentation.

Conclusion

HIV-positive patients presented at a young age, with STEMI being the most common mode of presentation. In these patients, atherosclerosis, as determined by VH-IVUS, was extensive. The left anterior coronary artery had the largest burden of disease and this disease burden was predominantly located in the proximal coronary arteries. Imaging using VH-IVUS demonstrated that atherosclerosis in young HIV-positive patients

comprised predominantly non-calcified fibrous and fibro-fatty plaque.

We acknowledge Dr Petra Gaylard of Data Management and Statistical Analysis, Johannesburg, South Africa; statistical analysis by Wits Donald Gordon Medical Centre, University of the Witwatersrand; and Ms Jacqui de Souza (JD), Philips Volcano. This publication was made possible in part by a grant from the Carnegie Corporation of New York. Dr Ahmed Vachiat was supported by a Research Grant from the Carnegie Foundation. The statements made and views expressed are, however, solely the responsibility of the authors.

References

1. World Health Organization. 10 facts on HIV/AIDS. Available at: http://www.who.int/features/factfiles/hiv/facts/en/. Accessed 16 August 2017.
2. UNAIDS. HIV and AIDS estimates (2015). Available at: http://www.unaids.org/en/regionscountries/countries/southafrica.Accessed 20 September 2017.
3. Grinspoon SK, Grunfeld C, Kotler DP, *et al*. State of the science conference: Initiative to decrease cardiovascular risk and increase quality of care for patients living with HIV/AIDS: executive summary. *Circulation* 2008; **118**: 198–210.
4. Currier JS, Taylor A, Boyd F, *et al*. Coronary heart disease in HIV-infected individuals. *J Acquir Immune Defic Syndr* 2003; **33**: 506–512.
5. Klein DB, Leyden WA, Xu L, *et al*. Declining relative risk for myocardial infarction among HIV-positive compared with HIV-negative individuals with access to care. *Clin Infect Dis* 2015; **60**: 1278–1280.
6. Triant VA, Lee H, Hadigan C, *et al*. Increased acute myocardial infarction rates and cardiovascular risk factors among patients with human immunodeficiency virus disease. *J Clin Endocrin Metab* 2007; **92**: 2506–2512.
7. Lang S, Boccara F, Mary-Krause M, *et al.* Epidemiology of coronary heart disease in HIV-infected versus uninfected individuals in developed countries. *Arch Cardiovasc Dis* 2015; **108**: 206–215.
8. Vachiat A, McCutcheon K, Tsabedze N, *et al*. HIV and ischemic heart disease. *J Am Coll Cardiol* 2017; **69**: 73–82.
9. Nair A, Kuban BD, Tuzcu EM, *et al*. Coronary plaque classification with intravascular ultrasound radiofrequency data analysis. *Circulation* 2002; **106**: 2200–2206.
10. Nasu K, Tsuchikane E, Katoh O, *et al*. Accuracy of *in vivo* coronary plaque morphology assessment: a validation study of *in vivo* virtual histology compared with *in vitro* histopathology. *J Am Coll Cardiol* 2006; **47**: 2405–2412.
11. Calvert PA, Obaid DR, O'Sullivan M, *et al*. Association between IVUS findings and adverse outcomes in patients with coronary artery disease: the VIVA (VH-IVUS in Vulnerable Atherosclerosis) Study. *J Am Coll Cardiol Cardiovasc Imaging* 2011; **4**: 894–901.
12. Tabib A, Leroux C, Mornex JF, *et al.* Accelerated coronary atherosclerosis and arteriosclerosis in young human-immunodeficiency-virus-positive patients. *Coron Artery Dis* 2000; **11**: 41–46.
13. Paton P, Tabib A, Loire R, *et al*. Coronary artery lesions and human immunodeficiency virus infection. *Res Virol* 1993; **144**: 225–231.
14. Lo J, Abbara S, Shturman L, *et al*. Increased prevalence of subclinical coronary atherosclerosis detected by coronary computed tomography angiography in HIV-infected men. *AIDS* 2010; **24**: 243–253.
15. O'Dwyer EJ, Bhamra-Ariza P, Rao S, *et al*. Lower coronary plaque burden in patients with HIV presenting with acute coronary syndrome. *Open Heart* 2016; **3**: e000511.
16. D'Ascenzo F, Cerrato E, Calcagno A, *et al*. High prevalence at computed coronary tomography of non-calcified plaques in asymptomatic HIV patients treated with HAART: a meta-analysis. *Atherosclerosis* 2015; **240**: 197–204.
17. Stein JH, Currier JS, Hsue PY. Arterial disease in patients with human immunodeficiency virus infection: what has imaging taught us? *J Am Coll Cardiol Cardiovasc Imaging* 2014; **7**: 515–525.
18. Fitch KV, Srinivasa S, Abbara S, *et al*. Noncalcified coronary atherosclerotic plaque and immune activation in HIV-infected women. *J Infect Dis* 2013; **208**: 1737–1746.
19. Kral BG, Becker LC, Vaidya D, *et al*. Noncalcified coronary plaque volumes in healthy people with a family history of early onset coronary artery disease. *Circ Cardiovasc Imaging* 2014; **7**: 446–453.
20. El-Sadr WM, Lundgren J, Neaton JD, *et al*. Strategies for Management of Antiretroviral Therapy (SMART) study group. CD4$^+$ count-guided interruption of antiretroviral treatment. *N Engl J Med* 2006; **355**: 2283–2296.
21. Kearns A, Gordon J, Burdo TH, *et al*. HIV-1-associated atherosclerosis: unraveling the missing link. *J Am Coll Cardiol* 2017; **69**: 3084–3098.
22. Hauguel-Moreau M, Boccara F, Boyd A, *et al*. Platelet reactivity in human immunodeficiency virus infected patients on dual antiplatelet therapy for an acute coronary syndrome: the EVERE2ST-HIV study. *Eur Heart J* 2017; **38**: 1676–1686.
23. Post WS, Budoff M, Kingsley L, *et al*. Associations between HIV infection and subclinical coronary atherosclerosis. *Ann Intern Med* 2014; **160**: 458–467.
24. Ahmadi N, Nabavi V, Hajsadeghi F, *et al*. Mortality incidence of patients with non-obstructive coronary artery disease diagnosed by computed tomography angiography. *Am J Cardiol* 2011; **107**: 10–16.
25. Becker AC, Sliwa K, Stewart S, *et al*. Acute coronary syndromes in treatment-naive black South africans with human immunodeficiency virus infection. *J Interv Cardiol* 2010; **23**: 70–77.
26. Ambrose JA, Gould RB, Kurian DC, *et al*. Frequency of and outcome of acute coronary syndromes in patients with human immunodeficiency virus infection. *Am J Cardiol* 2003; **92**: 301–303.
27. Hsue PY, Giri K, Erickson S, *et al*. Clinical features of acute coronary syndromes in patients with human immunodeficiency virus infection. *Circulation* 2004; **109**: 316–319.
28. Boccara F, Mary-Krause M, Teiger E, *et al*. Acute coronary syndrome in human immunodeficiency virus-infected patients: characteristics and 1 year prognosis. *Eur Heart J* 2011; **32**: 41–50.
29. Freiberg MS, Chang CC, Kuller LH, *et al*. HIV infection and the risk of acute myocardial infarction. *J Am Med Assoc Intern Med* 2013; **173**: 614–622.
30. Crane HM, Paramsothy P, Drozd DR, *et al*. Types of myocardial infarction among human immunodeficiency virus-infected individuals in the United States. *J Am Med Assoc Cardiol* 2017; **2**: 260–267.

Natural cocoa inhibits maternal hypercholesterolaemia-induced atherogenesis in rabbit pups

Richard Michael Blay, Saviour Kweku Adjenti, Kevin Kofi Adutwum-Ofosu, Bismarck Afedo Hottor, John Ahenkorah, Benjamin Arko-Boham, Frederick Kwaku Addai

Abstract

Atherosclerosis begins during foetal development and is enhanced by maternal hypercholesterolaemia during pregnancy. This study assessed the effect of natural cocoa on atherosclerosis in offspring conceived in maternal hypercholesterolaemia. Female rabbits were fed a cholesterol-enriched diet for two weeks and hypercholesterolaemia was confirmed, after which they were crossed with normocholesterolaemic males. One group of hypercholesterolaemic mothers (HCC) received natural cocoa powder (NCP) in their drinking water, whereas the other group (HC) received only water. Histological analysis of three segments of the aorta (arch, thoracic and abdominal) from offspring of both groups was compared with a control group (NC). Intima–media thickness of the aortic arch in offspring born to hypercholesterolaemic rabbits (HC: 146 µm) was higher compared to HCC (99 µm) and control rabbits (58.5 µm). All the sections from the aortic arch of the HC group had atherosclerotic lesions while none of the sections of the aortic arch from the NC and HCC groups had lesions present. Inferentially, regular and voluntary consumption of NCP during pregnancy may inhibit aortic atherogenesis in offspring of hypercholesterolaemic mothers.

Keywords: atherosclerosis, maternal hypercholesterolaemia, intima–media thickness, cocoa, antioxidants, foetal

Submitted 22/9/18, accepted 16/4/19
Published online 24/5/19
Cardiovasc J Afr 2019; 30: 208–215 www.cvja.co.za

DOI: 10.5830/CVJA-2019-019

Atherosclerosis is a progressive disease that is initiated by turbulent blood flow and the accumulation of lipids in the walls of large arteries, leading to dysfunction of the endothelium, and subsequently, the formation of lesions.[1,2] The disease leads to complications such as myocardial infarction and stroke, which are known to cause the death of about 17 million people globally each year.[3-5]

In humans, the process of atherogenesis begins during foetal development, and early lesions known as fatty streaks, containing cholesterol-rich macrophages or foam cells, occur in the first decade of life.[6] There is therefore a long time lag between the onset of atherogenesis and clinical manifestation,[7] and fatty streaks become precursors to advanced lesions later on in life.[1]

The relationship between serum cholesterol levels and atherosclerosis has long been established, and cholesterol-lowering therapy is known to reduce atherosclerosis.[8] The specific process that initiates atherosclerosis, however, needs to be further understood in order to develop effective therapeutic measures.

Three hypotheses have been proposed concerning the initiation of atherosclerosis, namely, the response-to-injury, the response-to-retention and the oxidative-modification hypotheses.[9] According to the response-to-injury theory, atherosclerosis is initiated when endothelial cells are denuded due to damage to the cells.[10] It is now known that endothelial injury alone does not initiate atherosclerosis, but injury results in the initiation of oxidation of low-density lipoprotein (LDL) and the activation of monocytes, which differentiate into macrophages and foam cells.[11,12]

In the response-to-retention hypothesis, sub-endothelial retention of apolipoprotein B-containing lipoproteins in the walls of arteries is the key pathological event during atherosclerosis.[9,13] The oxidative-modification hypothesis suggests that native LDL is oxidised in the vessel wall and the uptake of modified or oxidised LDL by macrophages leads to the formation of foam cells,[14] which become the pivot for the development of advanced atherosclerotic lesions.

Putting together the evidence supporting the various hypotheses, accumulation of cholesterol and its oxidation are key in the initiation of atherosclerosis. Hypercholesterolaemia, a condition characterised by elevated cholesterol levels in blood, is therefore the principal risk factor for cardiovascular diseases,[15] and understanding the role it plays during atherosclerosis is therefore likely to provide several novel treatment solutions.

Maternal hypercholesterolaemia during pregnancy results in the formation of significantly larger atherosclerotic lesions in foetuses,[7] and the formation of advanced lesions in adult life progresses faster in offspring of hypercholesterolaemic mothers.[16] Maternal hypercholesterolaemia may enhance atherosclerosis by differentially dysregulating the expression of aortic genes in the offspring,[17] resulting in a cascade of processes later in life that will increase lipid deposition and inflammation. Moreover, hypercholesterolaemia in pregnancy enhances endothelial dysfunction in foetal arteries and placental vasculature,[18] thereby decreasing nitric oxide-dependent vasodilation while increasing oxidative stress.[19] On the other hand, dietary intervention in humans using antioxidant-rich foods has an inverse relationship with the risk of cardiovascular diseases.[20,21]

Department of Anatomy, School of Biomedical and Allied Health Sciences, College of Health Sciences, University of Ghana, Korle-Bu campus, Accra, Ghana
Richard Michael Blay, PhD, rmblay@ug.edu.gh
Saviour Kweku Adjenti, PhD
Kevin Kofi Adutwum-Ofosu, PhD
Bismarck Afedo Hottor, PhD
John Ahenkorah, PhD
Benjamin Arko-Boham, PhD
Frederick Kwaku Addai, PhD

Cocoa powder is rich in antioxidants and several studies have shown that treating animals with cocoa powder inhibits the oxidation of LDL,[22] and reduces oxidative stress,[23] inflammation[24] and insulin resistance.[25] Moreover, consumption of natural cocoa powder reduced hypercholesterolaemia and atherosclerosis in apolipoprotein E knock-out mice by reducing the expression of genes related to metabolism, apoptosis and inflammation.[26] Our study therefore investigated the effect of maternal hypercholesterolaemia on the vascular morphology and atherosclerosis in the offspring of hypercholesterolaemic rabbits. It also sought to validate potential beneficial effects of consumption of natural cocoa powder (NCP) in the prevention of foetal onset of atherosclerosis.

Methods

This study was approved by the Ethical and Protocol Review Committee of the College of Health Sciences, University of Ghana. It was carried out in accordance with appropriate institutional regulations on the care and use of laboratory animals.

Ten New Zealand white female rabbits (age: 6 months, body weight: 1.5–2.8 kg) were obtained from the Animal Experimentation Unit of the Noguchi Memorial Institute for Medical Research (NMIMR), University of Ghana, Accra. The rabbits were transported to the animal house of the University of Ghana Medical School, Korle-Bu and kept for two weeks to acclimatise. The animals were housed under standard conditions of local temperature (30°C) and relative humidity (80%) and exposed to a 12-hour light/dark cycle.

Rabbits were then randomly assigned by lottery to three groups and housed individually in cages. The rabbits were arbitrarily numbered from one to 10 and the numbers were written on pieces of paper. After mixing up the pieces of paper, rabbits were placed in groups when the numbers were drawn.

The first two groups of four rabbits each were fed cholesterol-enriched feed (CEF). The CEF was prepared (adopted from Sun *et al.*[27]) by mixing standard feed (Kosher Feedmill Ltd, Accra) with 0.5% (w/w) cholesterol (Hopkin and William Ltd, London) and 10% (v/w) coconut oil (open market, Accra). The rabbits were fed CEF for two weeks, and when a routine lipid profile test confirmed hypercholesterolaemia, they were crossed with normocholesterolaemic males.

The normal cholesterol range for rabbits is 0.14–1.86 mmol/l (Olfert *et al.*[28]). Hypercholestrolaemia was defined as a total plasma cholesterol level higher than twice the upper level of the normal range.

One group of rabbits on CEF was given 2% (w/v) of NCP (GoodFood brand, Kakawa Enterprise Ltd, Accra) as an aqueous suspension instead of drinking water. This group (HCC) had 24-hour access to the NCP suspension, which they drank voluntarily, after being mated until they littered (28–30 days). The second group of rabbits on CEF (HC) were given 24-hour access to filtered tap water.

The third group of rabbits (n = 2), designated as normal control (NC), were given standard chow without cholesterol enrichment and filtered tap water throughout the duration of the experiment. Animals that were fed CEF were fed with standard chow after delivery and the cocoa drink was replaced with drinking water. Twelve pups were delivered by the HCC rabbits, six by the HC rabbits, and the NC rabbits delivered 12 pups.

Total levels of cholesterol were determined after an overnight fast by an enzymatic colorimetric test in a laboratory at the Medical Biochemistry Department (University of Ghana Medical School), using a semi-automated clinical analyser, Microlab 300 (Vital Scientific, the Netherlands).

Blood samples were obtained by the bleeding of the marginal ear vein. The skin over the ear of the rabbits was anaesthetised using a local anaesthetic cream containing lidocain (Lignocaine 2% Jelly, Purna Pharmaceuticals, Belgium) after the fur over the ear was shaved and the skin sanitised with alcohol. Blood samples were then drawn from the marginal ear vein and stored in sterilised test tubes containing heparin.

Maternal blood samples were collected before treatment with the cholesterol-enriched diet and after two weeks of feeding with the cholesterol-enriched diet. Blood samples from the offspring at the end of the experiment were obtained by cardiac puncture after chloroform inhalation had anaesthetised them.

The rabbit pups were euthanised by chloroform inhalation one week after birth and perfusion-fixed using 10% normal saline, followed by 10% phosphate-buffered formalin at pH 7.3. The aorta was dissected to remove the arch, thoracic and abdominal segments, which were post-fixed in 10% phosphate-buffered formalin for two to seven days. The aortae were taken through a routine histological processing.

Every 10th section of the arch, thoracic and abdominal segments of the aorta with a thickness of 10 µm was stained and analysed. Sections were stained with haematoxylin and eosin (H & E) for assessing intima–media thickness. In order to assess collagen and elastic fibre deposition in the vascular walls, Verhoeff–Van Gieson (VVG) staining of the sections was performed.

To determine the presence or absence of atherosclerotic lesions, frozen sections of the aortic segments were stained with Oil red O. Sections were counter-stained in alum haematoxylin. Five sections each of the aortic arch, thoracic and abdominal aorta were selected 100 µm apart and examined qualitatively for the presence or absence of atherosclerotic lesions.

Micrographs of stained sections were obtained using a digital microscope eyepiece (Premiere MA 88) fitted to a Leica Galen III light microscope. The digital eyepiece was connected to a computer and images from the microscope were captured using Microsoft Publisher software 2003 version. Images were analysed with Photoshop CS 4 (Adobe Systems, San Jose, CA, 2008).

A stage graticule (Nikon, Japan) was used to calibrate the ruler tool in Photoshop by mounting it onto the stage of a microscope and a micrograph, taken using the digital eyepiece, was connected to the ×10 objective lens. Intima–media thickness was measured using the ruler tool in Photoshop. Two lines (DD and EE) perpendicular to each other were drawn across the image of the artery through the centre, as shown in Fig. 1. Intima–media thickness readings were taken between points 1/2 and 3/4 on line EE and the average was calculated and recorded.

Statistical analysis

The results of the study were analysed using Graphpad Prism software (3.0). The t-test was used to compare the means of two groups, while one-way ANOVA was used to compare the

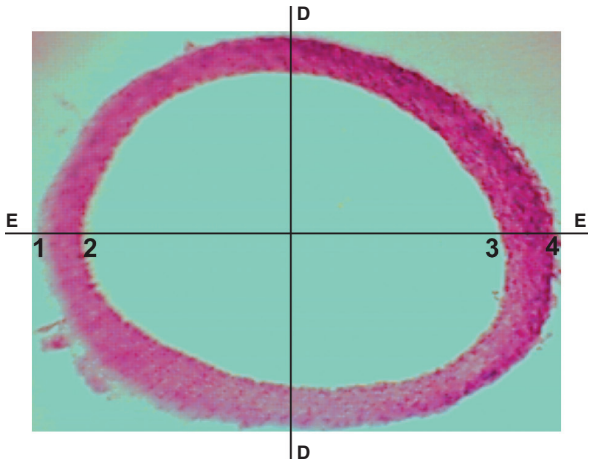

Fig. 1. Micrograph of H & E-stained section of the aorta illustrating intima–media thickness measurements. Two perpendicular lines (EE and DD) were drawn across the micrograph in Photoshop. Two measurements for intima–media thickness (IMT) were measured between points 1/2 and 3/4. The average IMT for each section was then computed.

means of three groups. Inherent in the Graphpad Prism is the *F*-test for variances to justify the *t*-test and the Bartlett's test to justify ANOVA. A *p*-value less than 0.05 was considered to be statistically significant. Bonferroni's multiple comparison test was done to show actual differences between the three groups.

Results

After feeding the female rabbits with a 0.5% cholesterol diet, the mean total plasma cholesterol of the HC and HCC groups were significantly higher than baseline concentrations. Cholesterol levels increased three-fold from the initial concentration for both groups after two weeks of treatment, as shown in Fig. 2A. In the HC group, total cholesterol levels increased from 2.38 (SD 0.81) to 7.33 (SD 1.93) mmol/l and that of the HCC group increased from 2.35 (SD 0.68) to 7.40 (SD 2.05) mmol/l. Cholesterol level of the control rabbits was unchanged at 1.8 (SD 0.28) before and after the same two-week period.

The mean total cholesterol levels of the offspring of the NC, HC and HCC rabbits were 9.47 (SD 1.56), 6.73 (SD 0.87) and 3.60 (SD 0.66) mmol/l, respectively (Fig. 2B). Statistical analysis showed significant differences between the total cholesterol levels of offspring of the different treatment groups ($p = 0.0002$, $F = 23.1$ and df = 2). Bonferroni's multiple comparison test indicated significant differences between the NC and HC groups ($p < 0.05$), the NC and HCC groups ($p < 0.0001$), and the HC and HCC groups ($p < 0.05$).

Histological sections of the aortic arch of the rabbit offspring showed intima–media thicknesses of 58.5 (SD 6.02) µm for the NC, 146 (SD 18.24) µm for the HC and 99 (SD 4.87) µm for the HCC groups. ANOVA showed significant differences ($p < 0.0001$, $F = 149.2$ and df = 2) between the intima–media thickness of the aortic arch between the three groups, as shown in Fig. 3. Bonferroni's multiple comparison test showed significant differences between the NC and HC groups ($p < 0.001$), the NC and HCC groups ($p < 0.001$), and the HC and HCC groups ($p < 0.001$).

Histological sections of the aortic arch revealed intimal lipid accumulations or lesions on all five sections per pup in the HC group (100%), whereas no lesions were observed on any of the five sections per pup from the NC and HCC groups (Fig. 4). In the descending thoracic segment of the aorta, again no lesions were found on sections from the NC group, as shown in Fig. 5. Lesions were present on 40% of the sections from the HC group and 20% of the sections from the HCC group. In the abdominal aorta, no lesions were present in any section of the three groups of rabbit pups.

Increased deposition of collagen and smooth muscle in vascular walls is associated with advanced atherosclerosis,[29] and so collagen and elastic fibre deposition were assessed by staining with VVG. Collagen and elastic fibres within the intima of the

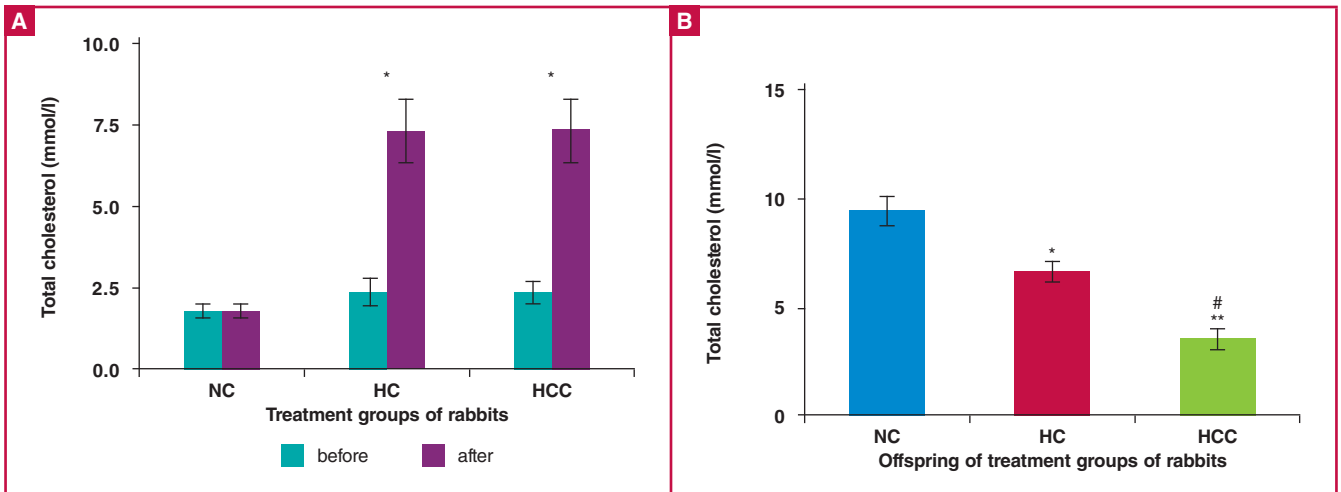

Fig. 2. Bar charts showing total plasma cholesterol concentrations. (A) shows total plasma cholesterol concentration of the mothers in all three groups before and after consuming a cholesterol-enriched diet for two weeks. (B) shows the mean plasma cholesterol level of the offspring. *$p < 0.05$ compared to control or baseline, **$p < 0.001$ and #$p < 0.05$ compared to the HC group. Error bars indicate standard deviation.

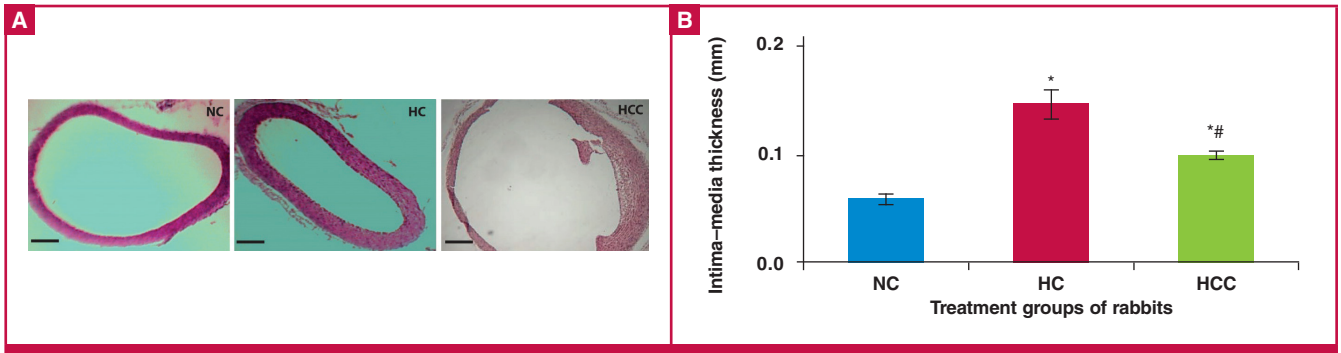

Fig. 3. (A) shows micrographs of H & E-stained sections of the aortic arch of rabbit pups born to the control rabbits (NC), hypercholesterolaemic rabbits without cocoa (HC) and hypercholesterolaemic rabbits given cocoa (HCC). The value of the scale bar is 140 µm. (B) shows a bar chart of the intima–media thickness of the aortic arch of offspring from the three groups. $^{*}p < 0.001$ and $^{\#}p < 0.001$ compared to the HC group. Error bars indicate standard deviation.

blood vessels stain blue-black and red/pink, respectively. Sections with more pink and black stain represent increased collagen and elastic fibres, as shown in Fig. 6.

Sections from the arch and abdominal aorta showed more deposition of collagen and elastic fibres in the intima of pups born to hypercholesterolaemic mothers in the HC group, but

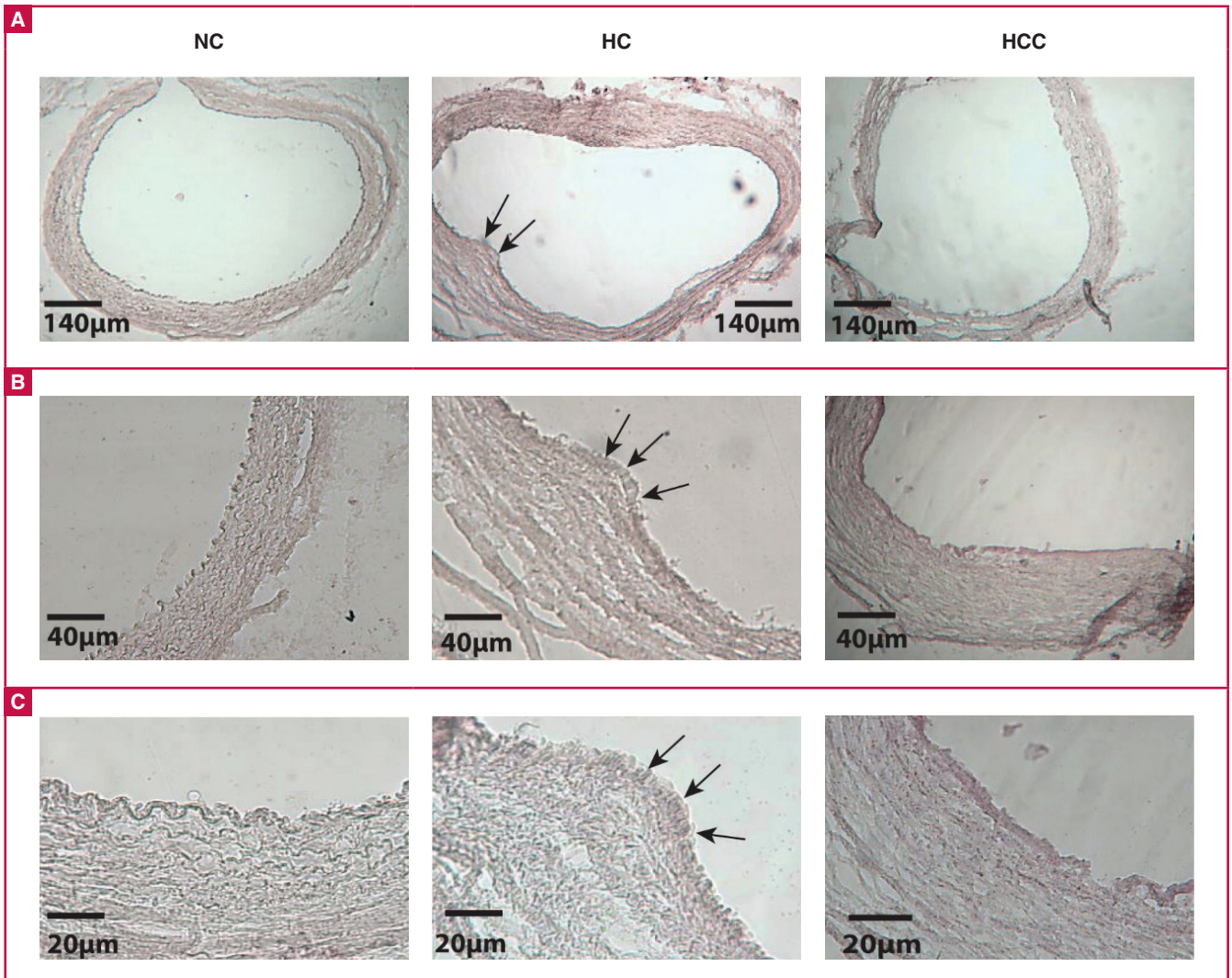

Fig. 4. Micrographs at different magnifications of Oil red O-stained sections of the aortic arch of offspring. (A) shows a whole section of the aortic arch. (B) and (C) show higher magnifications of the aortic arch and lesions (indicated with arrows). Sections from the NC and HCC pups show no lesions, whereas sections from the HC pups show the presence of atherosclerotic lesions.

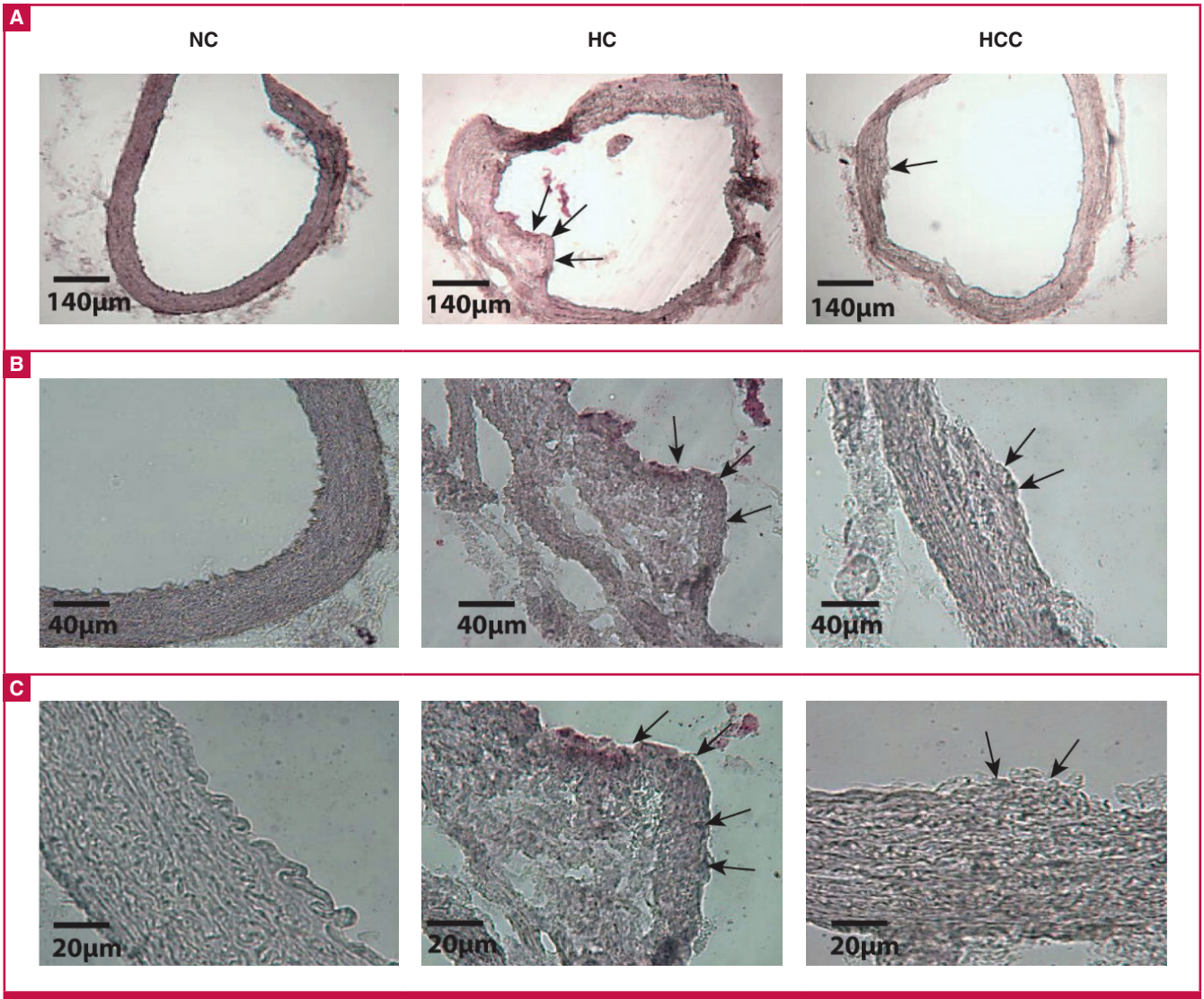

Fig. 5. Micrographs at different magnifications of Oil red O-stained sections of the descending thoracic aorta of offspring. (A) shows a whole section of the aortic arch. (B) and (C) show sections of thoracic aorta with atherosclerotic lesions. Sections from the NC pups show no lesions, whereas sections from the HC and HCC pups show the presence of atherosclerotic lesions.

less in those born to hypercholesterolaemic mothers fed on cocoa (HCC). Collagen and elastic fibre content of sections from the thoracic aorta did not show obvious differences between the two groups (Fig. 6).

Discussion

The causal role of maternal hypercholesterolaemia in foetal atherogenesis has been established and evidence suggests that both lipid-lowering and antioxidant interventions during pregnancy may inhibit atherosclerosis.[6] Previously, researchers seldom considered maternal hypercholesterolaemia to promote atherosclerosis in offspring because the placenta was thought to be impermeable to cholesterol and also because cholesterol levels of newborns were not correlated with maternal hypercholesterolaemia.[30,31] However, results from later studies have shown that serum cholesterol level is increased in early foetal life,[31] and the Fate of Early Lesions in Children (FELIC) study showed that increased maternal cholesterol levels enhanced the formation of fatty streaks in foetuses. Although with age, cholesterol levels in foetuses decrease, maternal hypercholesterolaemia increases the progression of atherosclerosis later in life.[16]

In this study, plasma cholesterol levels were significantly high in offspring of normocholesterolaemic as well as hypercholesterolaemic rabbits. Offspring of hypercholesterolaemic mothers that received cocoa powder, however, showed reduced cholesterol levels compared to the other two groups, suggesting that consumption of cocoa during pregnancy may reduce plasma cholesterol levels in the offspring of rabbits. It is not clear from this study the mechanism by which cocoa reduced plasma cholesterol levels of the offspring, however, this could have been due to antioxidant activity, as has already been shown by Napoli and colleagues.[6,26]

Interestingly, plasma cholesterol level was highest in offspring of normocholesterolaemic rabbits and this may have been because pregnancy induces a temporary condition of hypercholesterolaemia necessary for the normal development of the foetus.[18] However, beyond certain physiological levels, this

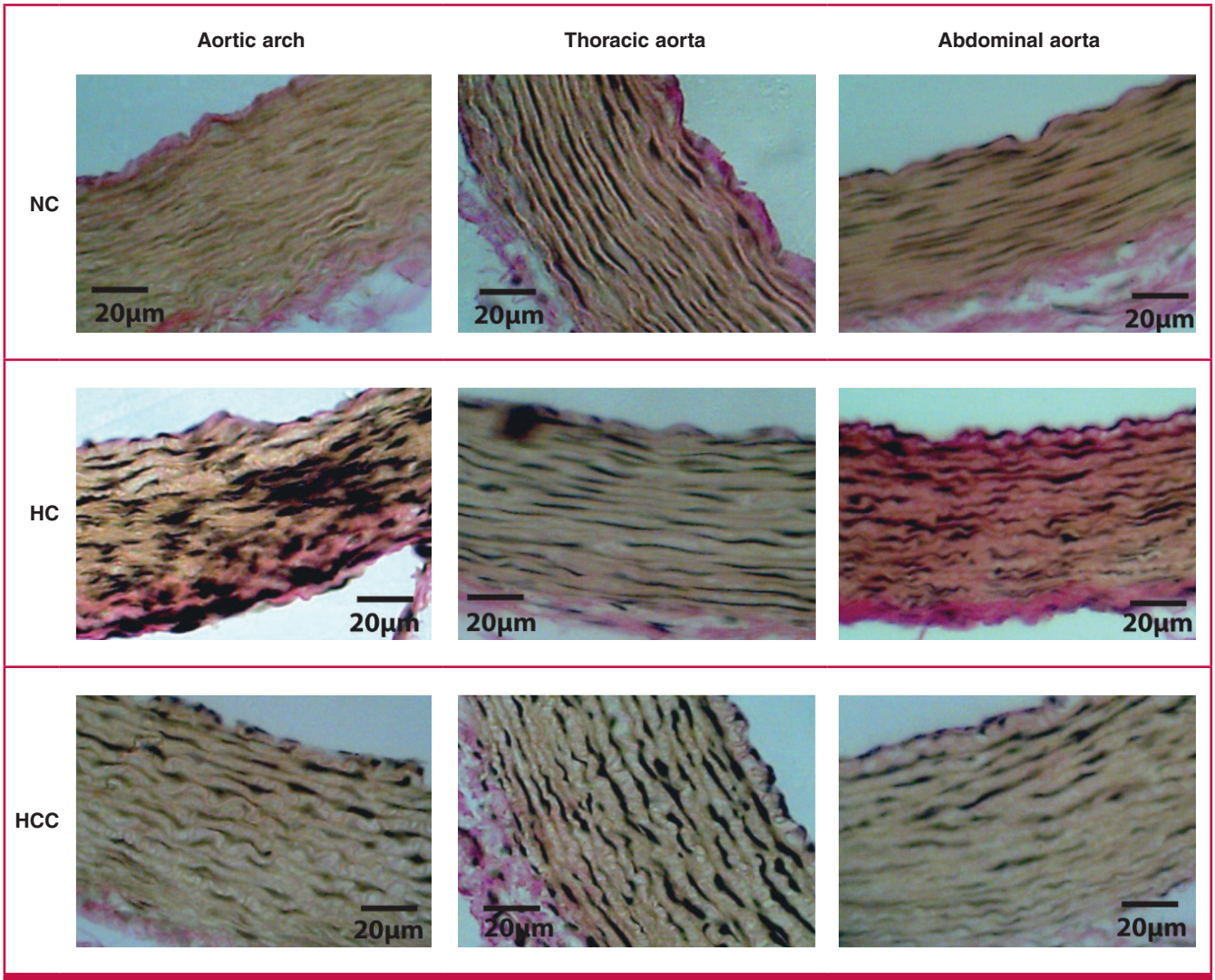

Fig. 6. Histomicrographs of Verhoeff–Van Gieson-stained sections of the arch, thoracic and abdominal segments of the aorta from offspring of NC, HC and HCC rabbits. Elastic fibres are stained blue-black or black and collagen fibres are stained red or pink.

condition may lead to the development of certain pathologies in both the mother and foetus.[32]

Although the placenta was thought to be impermeable to lipoproteins, Frantz *et al.*[33] showed that this may not be the case, and results from our study also suggest cholesterol possibly crossed the placenta into the foetus. This is consistent with earlier observations that foetal cholesterol levels showed an inverse correlation with maternal cholesterol level during the first six months of life.[16] Increased cholesterol levels in offspring of normocholesterolaemic mothers did not, however, result in atherosclerotic lesion formation in this study.

Maternal hypercholesterolaemia in rabbits led to the formation of atherosclerotic lesions in the aortic arch and descending thoracic aorta of offspring, as shown by increased intima–media thickness and the presence of lesions in sections of the aorta. Increased intima–media thickness of arteries, a consequence of pathological vascular remodelling, is associated with several risk factors for atherosclerosis, including age, systolic blood pressure, diabetes, LDL cholesterol, smoking and familial hypercholesterolaemia in humans.[34] The intima–media thickness is also increased in hypercholesterolaemic patients compared to controls,[35] and has become a convenient marker for atherosclerosis.[36]

Oxidation of LDL cholesterol is key in the initiation of atherosclerosis[7] and may also trigger vascular remodelling by enhancing smooth muscle cell proliferation and collagen deposition, leading to increased intima–media thickness. Increased deposition of elastic and collagen fibres was observed in the present study, shown by VVG-stained sections of aortic arch and thoracic aorta, suggesting increased atherogenesis, as shown previously.[37] Moreover, maternal hypercholesterolaemia has already been shown to increase the presence of collagen fibres in the intima–media of coronary arteries.[31] The association of cocoa intake with a smaller number of aortic sections with atherosclerotic lesions, as well as reduced collagen and elastic fibre staining in the rabbits may be explained by inhibition of LDL oxidation[20,22] and reduction in oxidative stress through high antioxidant[23,26] and anti-inflammatory[24] activity.

Maternal hypercholesterolaemia may also trigger the formation of fatty streaks and atherosclerosis in offspring by enhancing endothelial dysfunction,[32] a key event in the initiation and progression of atherosclerosis. It is known that flavanol-

rich cocoa inhibits endothelial dysfunction,[38,39] and hence the initiation of atherosclerosis during foetal development.

Conclusion

Regular consumption of cocoa powder during pregnancy reduced atherogenesis and intima–media thickening in pups of hypercholesterolaemic rabbits by inhibiting lesion formation and the deposition of elastic and collagen fibres in the aorta.

We acknowledge the College of Health Sciences, University of Ghana for providing financial support for this study and technicians from the departments of Anatomy, Medical Biochemistry and Pharmacology, University of Ghana, for their assistance. We also acknowledge Noguchi Memorial Institute of Medical Research, Accra for their support.

References

1. Lusis AJ, Atherosclerosis. *Nature* 2000; **407**(6801): 233–241. PMID: 11001066. PMC2826222.
2. Schober A, Nazari-Jahantigh M, Wei Y, Bidzhekov K, Gremse F, Grommes J, *et al.* MicroRNA-126-5p promotes endothelial proliferation and limits atherosclerosis by suppressing Dlk1. *Nat Med* 2014; **20**(4): 368–376. PMID: 24584117. PMC4398028.
3. Zimmer S, Grebe A, Latz E. Danger signaling in atherosclerosis. *Circ Re,* 2015; **116**(2): 323–340. PMID: 25593277.
4. Ladeiras-Lopes R, Agewall S, Tawakol A, Staels B, Stein E, Mentz RJ, *et al.* Atherosclerosis: Recent trials, new targets and future directions. *Int J Cardiol* 2015; **192**: 72–81. PMID: 26002254.
5. Benjamin EJ, Blaha MJ, Chiuve SE, Cushman M, Das SR, Deo R, *et al.* Heart disease and stroke statistics – 2017 update: A report From the American Heart Association. *Circulation* 2017; **135**(10): e146–e603. PMID: 28122885. 5408160.
6. Napoli C, Witztum JL, Calara F, de Nigris F, Palinski W. Maternal hypercholesterolemia enhances atherogenesis in normocholesterolemic rabbits, which is inhibited by antioxidant or lipid-lowering intervention during pregnancy: an experimental model of atherogenic mechanisms in human fetuses. *Circ Res* 2000; **87**(10): 946–952. PMID: 11073892.
7. Napoli C, D'Armiento FP, Mancini FP, Postiglione A, Witztum JL, Palumbo G, *et al.* Fatty streak formation occurs in human fetal aortas and is greatly enhanced by maternal hypercholesterolemia. Intimal accumulation of low density lipoprotein and its oxidation precede monocyte recruitment into early atherosclerotic lesions. *J Clin Invest* 1997; **100**(11): 2680–2690. PMID: 9389731. PMC508471.
8. Von-Birgelen C, Hartmann M, Mint GS, Baumgart D, Schmermund A, Erbel R. Relation between progression and regression of atherosclerotic left main coronary artery disease and serum cholesterol levels as assessed with serial long-term (≥ 12 months) follow-up intravascular ultrasound. *Circulation* 2003; **108**: 2757–2762. PMID: 14623804.
9. Williams KJ, Tabas I. The response-to-retention hypothesis of early atherogenesis. *Arterioscler Thromb Vasc Biol* 1995; **15**(5): 551–561. PMID: 7749869. PMC2924812.
10. Ross R, Glomset J, Harker L. Response to injury and atherogenesis. *Am J Pathol* 1977; **86**(3): 675–684. PMID: 842616. PMC2032127.
11. Ross R. The pathogenesis of atherosclerosis: a perspective for the 1990s. *Nature* 1993; **362**(6423): 801–809. PMID: 8479518.
12. DiCorleto PE, Chisolm GM, 3rd. Participation of the endothelium in the development of the atherosclerotic plaque. *Prog Lipid Res* 1986; **25**(1–4): 365–374. PMID: 3321089.
13. Tabas I, Garcia-Cardena G, Owens GK. Recent insights into the cellular biology of atherosclerosis. *J Cell Biol* 2015; **209**(1): 13–22. PMID: 25869663. PMC4395483.
14. Haberland ME, Olch CL, Folgelman AM. Role of lysines in mediating interaction of modified low density lipoproteins with the scavenger receptor of human monocyte macrophages. *J Biol Chem* 1984; **259**(18): 11305–11311. PMID: 6088540.
15. Andreadou I, Iliodromitis EK, Lazou A, Gorbe A, Giricz Z, Schulz R, *et al.* Effect of hypercholesterolaemia on myocardial function, ischaemia–reperfusion injury and cardioprotection by preconditioning, postconditioning and remote conditioning. *Br J Pharmacol* 2017; **174**(12): 1555–1569. PMID: 28060997. 5446572.
16. Napoli C, Glass CK, Witztum JL, Deutsch R, D'Armiento FP, Palinski W. Influence of maternal hypercholesterolaemia during pregnancy on progression of early atherosclerotic lesions in childhood: Fate of Early Lesions in Children (FELIC) study. *Lancet* 1999; **354**(9186): 1234–1241. PMID: 10520631.
17. Napoli C, de Nigris F, Welch JS, Calara FB, Stuart RO, Glass CK, *et al.* Maternal hypercholesterolemia during pregnancy promotes early atherogenesis in LDL receptor-deficient mice and alters aortic gene expression determined by microarray. *Circulation* 2002; **105**(11): 1360–1367. PMID: 11901049.
18. Leiva A, Fuenzalida B, Westermeier F, Toledo F, Salomon C, Gutierrez J, *et al.* Role for tetrahydrobiopterin in the fetoplacental endothelial dysfunction in maternal supraphysiological hypercholesterolemia. *Oxid Med Cell Longev* 2015; **2015**: 5346327. PMID: 26697136. PMC4677232.
19. Rodriguez-Porcel M, Lerman LO, Herrmann J, Sawamura T, Napoli C, Lerman A. Hypercholesterolemia and hypertension have synergistic deleterious effects on coronary endothelial function. *Arterioscler Thromb Vasc Biol* 2003; **23**(5): 885–891. PMID: 12663373.
20. Schroeter H, Heiss C, Balzer J, Kleinbongard P, Keen CL, Hollenberg NK, *et al.* (-)-Epicatechin mediates beneficial effects of flavanol-rich cocoa on vascular function in humans. *Proc Natl Acad Sci USA* 2006; **103**(4): 1024–1029. PMID: 16418281. PMC1327732.
21. Das S, Ray R, Snehlata, Das N, Srivastava LM. Effect of ascorbic acid on prevention of hypercholesterolemia induced atherosclerosis. *Mol Cell Biochem* 2006; **285**(1–2): 143–147. PMID: 16479321.
22. Kurosawa T, Itoh F, Nozaki A, Nakano Y, Katsuda S, Osakabe N, *et al.* Suppressive effects of cacao liquor polyphenols (CLP) on LDL oxidation and the development of atherosclerosis in Kurosawa and Kusanagi-hypercholesterolemic rabbits. *Atherosclerosis* 2005; **179**(2): 237–246. PMID: 15777537.
23. Martin MA, Ramos S, Cordero-Herrero I, Bravo L, Goya L. Cocoa phenolic extract protects pancreatic beta cells against oxidative stress. *Nutrients* 2013; **5**(8): 2955–2968. PMID: 23912326. PMC3775237.
24. Khan N, Khymenets O, Urpi-Sarda M, Tulipani S, Garcia-Aloy M, Monagas M, *et al.* Cocoa polyphenols and inflammatory markers of cardiovascular disease. *Nutrients* 2014; **6**(2): 844–880. PMID: 24566441. PMC3942736.
25. Cordero-Herrera I, Martin MA, Goya L, Ramos S. Cocoa flavonoids attenuate high glucose-induced insulin signalling blockade and modulate glucose uptake and production in human HepG2 cells. *Food Chem Toxicol* 2014; **64**: 10–19. PMID: 24262486.
26. Guan H, Lin Y, Bai L, An Y, Shang J, Wang Z, *et al.* Dietary cocoa powder improves hyperlipidemia and reduces atherosclerosis in apoE deficient mice through the inhibition of hepatic endoplasmic reticulum stress. *Mediators Inflamm* 2016; **2016**: 1937572. PMID: 26980943. PMC4770140.
27. Sun Y-P, Lu NC, Parmley WW, Hollenbeck CB. Effects of cholesterol diets on vascular function and atherogenesis in rabbits. *Proc Soc Exp Biol Med* 2000; **224** (3): 166–171. PMID: 10865232.

28. Olfert ED, Cross BM, McWilliam AA. Guide to the care and use of experimental animals. Volume 1: Appendix V. (1993). Accessed on May 22, 2017 from https://www.aaalac.org/accreditation/RefResources/CCAC_Experimental_Animals_Vol1.pdf
29. Stary HC, Chandler AB, Dinsmore RE, Fuster V, Glagov S, Insull W Jr, *et al.* A definition of advanced types of atherosclerotic lesions and a histological classification of atherosclerosis. A report from the committee on vascular lesions of the Council on Arteriosclerosis, American Heart Association. *Circulation* 1995; **92**(5): 1355–1374. PMID: 7648691.
30. Belknap WM, Dietschy JM. Sterol synthesis and low density lipoprotein clearance in vivo in the pregnant rat, placenta, and fetus. Sources for tissue cholesterol during fetal development. *J Clin Invest* 1988; **82**(6): 2077–2085. PMID: 3198766. 442791.
31. Palinski W, D'Armiento FP, Witztum JL, de Nigris F, Casanada F, Condorelli M, *et al.* Maternal hypercholesterolemia and treatment during pregnancy influence the long-term progression of atherosclerosis in offspring of rabbits. *Circ Res* 2001; **89**(11): 991–996. PMID: 11717155.
32. Leiva A, de Medina CD, Salsoso R, Saez T, San Martin S, Abarzua F, *et al.* Maternal hypercholesterolemia in pregnancy associates with umbilical vein endothelial dysfunction: role of endothelial nitric oxide synthase and arginase II. *Arterioscler Thromb Vasc Biol* 2013; **33**(10): 2444–2453. PMID: 23950140.
33. Frantz E, Menezes HS, Lange KC, Abegg MP, Correa CA, Zangalli L, *et al.* The effect of maternal hypercholesterolemia on the placenta and fetal arteries in rabbits. *Acta Cir Bras* 2012; **27**(1): 7–12. PMID: 22159432.
34. Lemne C, Jogestrand T, de Faire U. Carotid intima–media thickness and plaque in borderline hypertension. *Stroke* 1995; **26**(1): 34–39. PMID: 7839394.
35. Tonstad S, Joakimsen O, Stensland-Bugge E, Leren TP, Ose L, Russell D, *et al.* Risk factors related to carotid intima–media thickness and plaque in children with familial hypercholesterolemia and control subjects. *Arterioscler Thromb Vasc Biol* 1996; **16**(8): 984–991. PMID: 8696963.
36. Magnussen CG, Carotid artery intima–media thickness and hypertensive heart disease: a short review. *Clin Hypertens* 2017; **23**: 7. PMID: 28373912. PMC5376487.
37. Shindo J, Ishibashi T, Yokoyama K, Nakazato K, Ohwada T, Shiomi M, *et al.* Granulocyte-macrophage colony-stimulating factor prevents the progression of atherosclerosis via changes in the cellular and extracellular composition of atherosclerotic lesions in watanabe heritable hyperlipidemic rabbits. *Circulation* 1999; **99**(16): 2150–2156. PMID: 10217656.
38. Zoccali C, Mallamaci F. Cocoa flavanols: a magic potion for protecting the endothelium in kidney failure? *Clin J Am Soc Nephrol* 2016; **11**(1): 9–11. PMID: 26681133.
39. 39. Heiss C, Kleinbongard P, Dejam A, Perré S, Schroeter H, Sies H, Kelm M. Acute consumption of flavanol-rich cocoa and the reversal of endothelial dysfunction in smokers. *J Am Coll Cardiol* 2005; **46**(7): 1276–1283. PMID: 16198843.

…continued from page 197

The report says Esperion, which plans to set a $3 500 list price for bempedoic acid, believes it can play interloper. The list prices of PCSK9 treatments, which currently exceed $14 000 a year, have limited their use in the three years since they hit the market. Esperion's drug doesn't lower LDL as well as PCSK9 blockers, which can roughly halve bad cholesterol levels, but it would be cheaper and wouldn't require an injection.

But cracking the market may not be so simple. Earlier this year, Sanofi and Regeneron struck a deal with Express Scripts in which they'll discount their drugs by more than 50% in exchange for an easier path to patients. And, last week, Amgen made an unprecedented move to slash the list price of its treatment to $5 850 a year by 2020. According to the report, that could create a difficult market dynamic for Esperion. Zetia prescriptions, like statins, are practically free for patients with insurance, and each has an established effect on preventing heart attacks and strokes in the long term. The PCSK9 treatments have demonstrated dramatic long-term benefits of their own, and their impending price decreases could put them within reach of more patients than ever before.

Bempedoic acid has established that it can reduce LDL cholesterol levels, but its effects on cardiovascular health won't be known until a 13 000-patient trial reads out in 2022. That could leave Esperion struggling to make its case in a crowded market.

'I'm still not totally convinced that there's an obvious place for this drug,' said Dr Ethan Weiss, a cardiologist at the University of California – San Francisco Medical Centre, who wasn't involved in the study. 'We have a good drug with modest efficacy in statins, and then two drugs with significant efficacy in PCSK9. If you're a marketer, I don't know where you aim your gun at this one.'

The report says Esperion believes bempedoic acid will have plenty of room to compete. Despite the established benefits of PCSK9 therapy, only about 20 000 people are getting the drugs, Esperion CEO Tim Mayleben said. And that suggests there's pent-up demand for an alternative.

'There are 13 million people in the US who have elevated LDL cholesterol levels and have had a cardiovascular event and need more cholesterol lowering,' Mayleben said. 'The fact that the price of PCSK9s is being lowered, that's great. But it's still almost twice the list price of our drug.'

Source: Stat News report 2018

Unmasking right ventricular dysfunction in chronic rheumatic mitral regurgitation

Ruchika Meel, Ferande Peters, Elena Libhaber, Mohammed R Essop

Abstract

Aims: Right ventricular (RV) systolic function is an important predictor of mortality but has been poorly studied in chronic rheumatic mitral regurgitation (CRMR). We studied RV systolic function using speckle-tracking echocardiography (STE) in patients with CRMR.

Methods: Seventy-seven patients with CRMR and 40 healthy controls were enrolled in a cross-sectional study at Chris Hani Baragwanath Hospital between January and October 2014. RV peak systolic strain (PSS) and left ventricular (LV) global longitudinal strain (GLS) were measured using Philips Qlab 9 STE software.

Results: RVPSS was lower in CRMR patients compared to the controls (–16.8 ± 4.5 vs –19.2 ± 3.4%, $p = 0.003$) with no difference in conventional RV systolic function parameters ($p = 0.39$). RVPSS was lower in severe CRMR compared to moderate CRMR patients (–14.3 ± 4.23 vs –18 ± 4.18%, $p < 0.0001$). CRMR patients with LV systolic dysfunction had a greater reduction in RVPSS and LVGLS compared to those with preserved LV systolic function ($p = 0.001$). LVGLS and significant tricuspid regurgitation (TR) were independent predictors of RVPSS ($p < 0.001$).

Conclusion: In CRMR patients, RVPSS was a more sensitive marker for detecting earlier RV systolic dysfunction than traditional RV functional parameters.

Keywords: right ventricle, rheumatic mitral insufficiency, speckle-tracking echocardiography

Submitted 15/12/18, accepted 16/4/19
Published online 24/5/19
Cardiovasc J Afr 2019; **30**: 216–221 www.cvja.co.za

DOI: 10.5830/CVJA-2019-020

Systolic dysfunction of the right ventricle (RV) is a known predictor of mortality after acute myocardial infarction or coronary artery bypass grafting, and in heart failure and primary pulmonary hypertension (PHT).[1-4] In addition to left ventricular (LV) parameters, RV systolic function provides adjunctive information in the decision-making process regarding surgical intervention in mitral regurgitation (MR).[5,6]

Pre-operative RV function is an important determinant of intra-operative and postoperative outcomes in MR and therefore has prognostic implications.[5,7] Additionally, RV dysfunction may have important implications in terms of predicting greater haemodynamic impairment of the LV and secondary PHT due to MR.[8,9] Furthermore, it has been suggested that there may be direct involvement of the RV by the rheumatic process, resulting in necrosis of the myocytes, fibrosis and calcification of the myocardium, with resultant RV dysfunction.[10]

Recently, newer imaging techniques such as speckle-tracking-derived RV strain have emerged, which offer several advantages over traditional echocardiographic parameters for assessing overt and subclinical RV systolic dysfunction.[6,10,11,12,13] There are no studies that have assessed RV function in chronic rheumatic mitral regurgitation (CRMR). We therefore aimed to (1) study RV systolic function using speckle-tracking echocardiography (STE) in patients with CRMR; and (2) determine the predictors of RV free-wall peak systolic strain (PSS) in CRMR.

Methods

We conducted a cross-sectional study at the Chris Hani Baragwanath Academic Hospital. Patients were enrolled between January and October 2014. All patients were screened and patients deemed to have moderate or severe CRMR were referred for possible inclusion in the study. A total of 91 patients with presumed CRMR underwent clinical evaluation, resting electrocardiogram and detailed echocardiographic assessment according to a pre-determined protocol.

The inclusion criteria were patients aged 18 years or older with echocardiographic features of moderate or severe CRMR. Patients were excluded if they had significant aortic valve disease, concurrent mitral stenosis with a valve area of less than 2 cm^2, documented ischaemic heart disease, pre-existing non-valvular cardiomyopathy, prior cardiac surgery, congenital or pericardial disease, pregnancy, severe systemic disorders such as renal failure, uncontrolled hypertension (systolic blood pressure > 140 mmHg and diastolic blood pressure > 90 mmHg), were on medication or had severe anaemia (haemoglobin < 10 g/dl). Fourteen patients were excluded due to the following: atrial fibrillation, anaemia, renal dysfunction and inadequate image quality.

The final sample included 77 patients. Forty age- and gender-matched controls were also included in the study. All healthy volunteers with no known diseases and adequate echocardiographic windows were recruited from the community following an advertisement for the study. A tolerance of five years was allowed for age matching. The study was approved by the University of the Witwatersrand Ethics Committee (M140114).

Division of Cardiology, Chris Hani Baragwanath Academic Hospital and University of the Witwatersrand, Johannesburg, South Africa
Ruchika Meel, MB ChB, MMed (Int Med), Cert Card (SA), PhD, ruchikameel@gmail.com
Ferande Peters, MD
Elena Libhaber, PhD
Mohammed R Essop, MD

Transthoracic echocardiography was performed on all patients in the left lateral position by experienced sonographers using a S5-1 transducer on a Philips iE33 system (Amsterdam, the Netherlands). The images were obtained according to a standardised protocol. The data were transferred and analysed offline using the Xcelera workstation (Philips).

All linear chamber measurements were performed according to the American Society of Echocardiography (ASE) chamber guidelines.[14] Measurements relating to LV diastolic function were performed in accordance with the ASE guidelines on diastolic function and included pulse-wave Doppler at the mitral tips and tissue Doppler of both medial and lateral mitral annuli.[15] Measurements relating to the RV were based on the ASE guidelines on the RV.[16] All LV volumes were indexed to body surface area. We used a LV ejection fraction (EF) cut-off of < 60% to define decreased LV systolic function in MR.[17]

MR was considered of rheumatic aetiology when the morphology of the valve satisfied the proposed World Heart Federation criteria for the diagnosis of chronic rheumatic heart disease (RHD).[18] MR severity was assessed with an integrated approach using qualitative, semi-quantitative and quantitative methods as per ASE valvular regurgitation guidelines.[19]

Two-dimensional echocardiography images were obtained at end-expiration from LV long-axis apical four-, three- and two-chamber (A4C, A3C and A2C) views with frame rates of 60–80 frames per second.[20] Three consecutive cardiac cycles were recorded and averaged.[21] LV endocardial surface was traced manually in the three views by a point-and-click approach.[20,22] The speckle-tracking points were modified to allow for adequate speckle-tracking of the LV wall.[20,22] The LV was divided into 17 segments. Peak LV longitudinal systolic strain was calculated for long-axis A4C, A3C and A2C views, and global LV systolic strain was calculated by averaging the three apical views.[20,22]

RV free-wall PSS was derived from a modified A4C RV focused view.[10] Once three points, namely the RV apex, medial and lateral tricuspid annulus, were defined, the software automatically traced the endocardial and epicardial border.[10] Philips QLAB version 9.0 software allowed off-line semi-automated analysis of speckle-based strain. This results in the division of the RV into six standard segments in the A4C view.[10,23,24] The region of interest, once created, can be manually adjusted as needed to allow for adequate speckle-tracking.[6] The RV free-wall PSS was obtained by averaging three lateral segments (the basal, mid and apical RV wall).[25] The interventricular septum was excluded from analysis.[23,24] The longitudinal ε curves for each segment and a mean curve of all segments was generated by the software. These curves were used to derive peak negative RV free-wall PSS.

Statistical analysis

This was performed with Statistica (version 12.5, series 0414 for Windows). Continuous variables are expressed as mean ± SD or median (IQR). The Student's *t*-test or Mann–Whitney *U*-test were used to compare continuous variables. Categorical variables were evaluated with the chi-squared and Fisher's exact tests when necessary. A *p*-value of < 0.05 was recognised as statistically significant.

Univariate and multivariate linear regression analysis was used to identify possible independent determinants of RV free-wall PSS. The independent variables with $p \leq 0.05$ on univariate analyses were tested in multivariate models. Pearson's correlation coefficient was used to assess the co-linearity between variables. These models were further analysed using the forward and backward multiple linear regression methods.

The intra- and inter-observer variabilities were assessed for RV free-wall PSS and LVGLS. Measurements were done in 20 randomly selected subjects. Inter- and intra-observer reproducibility was assessed by calculating coefficients of variation. A *p*-value < 0.05 was considered statistically significant.

Results

There was no statistically significant difference in age, gender, systolic blood pressure, diastolic blood pressure, body mass index and heart rate between the patients with MR and the controls ($p > 0.05$) (Table 1). Hypertension, HIV and a combination of the two co-morbidities were identified in 41.5, 12.9 and 15.5% of patients, respectively. Forty-two per cent of the patients were in New York Heart Association functional class 1, the remainder were in class 2 (49%) and 3 (9%).

Among the CRMR patients, moderate MR was present in 51 (66%) and severe MR in 26 (34%) subjects. As expected, compared to controls, linear and volumetric measures of the LV revealed a greater degree of LV dilatation, and LV mass as well as left atrial volumes were increased. LVEF was significantly lower in CRMR patients compared to the controls. In addition, analysis of LV diastolic parameters revealed that compared to the controls, E′ of both annuli was lower and E/E′ was higher (Table 2).

Pulmonary artery systolic pressure (PASP) was significantly higher in the MR group compared to the controls (35.1 ± 16.9 vs 22.1 ± 5.6 mmHg, $p < 0.0001$). Grade ≥ 2+ tricuspid regurgitation (TR) was present in 30% of the patients with CRMR. No difference was noted between RV basal size, right atrial volume indexed, tricuspid annular plane systolic excursion (TAPSE) and RVS′ between the CRMR and control groups. However RV free-wall PSS was significantly lower in the CRMR patients compared to the controls (Table 2, Fig. 1).

Patients with severe CRMR had higher PASP and a greater degree of RV hypertrophy compared to those with moderate MR (Table 3). RV free-wall PSS was significantly lower in severe MR compared to patients with moderate MR, whereas no difference was detected between these groups for both TAPSE and tricuspid S′. A similar trend of depressed RVPSS with unchanged TAPSE and RVS′ was noted when comparing patients with LV dysfunction with those with preserved LVEF (Table 4).

Table 1. Baseline clinical characteristics of the study population

Variable	*CRMR patients (n = 77)*	*Controls (n = 40)*	p-*value*
Age (years)	44 ± 13.6	42 ± 13.4	0.4
Gender (M:F)	13:64	8:32	0.6
Body surface area (m^2)	1.7 ± 0.2	1.8 ± 0.2	0.01
Body mass index (kg/m^2)	27.1 ± 5.9	28.4 ± 6.2	0.3
Systolic blood pressure (mmHg)	124.2 ± 11.4	124 ± 17.5	0.94
Diastolic blood pressure (mmHg)	77 ± 9.1	75.7 ± 12.6	0.52
Heart rate (beats/min)	77.1 ± 12.6	76.3 ± 14.1	0.75

Data are presented as mean ± SD or %.
CRMR: chronic rheumatic mitral regurgitation.

Table 2. Echocardiographic parameters of the study population

Variable	*CRMR patients (n = 77)*	*Controls (n = 40)*	p-*value*
LV parameters			
EDD (mm)	54.8 ± 9.4	42.5 ± 4.8	< 0.0001
ESD (mm)	41.4 ± 9.4	27.1 ± 4.2	< 0.0001
LVPWD (mm)	8.5 ± 1.5	9.2 ± 1.9	0.03
EDVi (ml/m²)†	93.2 ± 30.1	47.9 ± 13.5	< 0.0001
ESVi (ml/m²)†	40.0 ± 22.2	17.8 ± 6.4	< 0.0001
LAVi (ml/m²)†	64.1 ± 39.9	21.9 ± 4.9	< 0.0001
EF (%)	58.5 ± 12.9	62.8 ± 11.2	0.07
LVMi (kg/m²)†	102.7 ± 36.3	65.6 ± 20.3	< 0.0001
E wave (cm/s)	133.8 ± 48.1	77.0 ± 17.6	< 0.0001
A wave (cm/s)	98.4 ± 33.5	59.6 ± 13.0	< 0.0001
E′ medial (cm/s)	7.3 ± 2.3	8.8 ± 2.8	0.002
E′ lateral (cm/s)	10.1 ± 4.0	13.4 ± 3.6	< 0.0001
E/E′ medial (cm/s)	20.1 ± 10.7	9.4 ± 3.0	< 0.0001
E/E′ lateral (cm/s)	15.4 ± 8.8	5.9 ± 1.6	< 0.0001
S′ medial (cm/s)	6.3 ± 1.3	7.1 ± 1.6	0.004
S′ lateral (cm/s)	7.3 ± 2.5	8.2 ± 2.6	0.07
LV GLS (%)	–16.1 ± 5.3	–17.9 ± 2.1	0.04
RV parameters			
RV base (mm)	32.1 ± 6.9	30.8 ± 4.7	0.28
RVS′ (cm/s)	11.5 (9.7–13.8)	11.6 (10.5–13.4)	0.29
TAPSE (cm)	2.1 ± 0.4	2.2 ± 3.2	0.78
RAVi (ml/m²)†	23.1 ± 12.9	18.6 ± 5.4	0.03
TR (grade ≥ 2+ TR) (%)	30%	–	–
PASP (mmHg)	35.1 ± 16.9	22.1 ± 5.6	< 0.0001
RV free-wall PSS (%)	–16.8 ± 4.5	–19.2 ± 3.4	0.003

Data are presented as mean ± SD or %. †Values are indexed to BSA. CRMR, chronic rheumatic mitral regurgitation; EDVi, end-diastolic volume indexed; ESVi, end-systolic volume indexed; IVSD, interventricular septal diameter; LAVi, left atrial volume indexed; EDD, end-diastolic diameter; EF, ejection fraction; ESD, end-systolic diameter; GLS, global longitudinal strain; LV, left ventricle; LVMi, left ventricular mass indexed; NYHA, New York Heart Association; PASP, pulmonary artery systolic pressure; PWD, posterior wall diameter; PSS, peak systolic strain; RAVi, right atrial volume indexed; RV, right ventricle; TAPSE, tricuspid annular plane systolic excursion.

Table 3. RV systolic function parameters according to severity of MR

Variable	*Moderate CRMR (n = 51)*	*Severe CRMR (n = 26)*	p-*value*
RV wall thickness (mm)	5.9 ± 1.6	7.2 ± 2.3	0.006
PASP (mmHg)	31.0 ± 12.3	43.9 ± 21.3	0.001
RVS′ (cm/s)	11.6 (9.9–14.6)	11.4 (9.4–13.4)	0.29
TAPSE (cm)	2.1 ± 0.38	2.0 ± 0.4	0.28
RV free-wall PSS (%)	–17.7 ± 4.2	–15 ± 4.7	0.01

Data are presented as median (IQR), mean ± SD. CRMR, chronic rheumatic mitral regurgitation; PASP, pulmonary artery systolic pressure; PSS, peak systolic strain; RV, right ventricle; TAPSE, tricuspid annular plane systolic excursion.

There was a positive correlation between RV free-wall PSS and LVGLS in patients with CRMR ($r = 0.3$, $p < 0.001$). The majority of patients (45%) had preserved RV free-wall PSS and LVGLS, 26% had decreased LVGLS and RV free-wall PSS, 18% had diminished LVGLS and preserved RV free-wall PSS, and a minority (11%) had preserved LVGLS with decreased RV free-wall PSS (Fig. 2).

By univariate linear regression analysis, severe MR, grade ≥ 2+ TR, PASP, LVEF, LV end-diastolic diameter, lateral S′ and LVGLS showed a significant association with RV free-wall PSS, with LVGLS having the strongest correlation (Table 5). By multivariate linear regression analysis after adjusting for age and gender, LVGLS and grade ≥ 2+ TR emerged as the most important predictors of RVPSS (Table 5).

RV free-wall PSS measurements were feasible in 76 patients. In one patient, RV free-wall PSS was not feasible due to poor imaging of the lateral wall, however, LVGLS could be quantified. The intra-observer coefficient of variation for RV free-wall PSS was 7% with a mean difference ± SD of 0.4 ± 2.7 ($p = 0.5$), and for LVGLS it was 2.4% with a mean difference ± SD of 1.1 ± 2.7 ($p = 0.09$). The inter-observer variability coefficient was 7.6% for RV free-wall PSS with a mean difference ± SD of 0.5 ± 3.8 ($p = 0.5$) and for LVGLS it was 9.8% with a mean difference ± SD of 0.25 ± 2.4 ($p = 0.6$).

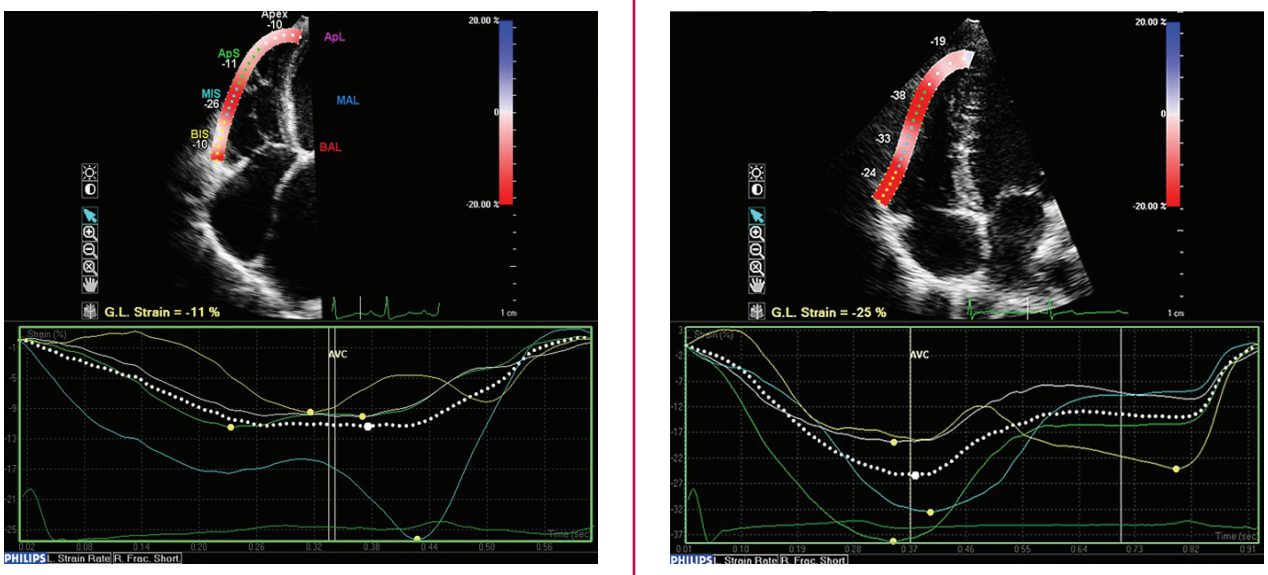

Fig. 1. Reduced RV free-wall peak systolic strain (PSS) in a chronic rheumatic mitral regurgitation patient (left) compared to normal RV free-wall PSS in a control subject (right).

Table 4. Comparison of RV systolic function parameters in CRMR according to LV systolic function

Variable	*LVEF < 60% (n = 32)*	*LVEF ≥ 60% (n = 45)*	p-*value*
RVS′ (cm/s)	11.3 (9.7–13.0)	12.0 (9.6–14.7)	0.27
TAPSE (cm)	1.9 ± 0.30	2.1 ± 0.41	0.07
LVGLS (%)	–13.1 ± 5.6	–18.2 ± 3.9	< 0.001
RVPSS (%)	–14.6 ± 4.1	–18.2 ± 4.2	0.0003
PASP (mmHg)	39.9 ± 21.5	31.6 ± 11.5	0.03

Data are presented as median (IQR), mean ± SD or %. EDD, end-diastolic diameter; GLS, global longitudinal strain; LV, left ventricle; PASP, pulmonary artery systolic pressure; PSS, peak systolic strain; RV, right ventricle; RVH, right ventricular hypertrophy; TAPSE, tricuspid annular plane systolic excursion.

Discussion

The pertinent findings of this study are firstly, that RV free-wall PSS is a sensitive marker of subclinical RV dysfunction in CRMR patients, as evidenced by depressed RV free-wall PSS when conventional clinical measures of RV function were normal. This trend was observed with CRMR patients compared to controls, moderate compared to severe MR and between those with normal LVEF and those with depressed LVEF. Secondly, LVGLS and significant TR were the most important determinant of RV free-wall PSS.

RV functional impairment and decreased LVEF are powerful predictors of cardiovascular and overall survival in degenerative MR.[6] The main determinants of RV function in MR are RV load, myocardial function, neuro-hormonal abnormalities and ventricular interaction.[5,26]

Only RV free-wall PSS was measured in this study as the interventricular septum contributes minimally to RV function.[27] RVPSS is known to have prognostic and predictive value in various cardiovascular disease states.[1,27] In this study RV systolic

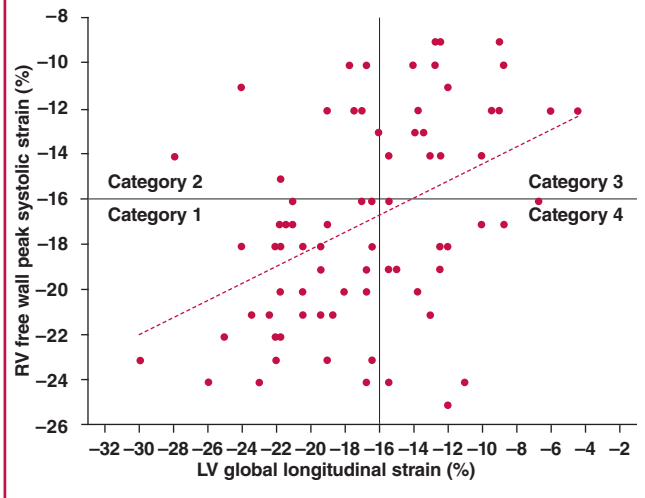

Fig. 2. Correlation between RV free-wall peak systolic strain (PSS) and LV global longitudinal strain (LVGLS) in chronic rheumatic mitral regurgitation (R^2 = 0.1984, p < 0.001). Category 1, normal LVGLS and normal RV free-wall PSS; category 2, normal LVGLS and decreased RV free-wall PSS; category 3, decreased LVGLS and decreased RV free-wall PSS; category 4, decreased LVGLS and normal RV free-wall PSS.

Table 5. Predictors of RV free-wall PSS in chronic rheumatic mitral regurgitation: uni- and multivariate linear regression analysis

Univariate models	R-*value*	*Adjusted* R^2	p-*value*
Age (years)	0.06	0.004	0.56
Gender (M)	0.14	0.008	0.20
LVEF (%)	0.33	0.09	0.003
LVEDD (mm)	0.29	0.07	0.009
Lateral S′ (cm/s)	0.24	0.04	0.03
PASP (mmHg)	0.31	0.08	0.006
Severe MR	0.29	0.07	0.008
LVGLS (%)	0.44	0.18	< 0.001
Grade ≥ 2+ TR	0.42	0.16	0.0001
Multivariate model $R = 0.56$, $p < 0.0001$			
LVGLS (%)	0.40	0.07	0.0004
Grade ≥ 2+ TR	0.37	0.07	0.001
Multivariate model $R = 0.58$, $p < 0.0001$			
LVGLS (%)	0.35	0.08	0.0009
Grade ≥ 2+ TR	0.38	0.46	0.005
PASP (mmHg)	–0.0007	0.44	0.99
Multivariate model $R = 0.57$, $p < 0.0001$			
LVGLS (%)	0.39	0.08	0.0006
Grade ≥ 2+ TR	0.29	0.24	0.01
Severe MR	0.12	0.26	0.27
Multivariate model $R = 0.56$, $p < 0.0001$			
LVGLS (%)	0.30	0.34	0.008
Grade ≥ 2+ TR	0.36	0.08	0.001
LVEF (%)	–0.08	0.31	0.45
Multivariate model $R = 0.55$, $p < 0.0001$			
LVGLS (%)	0.33	0.29	0.004
Grade ≥ 2+ TR	0.36	0.07	0.002
Lateral S′ (cm/s)	–0.04	0.38	0.69
Multivariate model $R = 0.5$, $p < 0.001$			
LVGLS (%)	0.34	0.16	0.002
Grade ≥ 2+ TR	0.36	0.05	0.001
LVEDD (mm)	0.13	0.14	0.26

EDD, end-diastolic diameter; EF, ejection fraction; GLS, global longitudinal strain; LV, left ventricle; MR, mitral regurgitation; PASP, pulmonary artery systolic pressure; TR, tricuspid regurgitation.

dysfunction was more prevalent by STE than with commonly used conventional markers of systolic function such as TAPSE and RVS′. STE-derived RVPSS has been shown to be feasible and reproducible for clinical use.[1,11,12] In this study RV free-wall PSS was feasible and reproducible in assessing RV function in CRMR. STE has been shown to be advantageous over conventional echocardiographic parameters used to measure RV systolic function in a variety of cardiovascular disorders such as heart failure, pulmonary hypertension and pre-operative and postoperative RV function assessment.[6,11,12,13,28]

This finding can be explained by technical aspects, as speckle-tracking is angle independent and less influenced by heart motion compared to TAPSE and RVS′.[1] Additionally, TAPSE and S′ only measure regional RV function, whereas RV free-wall PSS is able to provide more global assessment of RV function.[1] Furthermore, Focardi *et al.* recently showed that among all RV systolic function parameters, RVPSS had the best correlation with RVEF measured by cardiac magnetic resonance imaging.[29] Therefore, although STE is limited by image quality and load

dependence, unlike traditional echocardiographic parameters, it is able to detect subclinical longitudinal RV dysfunction.

The decreased RV free-wall PSS with preserved traditional markers of RV systolic function in this study implies subclinical RV dysfunction. The mechanism of reduced RV strain in this study may be related to the elevated PASP, as the RV is known to be extremely sensitive to afterload.[26,28] Even small increases in pulmonary vascular resistance can markedly decrease RV contractile function. Prior studies have noted a similar relationship between RV systolic performance and pulmonary hypertension in degenerative MR.[5,6]

Le Torneau *et al*. have shown in their study that, even though increased RV afterload secondary to PHT was an important cause of RV dysfunction in MR, LV dysfunction also contributed significantly to RV dysfunction, due to their interdependent relationship.[5] In this study PASP was only modestly elevated but the markers of LV remodelling and systolic function such as LVGLS, LVEDD and S′ velocity were markedly abnormal. Therefore, in agreement with Le Torneau *et al*.,[5] LV remodelling and LV dysfunction, in addition to the modest elevation in PASP, may be important causes of RV functional impairment in CRMR.

This is supported by the finding of reduced RV free-wall PSS in patients with LVEF < 60% and reduced LVGLS. Additionally, most patients had abnormal RV free-wall PSS in the presence of abnormal LVGLS, and those with normal RV free-wall PSS also had normal LVGLS. However, conventional RV systolic function parameters were still preserved even in the presence of LV systolic dysfunction. Hence, once abnormalities in LV systolic function are noted in MR, systematic RV function assessment must be done with not only traditional parameters but also STE, in order to detect subclinical RV dysfunction and reduce mortality associated with biventricular functional impairment.[5]

Severe MR was associated with worse RV function and was found to be a determinant of RVPSS in a study by Le Torneau *et al*.[5] Volume overload as a result of chronic MR results in LV remodelling, as noted in our study, and this in turn results in abnormalities of RV and LV interaction. RV free-wall PSS was lower in patients with severe MR compared to moderate MR. This association can be explained by greater chronic volume overload of the LV and left atrium, accompanied by increased PASP secondary to backward transmission of increased LV pressure, as well as remodelling of the pulmonary vasculature in severe compared to moderate MR.[30] However, a lack of difference in traditional RV systolic function parameters between the moderate and severe MR groups was present, and therefore quantitative RV function assessment in CRMR mandates evaluation by both conventional indices and RV longitudinal strain.

TR was an independent predictor of RV free-wall PSS. Significant TR is likely a reflection of deteriorating RV function secondary to left-sided disease. The increase in RV preload initially results in increased RV free-wall PSS due to increased myocardial lengthening in diastole and shortening in systole. Once RV myocardial contractile dysfunction ensues, however, RV systolic strain declines, as RV reaches the descending limb of the Frank–Starling curve.

Finally, the decline in RV free-wall PSS may be partially attributed to primary RV dysfunction. The intrinsic myocardial functional abnormality may be a result of longstanding activation of neuro-hormonal pathways and increased afterload secondary to chronic mitral regurgitation.[8,26] We further speculate that there may be direct involvement of the RV myocardium by the rheumatic process.

This study had two limitations: first, lack of reference standard for RV functional assessment such as additional imaging in the form of cardiac MRI and three-dimensional echocardiography, and second, we did not routinely perform right and left heart catheterisation to assess PASP, pulmonary vascular resistance and coronary anatomy.

Conclusion

In CRMR patients, RV free-wall PSS was a more sensitive marker for detecting earlier RV systolic dysfunction than traditional RV functional parameters. LVGLS and TR were important determinants of RV free-wall PSS in CRMR.

The first author was the recipient of the Carnegie PhD Fellowship award (Carnegie Corporation grant no. b8749.r01).

References

1. Lang RM, Plank C, Sadushi-Kolici R, Jakowitsch J, Klepetko W, Maurer G. Imaging in pulmonary hypertension. *J Am Coll Cardiol Cardiovasc Imaging* 2010; **3**(12): 1287–1295. DOI: 10.1016/j.jcmg.2010.09.013.
2. Anavekar NS, Skali H, Bourgoun M, Ghali JK, Kober L, Maggioni AP, *et al*. Usefulness of right ventricular fractional area change to predict death, heart failure, and stroke following myocardial infarction (from the VALIANT ECHO Study). *Am J Cardiol* 2008; **101**(5): 607–612. DOI: 10.1016/j.amjcard.2007.09.115.
3. Damy T, Viallet C, Lairez O, Deswarte G, Paulino A, Maison P, *et al*. Comparison of four right ventricular systolic echocardiographic parameters to predict adverse outcomes in chronic heart failure. *Eur J Heart Fail* 2009; **11**(9): 818–824. DOI: 10.1093/eurjhf/hfp111.
4. De Groote P, Fertin M, Goéminne C, Petyt G, Peyrot S, Foucher-Hossein C, *et al.* Right ventricular systolic function for risk stratification in patients with stable left ventricular systolic dysfunction: comparison of radionuclide angiography to echo Doppler parameters. *Eur Heart J* 2012; **33**(21): 2672–2679. DOI: 10.1093/eurheartj/ehs080.
5. Le Tourneau T, Deswarte G, Lamblin N, Foucher-Hossein C, Fayad G, Richardson M, *et al*. Right ventricular systolic function in organic mitral regurgitation: impact of biventricular impairment. *Circulation* 2013; **127**: 1597–608. DOI: 10.1161/CIRCULATIONAHA.112.000999.
6. Hyllén S, Nozohoor S, Ingvarsson A, Meurling C, Wierup P, Sjögren J. Right ventricular performance after valve repair for chronic degenerative mitral regurgitation. *Ann Thorac Surg* 2014; **98**(6): 2023–2030. DOI: 10.1016/j.athoracsur.2014.07.075.
7. Maffessanti F, Gripari P, Tamborini G, Muratori M, Fusini L, Alamanni F, *et al*. Evaluation of right ventricular systolic function after mitral valve repair: a two-dimensional Doppler, speckle-tracking, and three-dimensional echocardiographic study. *J Am Soc Echocardiogr* 2012; **25**(7): 701–708. DOI: 10.1016/j.echo.2012.03.017.
8. Polak JF, Holman BL, Wynne J, Colucci WS. Right ventricular ejection fraction: an indicator of increased mortality in patients with congestive heart failure associated with coronary artery disease. *J Am Coll Cardiol* 1983; **2**(2): 217–224. PMID: 6306086.
9. Grose R, Strain J, Yipintosoi T. Right ventricular function in valvular heart disease: relation to pulmonary artery pressure. *J Am Coll Cardiol* 1983; **2**(2): 225–232. PMID: 6408152.
10. Kumar V, Jose VJ, Pati PK, Jose J. Assessment of right ventricular strain

and strain rate in patients with severe mitral stenosis before and after balloon mitral valvuloplasty. *Indian Heart J* 2014; **66**(2): 176–182. DOI: 10.1016/j.ihj.2014.02.012.

11. Morris DA, Krisper M, Nakatani S, Köhncke C, Otsuji Y, Belyavskiy E, *et al*. Normal range and usefulness of right ventricular systolic strain to detect subtle right ventricular systolic abnormalities in patients with heart failure: a multicentre study. *Eur Heart J Cardiovasc Imaging* 2017; **18**(2): 212–223. DOI: 10.1093/ehjci/jew011.
12. Ternacle J, Berry M, Cognet T, Kloeckner M, Damy T, Monin JL, *et al*. Prognostic value of right ventricular two-dimensional global strain in patients referred for cardiac surgery. *J Am Soc Echocardiogr* 2013; **26**(7): 721–726. DOI: 10.1016/j.echo.2013.03.021.
13. Guendouz S, Rappeneau S, Nahum J, Dubois-Randé JL, Gueret P, Monin JL, *et al*. Prognostic significance and normal values of 2D strain to assess right ventricular systolic function in chronic heart failure. *Circ J* 2012; **76**(1): 127–136. PMID: 22033348.
14. Lang RM, Badano LP, Mor-Avi V, Afilalo J, Armstrong A, Ernande L, *et al*. Recommendations for cardiac chamber quantification by echocardiography in adults: an update from the American Society of Echocardiography and the European Association of Cardiovascular Imaging. *J Am Soc Echocardiogr* 2015; **28**(1): 1–39. DOI: 10.1016/j.echo.2014.10.003.
15. Nagueh SF, Appleton CP, Gillebert TC, Marino PN, Oh JK, Smiseth OA, *et al*. Recommendations for the evaluation of left ventricular diastolic function by echocardiography. *J Am Soc Echocardiogr* 2009; **22**(2): 107–133. PMID: 19187853.
16. Rudski LG, Lai WW, Afilalo J, Hua L, Handschumacher MD, Chandrasekaran K, *et al*. Guidelines for the echocardiographic assessment of the right heart in adults: a report from the American Society of Echocardiography: endorsed by the European Association of Echocardiography, a registered branch of the European Society of Cardiology, and the Canadian Society of Echocardiography. *J Am Soc Echocardiogr* 2010; **23**(7): 685–713. DOI: 10.1016/j.echo.2010.05.010.
17. Nishimura RA, Otto CM, Bonow RO, Carabello BA, Erwin JP, Guyton RA, *et al*. 2014 AHA/ACC guideline for the management of patients with valvular heart disease: a report of the American College of Cardiology/American Heart Association Task Force on Practice Guidelines. *J Am Coll Cardiol* 2014; **63**(22): e57–185. doi: 10.1016/j.jacc.2017.03.011.
18. Reményi B, Wilson N, Steer A, Ferreira B, Kado J, Kumar K, *et al*. World Heart Federation criteria for echocardiographic diagnosis of rheumatic heart disease – an evidence-based guideline. *Nature Rev Cardiol* 2012; **9**(5): 297–309. DOI: 10.1038/nrcardio.2012.7.
19. Zoghbi WA, Enriquez-Sarano M, Foster E, Grayburn PA, Kraft CD, Levine RA, *et al*. Recommendations for evaluation of the severity of native valvular regurgitation with two-dimensional and Doppler echocardiography. *J Am Soc Echocardiogr* 2003; **16**(7): 777–802. DOI: 10.1016/S0894-7317(03)00335-3.
20. Younan H. Role of two dimensional strain and strain rate imaging in assessment of left ventricular systolic function in patients with rheumatic mitral stenosis and normal ejection fraction. *Egyptian Heart J* 2015; **67**(3): 193–**19**8. https://doi.org/10.1016/j.ehj.2014.07.003.
21. Marciniak A, Claus P, Sutherland GR, Marciniak M, Karu T, Baltabaeva A, *et al*. Changes in systolic left ventricular function in isolated mitral regurgitation. Strain rate imaging study. *Eur Heart J* 2007; **28**(21): 2627–2636. DOI: 10.1093/eurheartj/ehm072.
22. Kocabay G, Muraru D, Peluso D, Cucchini U, Mihaila S, Padayattil-Jose S, *et al*. Normal left ventricular mechanics by two-dimensional speckle-tracking echocardiography. Reference values in healthy adults. *Rev Española Cardiología* (English edn) 2014; **67**(8): 651–658. doi: 10.1016/j.rec.2013.12.009.
23. Mingo-Santos S, Moñivas-Palomero V, Garcia-Lunar I, Mitroi CD, Goirigolzarri-Artaza J, Rivero B, *et al*. Usefulness of two-dimensional strain parameters to diagnose acute rejection after heart transplantation. *J Am Soc Echocardiogr* 2015; **28**(10): 1149–1156. doi: 10.1016/j.echo.2015.06.005.
24. Konishi K, Dohi K, Tanimura M, Sato Y, Watanabe K, Sugiura E, *et al*. Quantifying longitudinal right ventricular dysfunction in patients with old myocardial infarction by using speckle-tracking strain echocardiography. *Cardiovasc Ultrasound* 2013; **11**(1): 1. doi: 10.1186/1476-7120-11-23.
25. Todaro MC, Romano G, Carerj S, Clemenza F, Pilato M, Khandheria BK. Right ventricular free wall strain: a predictor of successful left ventricular assist device implantation. *Texas Heart Inst J* 2015; **42**(1): 87–89. DOI: 10.14503/THIJ-14-4111.
26. Friedberg MK, Redington AN. Right versus left ventricular failure differences, similarities, and interactions. *Circulation* 2014; **129**(9): 1033–1044. doi: 10.1161/circulationaha.113.001375.
27. Fine NM, Chen L, Bastiansen PM, Frantz RP, Pellikka PA, Oh JK, Kane GC. Reference values for right ventricular strain in patients without cardiopulmonary disease: a prospective evaluation and meta-analysis. *Echocardiography* 2015; **32**(5): 787–796. DOI: 10.1111/echo.12806.
28. Fukuda Y, Tanaka H, Sugiyama D, Ryo K, Onishi T, Fukuya H, *et al*. Utility of right ventricular free wall speckle-tracking strain for evaluation of right ventricular performance in patients with pulmonary hypertension. *J Am Soc Echocardiogr* 2011; **24**(10): 1101–1108. doi: 10.1016/j.echo.2011.06.005.
29. Focardi M, Cameli M, Carbone SF, Massoni A, de Vito R, Lisi M, Mondillo S. Traditional and innovative echocardiographic parameters for the analysis of right ventricular performance in comparison with cardiac magnetic resonance. *Eur Heart J Cardiovasc Imaging* 2015; **16**(1): 47–52. doi: 10.1093/ehjci/jeu156.
30. Mann DL, Zipes DP, Libby P, Bonow RO. *Braunwald's Heart Disease: A Textbook of Cardiovascular Medicine.* New York: Elsevier Health Sciences, 2014.

The effect of perindopril on echocardiographic parameters, NYHA functional class and serum NT-proBNP values in patients with diastolic heart failure

Umit Yuksek, Levent Cerit, Nihan Kahya Eren, Oktay Ergene

Abstract

Introduction: Growing evidence has demonstrated that diastolic heart failure occurs in about half of heart failure (HF) patients. We investigated the effects of perindopril on echocardiographic parameters, New York Heart Association (NYHA) functional class and serum N-terminal pro B-type natriuretic peptide (NT-proBNP) levels in patients with diastolic heart failure.

Methods: In total, 108 diastolic heart failure patients aged ≥ 50 years, who had diastolic dysfunction with an ejection fraction ≥ 50%, were enrolled and randomised to one of the two study groups. Perindopril was initiated in the study group and the control group was given standard therapy. Echocardiographic parameters, NT-proBNP levels and NYHA classes were recorded. The patients were followed for 11 (three to 16) months. Eighty-eight patients completed the study.

Results: Although diastolic parameters were not changed, A′ (septal) velocity (10.8 vs 9.9 cm/s) and Sm (septal) velocity (8.5 vs 7.6 cm/s) were significantly increased in the perindopril compared to the control group. A significant increase in A′ (septal) velocity (+0.61 vs –0.28 cm/s, $p = 0.04$) and a slight increase in Sm (septal) velocity (+0.99 vs 0.36 cm/s, $p = 0.054$) were noted in the perindopril group.

Conclusions: Tissue Doppler septal late diastolic velocities and septal systolic myocardial velocities increased in the perindopril group but NT-proBNP levels, and NYHA class was not changed in this study population.

Keywords: diastolic heart failure, perindopril, NT-proBNP, transthoracic echocardiography

Submitted 9/11/18, accepted 21/4/19
Published online 24/5/19
Cardiovasc J Afr 2019; **30**: 222–227 www.cvja.co.za

DOI: 10.5830/CVJA-2019-022

Department of Cardiology, Near East University Hospital, Nicosia, Cyprus
Umit Yuksek, MD
Levent Cerit, MD, drcerit@hotmail.com

Department of Cardiology, Izmir Ataturk Education and Research Hospital, Izmir, Turkey
Nihan Kahya Eren, MD

Department of Cardiology, 9 Eylul University Hospital, Izmir, Turkey
Oktay Ergene, MD

Heart failure (HF) with normal or preserved ejection fraction (HFpEF), also called diastolic heart failure (DHF), occurs in about half of HF patients. DHF is defined as a clinical syndrome in patients with symptoms and/or signs of HF who have an ejection fraction of ≥ 50%, accompanied by elevated natriuretic peptide levels and relevant structural heart disease (left ventricular hypertrophy and/or left atrial enlargement) or diastolic dysfunction on echocardiography according to 2016 European Society of Cardiology guidelines for heart failure.[1] Diastolic dysfunction (DD) is an important component of HFpEF.

In some previous studies, DD was an inclusion criterion for the study (e.g. PEP-CHF study), whereas it was not a prerequisite in others (e.g. I-PRESERVE or CHARM-Preserved trials). In an echocardiographic sub-study of the CHARM-Preserved trial, 67% of the patients had DD.[2] Left atrial (LA) function, which is a component of diastolic function, is also an important contributor to the pathophysiology of HFpEF. Several previous studies demonstrated that increased LA size and decreased LA systolic function are the most important part of the HFpEF.[3,4]

Parameters indicating LA systolic function may be found abnormal in HFpEF patients during exercise and may correlate with reduced exercise capacity in these patients.[5] There are many ways to assess LA systolic function, such as measurements of LA systolic strain, LA emptying fraction and end-diastolic mitral annular velocity in pulsed tissue Doppler. Doppler tissue imaging of the mitral annulus during atrial systole has been shown to be a practical method to quantify left atrial contractile function.[6] This parameter (Am) correlates well with the changes in LA fractional area, and it therefore provides an easy way to assess LA systolic function.

It has long been evident that this disease is not only a disease of diastolic function. A number of studies have shown that left ventricular longitudinal function, which is a component of systolic function that can be measured as myocardial systolic velocity (Sm) in tissue Doppler echocardiography (TDE), is also reduced in these patients, even though the ejection fraction is within the so-called 'normal' or 'preserved' limits.[7-13]

Benefits of some drugs were demonstrated on diastolic function in DHF patients. A calcium channel blocker (CCB), verapamil, was shown to have some benefit on diastolic function in patients with HFpEF.[14,15] Recently eplerenone induced improvements in diastolic echocardiographic measures (e.g. E/E′ parameter) in HFpEF patients.[16] In the Hong Kong diastolic heart failure study, both irbesartan and ramipril, added to diuretics in HFpEF patients, increased mean peak systolic (Sm) and early diastolic (Em) mitral annular velocities in TDE.[17] There are also some studies investigating the effects of perindopril on diastolic function in patients with hypertension (HT), diabetes mellitus (DM), or stable coronary artery disease

(CAD).[18-20] In those studies, perindopril improved the parameters of diastolic function in patients with HT and CAD but did not affect diastolic function in diabetic patients.

The effects of perindopril on the echocardiographic parameters of diastolic and systolic function have not been previously investigated in patients with DHF. Given the aforementioned studies, we aimed to investigate the effects of perindopril on the parameters of diastolic left atrial function and longitudinal myocardial function with TDE in patients with DHF. We also investigated whether perindopril treatment changed the NYHA functional class and serum NT-proBNP levels in this study population.

Methods

We enrolled 108 patients with DHF, aged ≥ 50 years, who presented to Izmir Ataturk Education and Research Hospital (IAERH) cardiology out-patient clinics with HF symptoms and were found to have an ejection fraction (EF) of ≥ 50% on transthoracic echocardiography (TTE) accompanied by an evidence of DD on TDE. The HF diagnosis was based on Framingham heart failure criteria.

Exclusion criteria included the following: EF < 50%, patient age < 50 years, severe valvular disease on echocardiography, a history of acute coronary syndrome, atrial fibrillation, cardiomyopathy or pericardial disease, anaemia (serum haemoglobin levels < 10 g/dl), hyperthyroidism, hypothyroidism, renal insufficiency (serum creatinine > 2 mg/dl or dialysis), serum potassium level > 5.5 mEq/l, moderate to severe pulmonary hypertension (sPAP > 50 mmHg), and/or intolerance to angiotensin converting enzyme inhibitors (ACEIs) or angiotensin receptor blockers (ARBs), bilateral renal artery stenosis, or any kind of malignancy. Patients with decompensated HF were also excluded.

The patients were randomised into two groups using a basic randomisation method. The first group (perindopril group) was started on oral perindopril treatment (5 mg/day) and the control group received standard DHF treatment alone. None of the patients was using ACEIs or ARBs before enrollment in the study. The study was designed as a randomised and prospective study.

All patients underwent a detailed clinical examination and comprehensive TTE (including TDE) using standardised equipment (Vivid 3 Pro Echocardiography, General Electric Corp, Milwaukee, WI, USA). EF was measured both visually and using the M-mode method. All echocardiographic parameters were measured and recorded.

Blood pressure measurements were taken after 10 minutes of rest. The height and weight of all patients were measured and body mass index (BMI) was calculated. The functional capacity of the patients was assessed according to the NYHA classification system (I-IV). Blood samples were drawn from all patients for biochemistry, complete blood count and NT-proBNP analyses. Blood samples for NT-proBNP measurements were stored in a –70°C refrigerator until the time of analysis, and were analysed using Siemens Corp Immulite-2000 NT-proBNP kites.

The study was approved by the local ethics committee of IAERH and was conducted in accordance with the Declaration of Helsinki.

The patients were followed for a mean period of 11 months (range: three to 16 months). After one month of follow up, blood samples were drawn from all patients for biochemistry analyses and complete blood counts. No significant deteriorations were noted in serum creatinine or potassium levels, and all patients had tolerated the study drug during this period. Accordingly, perindopril dose in the study group was up-titrated to 10 mg/day at the end of one month.

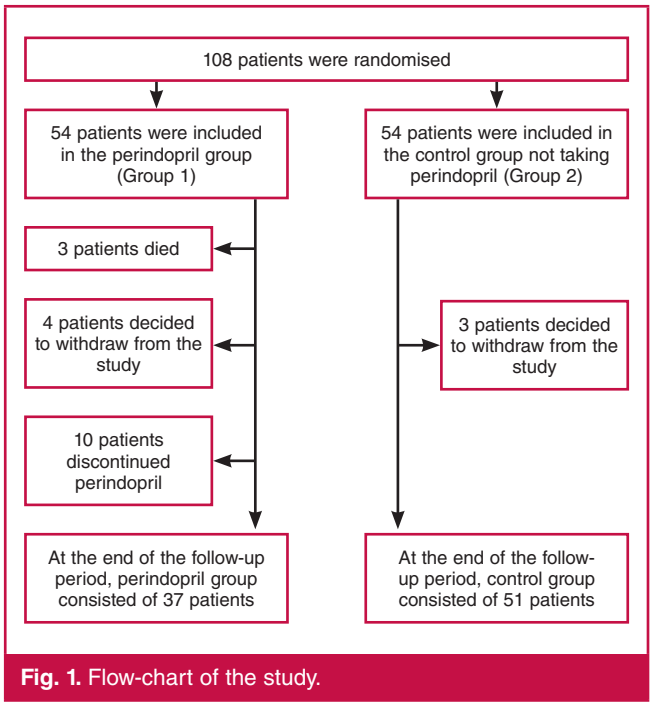

Fig. 1. Flow-chart of the study.

Over the 11-month follow-up period, seven patients decided to withdraw from the study and three patients died. Perindopril was discontinued in 10 patients for different reasons (due to any side effect). Therefore, at the end of the follow-up period, the perindopril group consisted of 37 patients and the control group included 51 patients (Fig. 1). At the end of the follow-up period, all patients were invited to the hospital and echocardiographic assessments were repeated. Blood samples were drawn for biochemistry and NT-proBNP measurements. NYHA functional classes were reassessed and recorded.

The primary endpoints of the study were the changes in E′, A′, and Sm velocities, E/E′, E/A, and E′/A′ ratios, isovolumic relaxation time (IVRT) and deceleration time (DT) at the end of the follow-up period. Secondary endpoints included the changes in NT-proBNP levels and NYHA functional classes.

Statistical analysis

The Statistical Package for the Social Sciences (SPSS) version 15.0 software program was used for statistical analysis. The Kolmogorov–Smirnov test was used to determine whether the numerical variables were normally distributed. A *t*-test was used to compare normally distributed variables between the two groups and the Mann–Whitney *U*-test was conducted for non-normally distributed variables. For categorical variables, cross-tables were made, and chi-squared analysis or Fisher's exact test was performed. The changes from baseline until the end of the 11-month follow-up period were assessed using the Wilcoxon test for non-normally distributed variables and a paired-samples *t*-test for normally distributed variables. A *p*-value of < 0.05 was accepted as statistically significant.

Table 1. Comparison of the baseline characteristics of the study groups

Variable	*Perindopril group (n = 37)*	*Control group (n = 51)*	p-*value*
Age (years)	62 ± 8	61 ± 8	0.879
Female, *n* (%)	31 (84)	38 (75)	0.432
Hypertension, *n* (%)	31 (84)	41 (80)	0.784
Diabetes mellitus, *n* (%)	19 (51)	17 (33)	0.124
Coronary artery disease, *n* (%)	4 (11)	11 (22)	0.254
Peripheral arterial disease, *n* (%)	2 (5)	0 (0)	0.174
Hyperlipidaemia, *n* (%)	18 (49)	30 (59)	0.390
Antihyperlipidaemics, *n* (%)	5 (14)	10 (20)	0.571
Aspirin, *n* (%)	15 (41)	20 (39)	1.000
Calcium antagonists, *n* (%)	28 (76)	26 (51)	0.026
Beta-blockers, *n* (%)	15 (41)	20 (39)	1.000
Antidiabetics, *n* (%)	15 (41)	12 (24)	0.105
Diuretics, *n* (%)	19 (51)	30 (59)	0.521
Body mass index (kg/m²)	33 ± 6	33 ± 5	0.914
Systolic blood pressure (mmHg)	126 ± 16	123 ± 19	0.341
Diastolic blood pressure (mmHg)	76 ± 12	73 ± 13	0.388
Serum creatinine level (mg/dl)	0.92 ± 0.14	0.98 ± 0.25	0.126
NYHA class, *n* (%)			
2	29 (78)	33 (65)	0.237
3	8 (22)	18 (35)	
NT-proBNP (pg/ml)			
Median	114	128	0.391

NYHA; New York Heart Association.

Results

The mean age of the patients was 62 years (50–83). Of all patients, 78% were women; 81.8% were hypertensive, and 31% had a history of heart failure. Sixty-one per cent of the patients were receiving CCBs, 39% were receiving beta-blockers, and 55.6% were using diuretics. One per cent of the patients were in NYHA functional class 1, 68% were in NYHA class 2, and 31% were in NYHA class 3.

During the 11 months of follow up, seven patients withdrew from the study and three patients died. Perindopril treatment was discontinued in 10 patients due to side effects (dry cough and hypotension). Therefore, at the end of the study period, the perindopril group consisted of 37 patients and the control group included 51 patients. The final analyses of the study were made on the data from 88 patients. The patients in the perindopril group used CCBs more frequently than the patients in the control group (76 vs 51%, $p = 0.026$). The other clinical and demographic characteristics were similar between the two groups (Table 1).

Echocardiographic parameters: At the study baseline, the mean visual EF of the patients was 64%, and the mean EF on M-mode was 65%. Mean left atrial volume index (LAVI) was 24 ml/m². The mean E/A ratio was 0.80, while the average E′ (mean) velocity was 6.5 cm/s. The average A′ (septal) velocity was measured as 10.1 cm/s, whereas A′ (lateral) velocity was 10.2 cm/s and A′ (mean) velocity was 10.2 cm/s. The E/E′ (mean) ratio was 11.2. The average Sm (septal) velocity was 7.2 cm/s, and Sm (lateral) velocity was 7.0 cm/s; Sm (mean) velocity was 7.2 cm/s. Twenty-six per cent of the patients had left ventricular hypertrophy (LVH); 85% had grade 1 DD, and 15% had grade 2 DD. None of the patients had grade 3 DD. There was no significant difference between the two groups in terms of the baseline echocardiographic parameters (Table 2).

Primary outcomes: At the end of the follow-up period, EF values were similar between the two groups. Mean LAVI values, mean E/A ratios, average E′ (mean) velocities, average A′ (mean) velocities, E/E′ (mean) ratios were also not significantly different between the two groups. LVH was found in 30 and 26% of the patients in the perindopril and control groups, respectively.

When we compared the echocardiographic parameters of the two groups at the end of the follow-up period, all parameters were comparable except for significant differences noted in A′ (sep), Sm (sep) and Sm (mean) velocities. A′ (sep), Sm (sep) and Sm (mean) velocities were significantly higher in the perindopril group (Table 3). A′ (sep) velocity in the perindopril group was significantly higher than in the control group (10.8 vs 9.9 cm/s, 95% CI: 0.065–1.795, $p = 0.036$). Sm (sep) velocity was also elevated in the perindopril group (8.5 vs 7.6 cm/s, 95% CI: 0.127–1.791, $p = 0.025$). Sm (mean) velocity was also higher in the perindopril group (8.3 vs 7.7 cm/s, 95% CI: 0.046–1.163, $p = 0.034$). DT and IVRT values were similar between the two

Table 2. Comparison of the baseline echocardiographic parameters in the study groups

Variable	*Perindopril group (n = 37)*	*Control group (n = 51)*	p-*value*
LA diameter (mm)	39 ± 5	40 ± 4	0.742
LVH, *n* (%)	11 (30)	12 (24)	0.624
LAV (ml)	44 ± 11	46 ± 11	0.382
LAVI (ml/m²)	24 ± 6	25 ± 6	0.726
EF (%)	66 ± 7	65 ± 8	0.591
E velocity (m/s)	0.75 ± 0.17	0.72 ± 0.17	0.446
A velocity (m/s)	0.94 ± 0.20	0.95 ± 0.24	0.902
E/A ratio	0.83 ± 0.26	0.80 ± 0.24)	0.537
E′ (sep) velocity (cm/s)	6.5 ± 1.0	6.5 ± 0.8	0.925
E′ (lat) velocity (cm/s)	6.7 ± 0.9	6.5 ± 1.0	0.327
A′ (sep) velocity (cm/s)	10.2 ± 1.7	10.2 ± 1.6	0.919
A′ (lat) velocity (cm/s)	10.3 ± 2.6	10.2 ± 2.1	0.867
E′ (mean) velocity (cm/s)	6.6 ± 0.8	6.5 ± 0.8	0.491
A′ (mean) velocity (cm/s)	10.3 ± 1.8	10.2 ± 1.5	0.872
E′/A′ (sep) ratio	0.65 ± 0.13	0.66 ± 0.11	0.880
E′/A′ (lat) ratio	0.67 ± 0.15	0.66 ± 0.16	0.569
E′/A′ (mean) ratio	0.66 ± 0.12	0.65 ± 0.12	0.684
E/E′ (sep) ratio	11.7 ± 2.8	11.2 ± 2.8	0.472
E/E′ (lat) ratio	11.3 ± 2.7	11.4 ± 3.1	0.953
E/E′ (mean) ratio	11.4 ± 2.5	11.2 ± 2.8	0.787
Sm (lat) velocity (cm/s)	7.3 ± 1.9	7.0 ± 1.5	0.450
Sm (sep) velocity (cm/s)	7.5 ± 2.0	7.2 ± 1.3	0.351
Sm (mean) velocity (cm/s)	7.4 ± 1.7	7.1 ± 1.1	0.350
DD grade, *n* (%)			
Grade 1	31 (84)	42 (82)	1.000
Grade 2	6 (16)	9 (18)	
IVRT, mean (msn)	132 ± 27	129 ± 21	0.533
DT, mean (msn)	238 ± 39	241 ± 35	0.658

LA: left atrium, LVH: left ventricular hypertrophy, LAV: left atrial volume, LAVI: left atrial volume index, EF: ejection fraction, E velocity: early diastolic mitral inflow velocity, A velocity: late diastolic mitral inflow velocity, E/A: ratio between early and late diastolic mitral inflow velocities, E′ (sep) velocity: septal tissue Doppler early diastolic mitral annular velocity, A′ (sep) velocity: septal tissue Doppler late diastolic mitral annular velocity, E′ (lat) velocity: lateral tissue Doppler early diastolic mitral annular velocity, A′ (lat) velocity: lateral tissue Doppler late diastolic mitral annular velocity, E′ (mean) velocity: mean tissue Doppler early diastolic mitral annular velocity, A′ (mean) velocity: mean tissue Doppler late diastolic mitral annular velocity, E′/A′ (sep, lat, mean): the ratio between septal/lateral/mean tissue Doppler early and late diastolic mitral annular velocities, E/E′ (sep, lat, mean): the ratio between septal/lateral/mean early diastolic mitral inflow velocities and tissue Doppler early diastolic mitral annular velocities, Sm (sep, lat, mean): septal/lateral/mean tissue Doppler systolic mitral annular velocities, DD: diastolic dysfunction, IVRT: isovolumic relaxation time, DT: deceleration time, SD: standard deviation.

Table 3. Comparison of the echocardiographic parameters at the end of the 11-month follow-up period

Variable	*Perindopril group (n = 37)*	*Control group (n = 51)*	p-*value*
LA diameter (mm)	40 ± 5	40 ± 4	0.994
LVH, *n* (%)	11 (30)	13 (26)	0.809
LAVI (ml/m²)	25 ± 6	25 ± 5	0.830
M-mode EF (%)	65 ± 7	64 ± 6	0.669
E/A ratio	0.86 ± 0.24	0.83 ± 0.21	0.520
E′ (sep) velocity (cm/s)	6.8 ± 0.7	6.6 ± 0.7	0.153
E′ (lat) velocity (cm/s)	7.2 ± 0.8	7.0 ± 0.9	0.460
A′ (sep) velocity (cm/s)	10.8 ± 2.4	9.9 ± 1.2	0.036
A′ (lat) velocity (cm/s)	10.5 ± 1.8	10.4 ± 1.5	0.710
E′ (mean) velocity (cm/s)	7.0 ± 0.5	6.8 ± 0.7	0.165
A′ (mean) velocity (cm/s)	10.7 ± 1.6	10.2 ± 1.2	0.093
E′/A′ (mean) ratio	0.67 ± 0.13	0.68 ± 0.11	0.628
E/E′ (mean) ratio	11.2 ± 2.4	11.6 ± 2.7	0.487
Sm (lat) velocity (cm/s)	8.1 ± 1.8	7.8 ± 1.3	0.399
Sm (sep) velocity (cm/s)	8.5 ± 2.2	7.6 ± 1.4	0.025
Sm (mean) velocity (cm/s)	8.3 ± 1.6	7.7 ± 1.1	0.034
DD grade, *n* (%)			
Grade 1	30 (81)	44 (86)	0.564
Grade 2	7 (19)	7 (14)	
IVRT, mean (msn)	118 ± 16	117 ± 17	0.806
DT, mean (msn)	224 ± 27	233 ± 29	0.128

Table 4. Comparison of the change in echocardiographic parameters during the 11-month follow-up period between the two groups

Variable	*Perindopril group (n = 37)*	*Control group (n = 51)*	p-*value*
Change in LA diameter (mm)	0.2 ± 2.0	–0.1 ± 1.9	0.449
Change in LAVI (ml/m²)	0.74 ± 2.77	0.55 ± 3.14	0.764
Change in M-mode EF (%)	–0.8 ± 6.7	–0.5 ± 6.9	0.864
Change in E/A ratio	0.03 ± 0.26	0.03 ± 0.20	0.977
Change in E′ (sep) velocity (cm/s)	0.35 ± 0.90	0.14 ± 0.83	0.253
Change in E′ (lat) velocity (cm/s)	0.48 ± 0.87	0.55 ± 0.92	0.737
Change in A′ (sep) velocity (cm/s)	0.61 ± 2.04	–0.28 ± 1.95	0.040
Change in A′ (lat) velocity (cm/s)	0.21 ± 2.47	0.16 ± 2.04	0.921
Change in E′ (mean) velocity (cm/s)	0.42 ± 0.69	0.35 ± 0.66	0.634
Change in A′ (mean) velocity (cm/s)	0.42 ± 1.54	–0.05 ± 1.65	0.171
Change in E′/A′ (mean) ratio	0.01 ± 0.11	0.03 ± 0.13	0.394
Change in E/E′ (mean) ratio	–0.2 ± 2.5	0.4 ± 2.0	0.259
Change in Sm (lat) velocity (cm/s)	0.84 ± 1.26	0.85 ± 1.43	0.995
Change in Sm (sep) velocity (cm/s)	0.99 ± 1.73	0.36 ± 1.28	0.054
Change in Sm (mean) velocity (cm/s)	0.90 ± 1.12	0.60 ± 1.07	0.210
Change in IVRT, according to DD grade (msn)			
Grade 1	–18 ± 18	–14 ± 18	0.373
Grade 2	– 2 ± 20	–3 ± 19	0.873
Change in DT, according to DD grade (msn)			
Grade 1	–15 ± 28	–12 ± 21	0.660
Grade 2	–8 ± 42	–10 ± 32	0 295

The change in the parameters was calculated as the value at 11 months – value at 0 months. Because the meaning of the change in DT and IVRT was different in diastolic dysfunction grades 1 and 2, the comparisons between DT and IVRT values were stratified according to the diastolic dysfunction grade.

groups, which suggested that perindopril treatment did not have a significant effect on these variables.

We also analysed the changes in the echocardiographic parameters from baseline until the end of the follow-up period. For this purpose, we compared the differences in the values recorded at the end of the follow-up period between the two groups. As a result, we found that only the change in the A′ (sep) velocity parameter was statistically significant. In the perindopril group, the A′ (sep) velocity increased, whereas it decreased in the control group. During the study we observed 0.61 cm/s increase in A′ (sep) velocity in the perindopril group and a decrease of 0.28 cm/s in the control group (0.61 vs –0.28 cm/s, 95% CI: 0.039–1.748, $p = 0.04$). The increase in Sm (sep) velocity in the perindopril group also reached near significance ($p = 0.054$). The changes observed in the other parameters were not statistically significant (Table 4).

Secondary outcomes: At the end of the follow-up period, the median NT-proBNP level was 150 pg/ml. In the perindopril group, the median level was 151 pg/ml and in the control group, it was 149 pg/ml. When the two groups were compared, the NT-proBNP levels were not found to be significantly different ($p = 0.688$ for the comparison of the median values). NT-proBNP levels did not change significantly with perindopril.

At the end of the follow-up period, 57 (65%) patients were in NYHA functional class 2, whereas 31 (35%) were in NYHA class 3. When we compared the two groups, no statistically significant difference was found in terms of the functional capacity at the end of the study ($p = 0.184$). When we analysed the two groups to determine the change in functional capacity during the follow-up period, no meaningful changes in NYHA functional class were found in either group (Table 5).

Discussion

HFpEF is a clinical syndrome that is becoming more frequently seen as the population ages worldwide. More strikingly, its mortality rate has not changed for decades while the mortality rate of systolic HF has declined significantly.[21] DD is an important component of HFpEF. Some small studies have reported improvements in DD with some drugs such as CCBs, aldosterone receptor blockers, ACEIs and ARBs in this patient population.[14-17] However, no previous study assessed the effect of perindopril on diastolic and systolic function in HFpEF patients.

In this study, we found that perindopril treatment increased tissue Doppler septal late diastolic velocity and slightly increased tissue Doppler septal systolic myocardial velocity in HFpEF patients. It did not improve the E/E′ ratio and tissue Doppler early diastolic velocity, which are markers of increased diastolic pressure in this population. The other diastolic parameters did not improve with perindopril treatment. In fact, only a few studies have reported improvements in systolic or diastolic echocardiographic parameters in HFpEF patients. One of these studies is the Hong Kong Diastolic Heart Failure study, which reported improvements in E′ and Sm velocities with ramipril and irbesartan.[17] It is well known that both E′ and Sm velocities

Table 5. Change in NYHA functional class of the patients in the two groups of the study at the end of the11-month follow-up period

	NYHA class, 11 months		
NYHA class, 0 months	*Class 2*	*Class 3*	p-*value*
Group 1			
Class 2	25	4	0.687
Class 3	2	6	
Group 2			
Class 2	28	5	0.453
Class 3	2	16	

are reduced in HFpEF patients, although EF is within normal limits.[9-13] Therefore, the systolic function cannot be considered normal in these patients.

The loss of longitudinal function may be compensated for by increased radial motion, which may preserve the EF in HFpEF patients; an effect that is also seen in diabetic patients.[22] The Sm velocity was shown to be a prognostic marker in patients with systemic hypertension and left ventricular hypertrophy, as well as patients with dilated cardiomyopathy.[23-25] The improvement in septal tissue Doppler myocardial systolic velocity may be an important finding of the present study, although it did not translate into an improvement in EF, likely due to the short duration of follow up. An improvement in EF also may be noticed in the long term.

To the best of our knowledge, this study is the first to show that perindopril treatment improved tissue Doppler systolic function in HFpEF patients. Improvement in systolic function may be related to several mechanisms, including reduction in myocardial fibrosis, left ventricular mass, ischaemia or afterload.

The improvement in tissue Doppler septal late diastolic velocity may also be another important finding of this study. Since this velocity represents LA systolic function in HFpEF patients, perindopril treatment also improved the left atrial function in these patients. This velocity is not the only way to assess left atrial function, but it is a practical way to show the contractile function of the left atrium.[6] Left atrial dysfunction was associated with exercise intolerance in HFpEF patients,[5] so improving this function may decrease exercise dyspnoea, which is an important symptom in these patients. We could not demonstrate symptomatic improvement in our patient group.

Future studies should investigate whether this improvement in left atrial systolic function is also seen during exercise in these patients. It may be more crucial to improve exercise left atrial function since the symptoms are generally exacerbated with exercise. A longer duration of follow up may also show some benefit on symptoms.

The median serum NT-proBNP level of the patients recruited to the present study was 135 pg/ml. This value may be considered low for an HFpEF diagnosis. In reality, there are not clearly defined cut-off values for the diagnosis of this syndrome. In the consensus document of the European Society of Cardiology (ESC) regarding HFpEF published in 2007, natriuretic peptides (NPs) were offered to aid the diagnosis when the E/E′ ratio was between eight and 15.[26] According to this document, an NT-proBNP value > 220 pg/ml supports the diagnosis of HFpEF, but NT-proBNP < 120 pg/ml makes the diagnosis unlikely. In the new 2016 ESC guidelines for heart failure, it is stated that an NT-proBNP value > 125 pg/ml supports the diagnosis of HFpEF.[1]

Other studies have also investigated NP levels in DHF patients. In one of those articles, in patients presenting to the out-patient clinic (similar to our study), if the patient's volume status was stable or optivolaemic, NP levels in HFpEF patients may be much lower.[27] A different study that enrolled 159 HFpEF patients reported that 29% of the patients had normal BNP values (≤ 100 pg/ml). These patients were symptomatic and had elevated pulmonary capillary wedge pressures.[28] The authors found that patients with normal BNP levels were younger, were more often female, were mostly obese and had higher BMIs. They concluded that a normal BNP level did not exclude an out-patient diagnosis of HFpEF. Obesity is known to reduce serum NT-proBNP levels, and this trend should be kept in mind when considering a diagnosis of HFpEF. NP levels decline linearly with increasing BMI, and low NP cut-off values should be used for the diagnosis of HFpEF when BMI is increased.[29,30]

In our study, the average BMI of the patients was 33 kg/m^2, which might have reduced the NT-proBNP levels. On the other hand, some drugs, such as diuretics and beta-blockers[31] are known to diminish serum NT-proBNP levels.

At the baseline of the present study, 54% of the patients were on diuretic drugs and 35% used beta-blockers. Therefore, concomitant drug use may be an additional factor that decreased baseline NT-proBNP levels. Nevertheless, we believe that the patients we recruited for this study had HFpEF. Framingham criteria were used to diagnose HF, and all patients were required to have evidence of DD on echocardiography, which is an important component of this disease. Another supporting fact not reported in the results section was that 24% of the patients in this study were hospitalised or presented to the emergency room because of HF decompensation during the follow-up period. These data, which are close to the number of hospitalisations characteristic to this population, provide another clue that our patients truly had HFpEF.[32]

Study limitations

There are many limitations of our study that are worth addressing. First of all, many patients discontinued the study drug or withdrew from the study. Seventeen patients, accounting for 16% of the total study population (20 patients, when three patients who died are also included), were excluded from the study after randomisation due to different reasons. This number may be large for this type of small-size study. The follow-up period may also have been too short to accurately investigate the outcomes associated with the study drug. Over a longer period, the study drug might have shown more pronounced benefits in HFpEF patients. LA systolic function was assessed by tissue Doppler annular late diastolic velocities. This method provides a rapid way to assess LA systolic function, but it might be more accurately assessed by LA systolic strain or LA emptying fraction methods.

Conclusion

Tissue Doppler septal late diastolic velocity and septal systolic myocardial velocity were increased in the perindopril group. NT-proBNP level and NYHA functional status were not changed in this study population.

References

1. Ponikowski P, Voors AA, Anker SD, Bueno H, Cleland JG, *et al*. 2016 ESC guidelines for the diagnosis and treatment of acute and chronic heart failure: the task force for the diagnosis and treatment of acute and chronic heart failure of the European Society of Cardiology (ESC). Developed with the special contribution of the Heart Failure Association (HFA) of the ESC. *Eur J Heart Fail* 2016; **18**: 891–975.
2. Persson H, Lonn E, Edner M, Baruch L, Lang CC, *et al.* Investigators of the CHARM Echocardiographic Substudy – CHARMES. Diastolic dysfunction in heart failure with preserved systolic function: need

for objective evidence: results from the CHARM Echocardiographic Substudy – CHARMES. *J Am Coll Cardiol* 2007; **49**: 687–694.
3. Gottdiener JS, Kitzman DW, Aurigemma GP, Arnold AM, Manolio TA. Left atrial volume, geometry and function in systolic and diastolic heart failure of persons ≥ 65 years of age (the Cardiovascular Health study). *Am J Cardiol* 1997; **97**: 83–89.
4. Kurt M, Wang J, Torre-Amione G, Nagueh SF. Left atrial function in diastolic heart failure. *Circ Cardiovasc Imaging* 2009; **2**: 10–15.
5. Tan YT, Wenzelburger F, Lee E, Nightingale P, Heatlie G, *et al*. Reduced left atrial function on exercise in patients with heart failure and normal ejection fraction. *Heart* 2010; **96**: 1017–1023.
6. Hesse B, Schuele SU, Thamilasaran M, Thomas J, Rodriguez L. A rapid method to quantify left atrial contractile function: Doppler tissue imaging of the mitral annulus during atrial systole. *Eur J Echocardiogr* 2004; **5**: 86–92.
7. Yip G, Wang M, Zhang Y, Fung JW, Ho PY, *et al.* Left ventricular long-axis function in diastolic heart failure is reduced in both diastole and systole: time for a redefinition? *Heart* 2002; **87**: 121–125.
8. Petrie MC, Caruana L, Berry C, McMurray JJ. 'Diastolic heart failure' or heart failure caused by subtle left ventricular systolic dysfunction? *Heart* 2002; **87**: 29–31.
9. Yu CM, Lin H, Yang H, Kong SL, Zhang Q, *et al*. Progression of systolic abnormalities in patients with 'isolated' diastolic heart failure and diastolic dysfunction. *Circulation* 2002; **105**: 1195–1201.
10. Nikitin NP, Witte KK, Clark AL, Cleland JG. Color tissue Doppler-derived long-axis left ventricular function in heart failure with preserved global systolic function. *Am J Cardiol* 2002; **90**: 1174–1177.
11. Bruch C, Gradaus R, Gunia S, Breithardt G, Wichter T. Doppler tissue analysis of mitral annular velocities: evidence for systolic abnormalities in patients with diastolic heart failure. *J Am Soc Echocardiogr* 2003; **16**: 1031–1036.
12. Vinereanu D, Nicolaides E, Tweddel AC, Fraser AG. 'Pure' diastolic dysfunction is associated with long-axis systolic dysfunction. Implications for the diagnosis and classification of heart failure. *Eur J Heart Fail* 2005; **7**: 820–828.
13. Garcia EH, Perna ER, Farias EF, Obregón RO, Macin SM, *et al*. Reduced systolic performance by tissue Doppler in patients with preserved and abnormal ejection fraction: new insights in chronic heart failure. *Int J Cardiol* 2006; **108**: 181–188.
14. Setaro JF, Zaret BL, Schulman DS, Black HR, Soufer R. Usefulness of verapamil for congestive heart failure associated with abnormal left ventricular diastolic filling and normal left ventricular systolic performance. *Am J Cardiol* 1990; **66**: 981–986.
15. Hung MJ, Cherng WJ, Kuo LT, Wang CH. Effect of verapamil in elderly patients with left ventricular diastolic dysfunction as a cause of congestive heart failure. *Int J Clin Pract* 2002; **56**: 57–62.
16. Deswal A, Richardson P, Bozkurt B, Mann DL. Results of the Randomised Aldosterone Antagonism in Heart Failure with Preserved Ejection Fraction trial (RAAM-PEF). *J Card Fail* 2011; **17**: 634–642.
17. Yip GWK, Wang M, Wang, T, Chan S, Fung JW, *et al*. The Hong Kong diastolic heart failure study: a randomised controlled trial of diuretics, irbesartan and ramipril on quality of life, exercise capacity, left ventricular global and regional function in heart failure with a normal ejection fraction. *Heart* 2008; **94**: 573–580.
18. Wang JG, Pimenta E, Chwallek F. Comparative review of the blood pressure-lowering and cardiovascular benefits of telmisartan and perindopril. *Vasc Health Risk Manag* 2014; **10**: 189–200.
19. ADVANCE Echocardiography Substudy Investigators; ADVANCE collaborative group. Effects of perindopril–indapamide on left ventricular diastolic function and mass in patients with type 2 diabetes: the ADVANCE Echocardiography Substudy. *J Hypertens* 2011; **29**: 1439–1447.
20. Pela G, Pattoneri P, Passera M, Tirabassi G, Reverberi C, *et al.* Long-term effects of perindopril on left ventricular structure and function in patients with stable coronary artery disease: a conventional and Doppler tissue echocardiographic pilot study. *J Cardiovasc Med* (Hagerstown) 2009; **10**: 781–786.
21. Owan T, Hodge DO, Herges RM, Jacobsen SJ, Roger VL, *et al*. Secular trends in renal dysfunction and outcomes in hospitalized heart failure patients. *J Card Fail* 2006; **12**: 257–262.
22. Vinereanu D, Nicolaides E, Tweddel AC, Mädler CF, Holst B, *et al*. Subclinical left ventricular dysfunction in asymptomatic patients with Type II diabetes mellitus, related to serum lipids and glycated haemoglobin. *Clin Sci* (Lond) 2003; **105**: 591–599.
23. Wang M, Yip GW, Wang AY, Zhang Y, Ho PY, *et al.* Tissue Doppler imaging provides incremental prognostic value in patients with systemic hypertension and left ventricular hypertrophy. *J Hypertens* 2005; **23**: 183–191.
24. Galrinho A, Branco L, Soares R, Timóteo A, Abreu J, *et al*. Prognostic implications of tissue Doppler in patients with dilated cardiomyopathy. *Rev Port Cardiol* 2006; **25**: 781–793.
25. Terzi S, Sayar N, Bilsel T, Enc Y, Yildirim A, *et al*. Tissue Doppler imaging adds incremental value in predicting exercise capacity in patients with congestive heart failure. *Heart Vessels* 2007; **22**: 237–244.
26. Paulus WJ, Tschöpe C, Sanderson JE, Rusconi C, Flachskampf FA, *et al*. How to diagnose diastolic heart failure: a consensus statement on the diagnosis of heart failure with normal left ventricular ejection fraction by the Heart Failure and Echocardiography Associations of the European Society of Cardiology. *Eur Heart J* 2007; **28**: 2539–2550.
27. Maisel A, Mueller C, Adams K Jr, Anker SD, Aspromonte N, *et al*. State of the art: using natriuretic peptide levels in clinical practice. *Eur J Heart Fail* 2008; **10**: 824–839.
28. Anjan VY, Loftus TM, Burke MA, Akhter N, Fonarow GC, *et al.* Prevalence, clinical phenotype, and outcomes associated with normal B-type natriuretic peptide levels in heart failure with preserved ejection fraction. *Am J Cardiol* 2012; **110**: 870–876.
29. Horwich TB, Hamilton MA, Fonarow GC. B-type natriuretic peptide levels in obese patients with advanced heart failure. *J Am Coll Cardiol* 2006; **47**: 85–90.
30. Bayes-Genis A, Lloyd-Jones DM, van Kimmenade RR, Lainchbury JG, Richards AM, *et al*. Effect of body mass index on diagnostic and prognostic usefulness of amino-terminal pro-brain natriuretic peptide in patients with acute dyspnea. *Arch Intern Med* 2007; **167**: 400–407.
31. Li N, Wang JA. Brain natriuretic peptide and optimal management of heart failure. *J Zhejiang Univ Sci B*, 2005; **6**: 877–884.
32. Hogg K, Swedberg K, McMurray J. Heart failure with preserved left ventricular systolic function: epidemiology, clinical characteristics and prognosis. *J Am Coll Cardiol* 2004; **43**: 317–327.

Plasma phospholipid fatty acid patterns are associated with adiposity and the metabolic syndrome in black South Africans: a cross-sectional study

Alice Achieng Ojwang, Herculina Salome Kruger, Manja Zec, Cristian Ricci, Marlien Pieters, Iolanthé Marike Kruger, Edelweiss Wentzel-Viljoen, Cornelius Mattheus Smuts

Abstract

Background: Diets rich in n-6 polyunsaturated fatty acids (PUFAs) and saturated fatty acids (SFA) have been associated with increased risk of obesity and the metabolic syndrome (MetS), but the evidence is inconsistent, whereas diets high in n-3 long-chain (LC)-PUFAs are associated with lower risk. There is limited information about the association of plasma phospholipid fatty acids (FAs) with obesity and the MetS among black South Africans.

Objective: To investigate the association of dietary FAs and plasma phospholipid FA patterns, respectively, with measures of adiposity (body mass index, waist circumference, waist-to-height ratio) and the MetS in black South Africans.

Methods: Factor analysis was used to identify FA patterns from 11 dietary FAs and 26 individual plasma phospholipid FAs. Cross-sectional association of the identified patterns with measures of adiposity and the MetS was investigated. A random sample of 711 black South African adults aged 30 to 70 years (273 men, 438 women) from the North West Province was selected from the South African leg of the Prospective Urban and Rural Epidemiology (PURE) study. Sequential regression models adjusted for confounders were applied to investigate the association between dietary FAs and plasma phospholipid FA patterns with measures of adiposity and the MetS.

Results: Two patterns were derived from dietary FAs and six patterns from plasma phospholipid FAs that explained the cumulative variance of 89 and 73%, respectively. The association of FA patterns with adiposity and the MetS was weaker for dietary FA patterns than for plasma phospholipid FA patterns. The plasma phospholipid FA pattern with high loadings of saturated FAs (high-Satfat) and another with high loadings of n-3 very-long-chain PUFAs (n-3 VLC-PUFAs) were positively associated with measures of adiposity and the MetS, while patterns with positive loadings of LC mono-unsaturated fatty acids (n-9 LC-MUFA) and a positive loading of n-3 essential FAs (n-3 EFA) showed inverse associations with the MetS and some measures of adiposity.

Conclusions: The n-9 LC-MUFA and n-3 EFA patterns seemed to provide possible protective associations with adiposity and the MetS, whereas the high-Satfat and n-3 VLC-PUFA patterns were associated with adiposity and the MetS in our study participants. The results are reflective of the metabolic difference between overweight and obese compared to lean individuals.

Keywords: phospholipid fatty acid patterns, dietary fatty acid patterns, adiposity, metabolic syndrome, waist:height ratio

Submitted 23/1/19, accepted 3/5/19
Published online 11/7/19
Cardiovasc J Afr 2019; **30**: 228–238 www.cvja.co.za

DOI: 10.5830/CVJA-2019-026

Centre of Excellence for Nutrition, North-West University, Potchefstroom, South Africa
Alice Achieng Ojwang, M Nutr, RDN, ojwangaa@gmail.com
Herculina Salome Kruger, PhD, RD (SA)
Manja Zec, PhD
Cristian Ricci, PhD
Marlien Pieters, PhD, RD (SA)
Edelweiss Wentzel-Viljoen, PhD, RD (SA), RNT (SA)
Cornelius Mattheus Smuts, PhD, RNT (SA)

Medical Research Council Hypertension and Cardiovascular Disease Research Unit, North-West University, Potchefstroom, South Africa
Herculina Salome Kruger, PhD, RD (SA)

Excellence in Nutrition and Metabolism, Institute for Medical Research, University of Belgrade, Serbia
Manja Zec, PhD

Africa Unit for Transdisciplinary Health Research, North-West University, Potchefstroom, South Africa
Iolanthé Marike Kruger, PhD

South Africa is currently experiencing rapid nutritional, economic, demographic and epidemiological transitions with likely consequences for lifestyle and health.[1] The prevalence of overweight and obesity in South Africa in 2012 was 31% in men and 64% for women.[2] This increased in 2016 to 68% in women but remained the same for men.[3] Abdominal obesity among black South African women is particularly associated with elevated blood pressure (BP), lower high-density lipoprotein cholesterol, higher serum triglycerides, and elevated fasting plasma glucose, indicative of insulin resistance.[4] Unhealthy diet is a major risk factor associated with the rising prevalence of obesity and the metabolic syndrome (MetS).[5,6]

Fat intake among the black urban population of South Africa has increased from 16.4 to 26.2% of total energy over the past 50 years.[7] The transition from more traditional to Western diets, characterised by an increase in n-6 polyunsaturated fatty acids (PUFA), saturated fatty acids (SFA), industrial trans fatty acids (FAs),[8] as well as a decrease in n-3 PUFA intake, is also prevalent in this population.[9] Diets high in percentage energy from animal protein and total fat intake may increase the risk of non-communicable diseases in rural and urban black South Africans,[10] and this may be related to meat intake, which is a major source of both MUFAs and SFAs in South Africans.[11]

By contrast with this, however, a study that investigated dietary intake of carbohydrate and SFAs in 18 countries undergoing rapid nutritional transition documented that SFA intake was associated with lower risk of mortality.[12]

Studies investigating circulating FAs have also reported some conflicting results. A recent study examined the relationship between body mass index (BMI) and plasma phospholipid FA composition in men aged between 48 and 65 years and reported higher plasma phospholipid levels of palmitic (C16:0) and stearic acid (C18:0) in obese individuals.[13] Furthermore, plasma concentrations of C16:0 were positively associated with risk for total mortality in men and women in a prospective study in the USA.[14] SFAs, myristic acid (C14:0), C16:0 and C18:0 in plasma were positively associated with the MetS, while longer-chain SFAs, and arachidic (C20:0), behenic (C22:0) and lignoceric acid (C24:0) were inversely associated in men and women from Taiwan.[15] Another study also reported lower levels of plasma C22:0 and C24:0 in the MetS participants.[16] Palmitoleic acid (C16:1n-7) level in plasma phospholipids was positively associated with BMI in men and women,[13,17] and higher levels of plasma C16:1n-7 were associated with multiple metabolic risk factors in men and women.[18,19]

In different populations, total n-3 FAs in plasma were associated with lower BMI, waist circumference (WC) and hip circumference[20] and inversely associated with the MetS,[21] while omega-6 PUFA have been associated with obesity and the MetS. Pickens and associates reported higher plasma phospholipid levels of dihomo-γ-linolenic acid (C20:3n-6) in overweight and obese individuals.[13] Positive associations of serum phospholipid C20:3n-6 with BMI, as well as total n-6 PUFAs with waist:hip ratio were also documented in a study of Mexican women.[17] Some studies also report positive associations of specific plasma phospholipids n-6 PUFAs with metabolic risk,[18,22] while other studies report inverse associations of total n-6 PUFAs in erythrocytes and serum, respectively, with the MetS.[23,24] Due to inconsistent results in different studies relating to circulating n-6 PUFAs, further research to understand their role in association with obesity and the MetS is highly recommended.[25]

Since people consume food rather than individual nutrients, it is difficult to isolate the individual nutrients in the diet and link them to disease and health.[26] Therefore, the analysis of food intakes into patterns derived from various combinations of nutrients or foods has developed as a preferred alternative to investigating associations between nutrients and diseases.[27] Several studies have applied factor and cluster analysis to derive patterns from food and tissues in investigating the association of these patterns with health and diseases.[28]

FA patterns from adipose tissue and plasma have been employed to describe associations of FAs with obesity[29] and the MetS.[22,30] Despite the extensive use of plasma FAs in research, there is limited epidemiological research on the use of both dietary and circulating FA patterns in association with obesity and the MetS in black populations in Africa. To address the key gaps in the current knowledge, the aim of this study was to investigate the associations of dietary and plasma phospholipid FA patterns with adiposity measures [BMI, waist circumference (WC) and waist-to-height ratio (WHtR)] and the MetS in a selected group of black South African adults. This study was based on a random sub-sample of 711 participants selected from the South African site (North West Province) of the multi-country Prospective Urban and Rural Epidemiological (PURE) study. This study made use of cross-sectional data collected at baseline during the months of August to November 2005.

Methods

A sub-sample of 711 black South African participants were randomly selected from 2 010 adults recruited at baseline (in 2005) from urban (1 004) and rural (1 006) households in the North West Province to assess dietary FA intake and plasma phospholipid FA status. Those included were apparently healthy subjects older than 30 years at baseline, with no reported diseases of lifestyle, tuberculosis or HIV, and used chronic medication for diabetes and hypertension only.

Ethical approval for the South African PURE study was obtained from the Ethics Committee of North-West University (Ethics number 04M10). Participants provided written informed consent and participation was voluntarily.

Transportation was provided for the study subjects to reach the data-collection centres in both rural and urban areas. During face-to-face interviews by trained fieldworkers, each participant completed questionnaires in his or her preferred language (Afrikaans, Setswana or English). The questionnaires included demographic,[31] physical activity[32] and quantitative food-frequency questions (QFFQ),[33,34] and made use of, among others, validated food photo-books to estimate portion sizes.[35] Reproducibility[33] and details of dietary assessments have been published elsewhere.[10]

Dietary macronutrients and FAs were calculated using the South African Medical Research Council food composition tables.[36] Twenty-eight dietary FAs were included initially, but FAs that had a daily median intake of less than 0.10 mg were excluded. A total of 11 dietary FAs were used to derive FA patterns for investigation in this study.

Anthropometric measurements were performed by trained research assistants according to standards prescribed by the International Society for the Advancement of Kinanthropometry.[37] A portable electronic scale (Precision Health Scale, A&D Company, Tokyo, Japan) was used to measure weight. Height was measured using a calibrated stadiometer (Seca, Hamburg, Germany). Waist and hip circumferences were recorded using steel tapes (Lufkin, Apex, NC, USA). BMI and WHtR were calculated using weight (kg)/height (m^2) and waist (cm)/height (cm) formulas, respectively. Blood pressure (mmHg) was measured in duplicate (five minutes apart) on the right upper arm. Appropriately sized cuffs were used for obese subjects.

Fasting blood samples were collected from the antecubital vein with a sterile winged infusion set with minimal stasis. The samples were collected and plasma and serum were prepared and aliquoted by a registered nurse and then stored at –80°C in the urban areas. In rural areas, the samples were stored at –18°C for up to five days, where after it was transported to the laboratory facility and stored at –80°C until analysed.

Fasting plasma glucose concentration was determined by the hexokinase method using the Synchron® system (Beckman Coulter Co, Fullerton, CA, USA). The sequential multiple analyser computer (SMAC) using the Konelab™ auto-analyser (Thermo Fisher Scientific Oy, Vantaa, Finland) performed quantitative determinations of high-density lipoprotein cholesterol (HDL-C), triglycerides and total cholesterol (TC).

Low-density lipoprotein cholesterol (LDL-C) was calculated using the Friedewald equation.[38]

EDTA plasma samples were thawed and extracted with chloroform:methanol (2:1 v/v) according to the modified Folch method.[39] The plasma phospholipid FA fraction was isolated by thin-layer chromatography from the extracted lipids.[40] Subsequently, the phospholipid FA fraction was transmethylated to FA methyl esters and analysed by quadrupole gas chromatography electron ionisation mass spectrometry by means of an Agilent Technologies 7890 A GC system, as described by Baumgartner *et al*.[40]

Thirty-two FAs were measured in fasted plasma samples from 711 participants. Six FAs, i.e. pentadecanoic acid (C15:0), margaric acid (C17:0), trans vaccenic acid (C18:1n-7t), rumenic acid (C18:2n-7tt), stearidonic acid (C18:4n-3) and eicosatrienoic (C20:3n-3) were below the limit of quantification and therefore not included. The remaining 26 plasma phospholipid FAs were quantified and expressed as a percentage of total FAs. Quality of data was assured with a separate calibration for each FA, monitoring of internal standard (1,2-diheptadecanoyl-sn-glycerol-3 phosphorylchloline, Matreya, Pennsylvania, USA) and Levey Jennings graphs for a pooled plasma control analysed with each batch.

The MetS was defined according to recommendations by the Joint Interim Statement of six international associations as the presence of three or more of the following: (1) fasting plasma glucose levels ≥ 5.6 mmol/l or the use of oral hypoglycaemic medication; (2) serum triglycerides ≥ 1.7 mmol/l; (3) serum HDL ≤ 1.0 mmol/l for men and ≤ 1.3 mmol/l for women; (4) BP ≥ 130/85 mmHg or the use of BP medication; and (5) WC of ≥ 94 cm for men and ≥ 80 cm for women.[41]

Statistical analysis

Continuous variables were described as medians and interquartile ranges if data deviated from the normal distribution according to the Kolmogorov–Smirnov test, whereas categorical variables were presented as percentages. Non-normally distributed data were log transformed before inclusion in regression models. Participants' characteristics were compared by gender and BMI categories using the Mann–Whitney *U*-test or chi-squared test for continuous and categorical variables, respectively. Differences between individual FAs and ratios by BMI and gender groups were tested with the Mann–Whitney test. A BMI < 25 kg/m^2 was considered as underweight and/or normal-weight or lean, whereas BMI ≥ 25 kg/m^2 was considered overweight and/or obese. The effect size of the differences between groups was calculated using the Man–Whitney *U*-value and sample size of the groups.[42]

Principal-component-based varimax factor analysis of the correlation matrix was used to define dietary FA (based on the QFFQ) and plasma phospholipid FA patterns. The identification and naming of 11 dietary FAs and 26 plasma phospholipid FAs used in this study are based on relevant literature and the levels of specific FAs observed in our population.[43] The number of factors to retain was established by the Kaiser criterion (eigenvalues > 1) and scree-plot visual inspection. Loadings with absolute values > 0.5 were considered as relevant for the contribution to each FA pattern. The associations between FA patterns and outcomes were evaluated by sequential regression models, logistic regression for the dichotomous outcome (MetS), and generalised linear models for continuous outcomes (WC, BMI and WHtR).

The first step of the sequential modelling analyses was based on models that contained only dietary FAs or plasma phospholipid FA patterns and was referred to as a crude model. The crude model was then adjusted for gender and age (adjusted model$_1$). This model was further adjusted for lifestyle confounders, including the level of education, physical activity, alcohol and total energy intake, and self-reported smoking status, creating a fully adjusted model. We further adjusted this model for contraceptives (adjusted for in plasma phospholipid FA pattern models only) and dietary factors, including total fats, carbohydrates, dietary fibre and energy from added sugar as individual confounders and as combined covariates.

Model fitting was evaluated using the adjusted *R*-square for linear regression and maximum re-scaled *R*-square statistic

Table 1. Demographics, health and dietary intake data of an apparently healthy cohort of 711 black South African adults participating in the PURE study

Variables	*Men* (n = 273) *Median* (Q_1, Q_3)[b]	*Women* (n = 438) *Median* (Q_1, Q_3)[b]	p-*value*[c]
Demographics			
Age (years)	52 (46, 60)	52 (45, 59)	0.80
Education (educated), *n* (%)	155 (57.6)	263 (62.2)	0.22
Tobacco use (current smoker), *n* (%)	163 (59.7)	205 (46.8)	0.0008
Alcohol (g/week)	6.4 (0, 24.9)	0 (0, 3.9)	< 0.0001
Physical activity index	2.8 (2.5, 3.1)	2.8 (2.5, 3.3)	0.71
Waist circumference (cm)	75.4 (69.7, 82.4)	82.0 (71.7, 92.6)	< 0.0001
Waist-to-height ratio	0.45 (0.4, 0.5)	0.52 (0.5, 0.6)	< 0.0001
Body mass index (kg/m^2)	20.0 (18.1, 23.2)	26.0 (21.8, 31.9)	< 0.0001
Systolic blood pressure (mmHg)	135 (121, 152)	132 (118, 150)	0.06
Diastolic blood pressure (mmHg)	88 (78, 98)	88 (70, 97)	0.84
Fasting glucose (mmol/l)	4.8 (4.3, 5.4)	4.9 (4.3, 5.4)	0.53
Total cholesterol (mmol/l)	5.0 (4.1, 6.0)	5.1 (4.4, 6.2)	0.35
High-density lipoprotein cholesterol (mmol/l)	1.54 (1.2, 2.1)	1.5 (1.2, 1.8)	0.04
Low-density lipoprotein cholesterol (mmol/l)	3.1 (2.3, 4.0)	3.4 (2.7, 4.2)	0.06
Triglycerides (mmol/l)	1.0 (0.8, 1.5)	1.2 (0.9, 1.8)	0.002
Dietary intake[a]			
Total energy (kcal/day)	1874 (1377, 2612)	1628 (1189, 2212)	0.001
Total carbohydrate (g/day)	285.4 (199, 378)	248.8 (180.6, 325.1)	0.01
Total fibre (g/day)	14.8 (25, 30)	17.9 (12.7, 25.2)	0.004
Total protein (g/day)	55.0 (38, 75.7)	46.2 (33.1, 65.0)	< 0.0001
Total fat (g/day)	45.3 (28.5, 63.7)	40.5 (26.3, 64.4)	0.10
Total saturated fatty acids (g/day)	10.5 (6.5, 15.7)	9.5 (5.6, 16.6)	0.13
Total mono-unsaturated fatty acids (g/day)	11.4 (6.8, 17.8)	10.4 (6.0, 18.3)	0.14
Total polyunsaturated fatty acids (g/day)	13.6 (8.8, 19.6)	13.1 (7.5, 20.0)	0.47
Total n-3 polyunsaturated fatty acids (g/day)	0.4 (0.2, 0.6)	0.33 (0.20, 0.5)	0.15
Total n-6 polyunsaturated fatty acids (g/day)	13.3 (8.8, 19.2)	12.9 (7.3, 19.6)	0.55

[a]Baseline demographic details of participants.
[b]Data are presented as median (interquartile range): Q_1, lower interquartile range; Q_3, upper interquartile range.
[c]Significance levels of differences in parameters between men and women, based on Mann–Whitney and chi-squared tests for continuous and categorical variables, respectively.

for logistic regression. Linear regression results are presented as standardised β and 95% confidence intervals (CI) with their significance levels, and odds ratio and 95% CI with significance levels for logistic regression. All analyses were performed using SAS Version 9.4 (SAS Institute, Cary, NC, USA)[44] and $p < 0.05$ was considered significant.

Results

The baseline characteristics of the 711 participants are shown in Table 1. The majority were women (61.6%) and the median age was comparable between men and women. Men had higher HDL levels and were more likely to smoke. By contrast, the women had higher serum triglycerides, as well as higher levels of measures of adiposity ($p < 0.0001$). The dietary intake data revealed that men had higher total energy, total carbohydrate and total protein intakes, whereas the women, on the other hand, had higher total dietary fibre intake.

Table 2 shows that total intakes of fat, SFAs and MUFAs were significantly higher in overweight/obese women compared to lean women. Plasma phospholipid FAs within SFA, MUFA and PUFA classes differed across BMI categories and gender. In men, the plasma levels of SFAs, C18:0, C20:0, C22:0, C24:0 and n-6 PUFA C20:3n-6 were significantly higher in overweight

Table 2. Dietary intake of fats, individual fatty acids and plasma phospholipid fatty acid profile by BMI categories and gender in 711 black South African adults

	Men (n = 273)				*Women (n = 438)*			
	BMI[a] < 25 kg/m² (n = 233)	*BMI ≥ 25 kg/m² (n = 40)*		*Effect size*	*BMI < 25 kg/m² (n = 191)*	*BMI ≥ 25 kg/m² (n = 247)*		*Effect size*
Variables		*Median (Q_1, Q_3)*	p-*value*		*Median (Q_1, Q_3)*	*Median (Q_1, Q_3)*	p-*value*	
Total energy, dietary fat intake								
Total energy (kcal/day)	1856 (1374, 2599)	2052 (1370, 2681)	0.48		1579 (1139, 2188)	1651 (123, 2224.)	0.50	
Total fat (g/day)	44.8 (28.5, 63.0)	46.8 (31.5, 66.9)	0.71		35.5 (22.8, 59.2)	44.9 (27.9, 68.0)	0.002	
Total saturated fatty acids (g/day)	10.4 (6.5, 15.4)	12.4 (8.1, 16.3)	0.71		8.4 (4.7, 15.5)	10.8 (6.2, 17.1)	0.003	
Total polyunsaturated fatty acids (g/day)	13.8 (8.8, 19.6)	12.8 (8.7, 18.7)	0.32		11.8 (7.0, 19.5)	13.5 (8.2, 20.9)	0.29	
Total n-3 PUFAs (g/day)	0.4 (0.2, 0.6)	0.34 (0.2, 0.6)	0.58		0.3 (0.2, 0.5)	0.4 (0.2, 0.5)	0.09	
Total n-6 PUFAs (g/day)	13.5 (8.7, 19.1)	12.4 (9.2, 19.8)	0.39		12.1 (6.9, 18.9)	13.4 (8.1, 20.2)	0.27	
n-6/n-3 ratio	33.1 (24.4, 152.4)	34.2 (22.5, 53.1)	0.84		37.3 (27.57,49.73)	36.8 (26.1, 51.9)	0.76	
Total mono-unsaturated fatty acids (g/day)	11.2 (6.8, 16.4)	13.4 (7.2, 19.7)	0.48		8.5 (5.0, 16.4)	12.0 (6.4, 19.4)	< 0.0001	
Plasma phospholipid fatty acids (% total FAs)[c]								
Saturated fatty acids								
Myristic acid (C14:0)	0.25 (0.2, 0.3)	0.25 (0.2, 0.3)	0.75		0.26 (0.2, 0.3)	0.27 (0.2, 0.3)	0.21	
Palmitic acid (C16:0)	27.6 (25.2, 29.5)	26.3 (24.6, 28.0)	0.002	0.37	26.7 (24.8, 29.2)	25.7 (24.0, 27.6)	0.21	
Stearic acid (C18:0)	14.0 (12.4, 15.5)	15.1 (14.4, 16.2)	< 0.0001	0.31	14.8 (13.5, 16.3)	15.5 (14.3, 17.0)	0.0004	0.38
Arachidic acid (C20:0)	0.27 (0.21, 0.34)	0.34 (0.27, 0.39)	0.02	0.33	0.30 (0.25, 0.37)	0.36 (0.30, 0.43)	< 0.0001	0.35
Behenic acid (C22:0)	0.94 (0.66, 1.17)	1.22 (0.97, 1.43)	0.0006	0.32	1.03 (0.78, 1.35)	1.27 (1.07, 1.54)	< 0.0001	0.35
Lignoceric acid (C24:0)	1.01 (0.81, 1.23)	1.13 (0.91, 1.36)	0.02	0.40	1.00 (0.81, 1.24)	1.07 (0.9, 1.27)	0.03	0.45
Mono-unsaturated fatty acids								
Palmitoleic acid (C16:1n-7)	0.88 (0.5, 1.6)	0.6 (0.4, 0.8)	0.0007	0.34	0.8 (0.5, 1.2)	0.6 (0.4, 0.8)	0.003	0.40
Cis-vaccenic acid (C18:1n-7)	1.46 (1.26, 1.69)	1.19 (1.01, 1.44)	0.002	0.30	1.41 (1.20, 1.65)	1.30 (1.12, 1.5)	0.03	0.41
Oleic acid (C18:1n-9)	10.0 (7.6, 13.0)	7.5 (6.2, 9.3)	0.0002	0.30	8.2 (7.0, 11.3)	7.16 (6.3, 8.3)	< 0.0001	0.35
Elaidic acid (C18:1n9t)	0.31 (0.20, 0.56)	0.27 (0.20, 0.5)	0.32		0.34 (0.21, 0.81)	0.32 (0.21, 0.61)	0.50	
Gondoic acid (C20:1n-9)	0.11 (0.09, 0.12)	0.10 (0.08, 0.11)	0.04	0.36	0.11 (0.09, 0.12)	0.10 (0.09, 0.12)	0.02	0.42
Erucic acid (C22:1n-9)	0.06 (0.04, 0.08)	0.07 (0.04, 0.09)	0.29		0.06 (0.05, 0.09)	0.07 (0.05, 0.09)	0.50	
Nervonic acid (C24:1n-9)	1.66 (1.44, 1.95)	1.61 (1.35, 1.95)	0.75		1.69 (1.42, 2.02)	1.88 (1.55, 2.21)	0.005	0.41
n-3 polyunsaturated fatty acids								
α-linolenic acid (c18:3n-3)	0.09 (0.07, 0.12)	0.08 (0.05, 0.10)	0.18		0.08 (0.06, 0.1)	0.1 (0.05, 0.1)	0.77	
Eicosapentaenoic acid (C20:5n-3)	0.6 (0.5, 0.9)	0.6 (0.5, 0.9)	0.32		0.6 (0.4, 0.9)	0.6 (0.4, 0.8)	0.92	
Docosapentaenoic acid (C22:5n-3)	0.5 (0.4, 0.7)	0.6 (0.4, 0.8)	0.51		0.6 (0.5, 1.0)	0.5 (0.4, 0.8)	0.92	
Docosahexaenoic acid (C22:6n-3)	3.8 (3.0, 4.8)	4.29 (3.2, 5.6)	0.09		4.4 (3.5, 5.5)	5.0 (4.05, 5.8)	0.0008	0.39
n-6 and n-9 polyunsaturated fatty acids								
Linoleic acid (C18:2n-6)	16.1 (13.6, 18.5)	16.4 (14.1, 18.6)	0.71		15.9 (12.8, 18.4)	16.0 (13.8, 18.7)	0.50	
γ-linolenic acid (C18:3n-6)	0.13 (0.1, 0.2)	0.10 (0.07, 0.14)	0.04	0.39	0.1 (0.1, 0.2)	0.10 (0.07, 0.13)	0.07	
Eicosadienoic acid (C20:2n-6)	0.34 (0.29, 0.39)	0.35 (0.29, 0.4)	0.71		0.36 (0.31, 0.42)	0.38 (0.33, 0.44)	0.07	
Dihomo-γ-linolenic acid (C20:3n-6)	2.7 (2.4, 3.3)	3.1 (2.7, 3.9)	0.006	0.32	2.8 (2.4, 3.2)	3.1 (2.72, 3.61)	< 0.0001	0.35
Arachidonic (C20:4n-6)	12.9 (11.5, 14. 3)	14.1 (12.6, 15.7)	0.08		13.5 (12.0, 15.0)	14.2 (12.7, 15.6)	0.007	0.44
Docosadienoic acid (C22:2-n6)	0.018 (0.013, 0.023)	0.018 (0.014, 0.022)	0.75		0.02 (0.014, 0.027)	0.025 (0.018, 0.032)	< 0.0001	0.37
Adrenic acid (C22:4n-6)	0.6 (0.5, 0.7)	0.6 (0.5, 0.7)	0.51		0.6 (0.5, 0.7)	0.6 (0.5, 0.7)	0.29	
Osbond acid (C22:5n-6)	1.4 (1.2, 1.6)	1.4 (1.1, 1.7)	0.71		1.4 (1.2, 1.6)	1.4 (1.1, 1.6)	0.15	
Mead acid (C20:3n-9)	0.3 (0.2, 0.4)	0.2 (0.1, 0.3)	0.09		0.2 (0.1, 0.3)	0.17 (0.1, 0.3)	0.0003	0.41

[a]BMI, body mass index; PUFA, polyunsaturated fatty acids.
[b]Median (Q_1, Q_3) = differences between FAs across BMI and gender were tested by independent *t*-test according to BMI < 25 and BMI ≥ 25 kg/m². Data are presented as median; Q_1: lower interquartile range, Q_3: upper interquartile range.
[c]Plasma phospholipid fatty acids (% total FAs) = fatty acids are expressed as a percentage (%) of total FA. Significance levels of differences in parameters between men and women based on Mann–Whitney tests.

men than in lean men, whereas C16:0, C18:3n-6 and MUFAs, C16:1n-7, *cis*-vaccenic acid (C18:1n-7), oleic acid (C18:1n-9) and gondoic acid (C20:1n-9) were higher in lean than in overweight men. Although significant differences were observed for these FAs between overweight and lean groups in men, most had a small effect size of approximately 0.30 to 0.40.

Plasma levels of similar SFAs, i.e. C18:0, C20:0, C22:0 and C24:0, as well as nervonic acid (C24:1n-9), docosahexaenoic acid (C22:6n-3), C20:3n-6, arachidonic acid (C20:4n-6) and docosadienoic acid (C22:2-n6) were higher in overweight women than in their lean counterparts. Similar MUFAs, i.e. C16:1n-7, C18:1n-7, C18:1n-9 and C20:1n-9, but also mead acid, were

Table 3. Factor loadings for dietary and plasma phospholipid fatty acids

	Dietary fatty acid patterns[a]	
Dietary fatty acids	*Non-marine* ($\lambda_1 = 60\%$)[b]	*Marine* ($\lambda_2 = 29\%$)
Saturated fatty acids		
Myristic acid (C14:0)	0.78	0.10
Palmitic acid (C16:0)	0.97	0.22
Stearic acid (C18:0)	0.94	0.21
Behenic acid (C22:0)	0.67	0.29
Mono-unsaturated fatty acids		
Palmitoleic acid (C16:1n-7)	0.89	0.28
Oleic acid (C18:1n-9)	0.95	0.23
n-3 fatty acids		
α-Linolenic acid (C18:3n-3)	0.89	0.22
Eicosapentaenoic acid (C20:5n-3)	0.21	0.96
Docosahexaenoic acid (C22:6n-3)	0.23	0.96
n-6 fatty acids		
Linoleic acid (C18:2n-6)	0.80	0.31
Arachidonic acid (C20:4n-6)	0.70	0.48
The Kaiser's measure of sampling adequacy = 0.0.84		

	Plasma phospholipid fatty acid patterns[c]					
Plasma phospholipid fatty acids	*High-Satfat* ($\lambda 1 = 24\%$)	*n-3 VLC-PUFA* ($\lambda 2 = 11\%$)	*High-LA* ($\lambda 3 = 11\%$)	*n-6 VLC-PUFA* ($\lambda 4 = 10\%$)	*n-9 LC-MUFA* ($\lambda 5 = 10\%$)	*n-3 EFA* ($\lambda 6 = 7\%$)
Saturated fatty acids						
Myristic acid (C14:0)	–0.13	–0.28	–0.06	–0.06	–0.56	0.01
Palmitic acid (C16:0)	–0.10	–0.54	–0.47	–0.40	–0.34	–0.05
Stearic acid (C18:0)	0.80	–0.21	–0.04	0.08	–0.04	–0.16
Arachidic acid (C20:0)	0.86	–0.08	0.01	–0.04	0.36	–0.08
Behenic acid (C22:0)	0.92	–0.03	0.06	–0.07	0.24	–0.07
Lignoceric acid (C24:0)	0.81	–0.19	–0.01	–0.06	0.34	0.10
Mono-unsaturated fatty acids						
Palmitoleic acid (C16:1n-7)	–0.84	–0.13	–0.25	0.08	-0.12	0.23
Cis-vaccenic acid (C18:1n-7)	–0.73	0.10	0.16	0.08	0.40	–0.20
Oleic acid (C18:1n-9)	–0.82	–0.15	–0.26	0.11	-0.01	0.35
Elaidic acid (C18:1n9t)	0.44	–0.58	–0.25	–0.04	0.09	–0.02
Gondoic acid (C20:1n-9)	–0.17	–0.07	0.52	–0.05	0.54	–0.13
Erucic acid (C22:1n-9)	0.35	–0.01	0.05	0.22	0.42	–0.05
Nervonic acid (C24:1n-9)	0.16	0.09	0.07	–0.01	0.85	–0.04
n-3 fatty acids						
α-linolenic acid (C18:3n-3)	–0.23	0.02	0.28	–0.15	–0.09	0.71
Eicosapentaenoic acid (C20:5n-3)	–0.37	0.57	–0.25	–0.32	–0.01	0.42
Docosapentaenoic acid (C22:5n-3)	–0.08	0.71	–0.01	0.12	0.15	0.27
Docosahexaenoic acid (C22:6n-3)	0.05	0.79	0.25	–0.08	0.08	–0.24
n-6 and n-9 fatty acids						
Linoleic acid (C18:2n-6)	0.08	0.31	0.80	–0.10	0.05	0.16
γ-linolenic acid (C18:3n-6)	–0.41	–0.08	–0.17	0.27	–0.37	0.49
Eicosadienoic acid (C20:2n-6)	0.09	0.06	0.82	0.30	0.15	0.13
Dihomo-γ-linolenic acid (C20:3n-6)	0.00	0.29	0.14	0.65	–0.06	0.30
Arachidonic acid (C20:4n-6)	0.04	0.66	0.12	0.42	0.24	–0.31
Docosadienoic acid (C22:2-n6)	0.44	0.08	0.47	–0.06	0.45	–0.24
Adrenic acid (C22:4n-6)	–0.13	0.02	0.03	0.83	0.08	0.01
Osbond acid (C22:5n-6)	–0.12	–0.04	–0.09	0.82	0.01	–0.32
Mead acid (C20:3n-9)	–0.58	–0.15	–0.53	0.32	0.05	0.28
The Kaiser's measure of sampling adequacy = 0.78						

[a]Fatty acid patterns derived from dietary fatty acids. [b]Variance explained by the single factor. [c]Fatty acid patterns derived from plasma phospholipids.
High-Satfat, saturated fatty acid pattern; n-3 VLC-PUFA, n-3 very-long-chain polyunsaturated fatty acid pattern; high-LA, high linoleic acid pattern; n-6 VLC-PUFA, n-6 very-long-chain polyunsaturated fatty acid pattern; n-9 LC-MUFA, n-9 long-chain mono-unsaturated fatty acid pattern; n-3 EFA, n-3 essential fatty acid pattern.

Table 4. Associations of dietary fatty acid patterns with adiposity and the MetS in 711 black South African adults in regression models

	Linear regression models						*Logistic regression models*	
	Body mass index		*Waist circumference*		*Waist:height ratio*		*Metabolic syndrome*	
	β[a] *(95% CI)*[a]	p-*value*	β (95% CI)	p-*value*	β (95% CI)	p-*value*	*OR (95% CI)*[b]	p-*value*
Crude model[c]								
Non-marine	0.05 (–0.02, 0.13)	0.15	0.07 (–0.004, 0.14)	0.07	0.06 (–0.02, 0.13)	0.14	1.13 (0.96, 1.32)	0.14
Marine	–0.015 (–0.09, 0.06)	0.69	0.007 (–0.07, 0.08)	0.85	0.004 (–0.07, 0.08)	0.92	0.99 (0.84, 1.16)	0.88
R^2 (%)		0.03		0.02		0.03		0. 43
Adjusted model$_1$[d]								
Non-marine	0.04 (–0.02, 0.11)	0.20	0.06 (–0.01, 0.13)	0.09	0.04 (–0.02, 0.11)	0.19	1.12 (0.95, 1.33)	0.19
Marine	–0.02 (–0.09, 0.05)	0.55	0.004 (–0.07, 0.08)	0.91	–0.0015 (–0.07, 0.07)	0.97	0.98 (0.82, 1.16)	0.78
R^2 (%)		20.48		6.35		17.25		17.69
Fully adjusted model[e]								
Non-marine	0.04 (–0.02, 0.11)	0.21	0.06 (–0.01, 0.13)	0.09	0.04 (–0.03, 0.11)	0.25	1.15 (0.96, 1.38)	0.12
Marine	–0.02 (–0.10, 0.04)	0.47	0.002 (–0.07, 0.07)	0.96	–0.005 (–0.07, 0.06)	0.88	0.94 (0.78, 1.14)	0.53
R^2 (%)		26.68		13.34		22.72		20.39

[a]Standardised betas and standardised 95% confidence intervals (CI). [b]OR, odds ratio and 95% CI. [c]Crude model; consisted of plasma phospholipid fatty acid patterns only. [d]Adjusted model$_1$; crude model and additionally adjusted for age and gender. [e]Fully adjusted model; adjusted model$_1$, additionally adjusted for lifestyle confounders (physical activity, self-reported smoking, total dietary energy and alcohol intake (Kcal) and level of education).

Table 5. Associations of plasma phospholipid fatty acid patterns with adiposity and the MetS in 711 black South African adults in regression models

	Linear regression models						*Logistic regression models*	
	Body mass index		*Waist circumference*		*Waist:height ratio*		*Metabolic syndrome*	
	β[a] *(95% CI)*[a]	p-*value*	β (95% CI)	p-*value*	β (95% CI)	p-*value*	*Exponent of* β *(95% CI)*	p-*value*
Crude model[b]								
High-Satfat	0.37 (0.31, 0.44)	< 0.0001	0.28 (0.21, 0.35)	< 0.0001	0.31 (0.24, 0.38)	< 0.0001	1.62 (1.34, 1.96)	< 0.0001
n-3 VLC-PUFA	0.21 (0.15, 0.28)	< 0.0001	0.22 (0.15, 0.28)	< 0.0001	0.22 (0.15, 0.28.)	< 0.0001	1.76 (1.44, 2.15)	< 0.0001
High-LA	0.04 (–0.02, 0.11)	0.20.	–0.05 (–0.12, 0.02)	0.16	–0.04 (–0.10, 0.03)	0.29	1.09 (0.92, 1.30)	0.33
n-6 VLC-PUFA	0.05 (–0.0, 0.12)	0.13	0.06 (–0.005, 0.13)	0.07	0.07 (0.001, 0.14)	0.045	1.28 (1.08, 1.53)	0.006
n-9 LC-MUFA	–0.05 (–0.11, 0.02)	0.17	–0.10 (–0.16, –0.03)	0.007	–0.09 (–0.16, –0.02)	0.009	0.63 (0.52, 0.75)	< 0.0001
n-3 EFA	–0.12 (–0.18, –0.05)	0.0007	–0.06 (–0.13, 0.006)	0.07	–0.09 (–0.16, –0.02)	0.009	0.81 (0.68, 0.96)	0.02
R^2 (%)		19.72		13.87		15.62		18.30
Adjusted model$_1$[d]								
High-Satfat	0.29 (0.22, 0.35)	< 0.0001	0.25 (0.18, 0.32)	< 0.0001	0.23 (0.16, 0.30)	< 0.0001	1.44 (1.17, 1.76)	0.0004
n-3 VLC-PUFA	0.18 (0.12, 0.24)	< 0.0001	0.20 (0.13, 0.27)	< 0.0001	0.18 (0.12, 0.24)	< 0.0001	1.70 (1.37, 2.10)	< 0.0001
High-LA	0.03 (–0.04, 0.09)	0.43	–0.04 (–0.11, 0.03)	0.26	–0.04 (–0.11, 0.02)	0.21	1.10 (0.89, 1.30)	0.43
n-6 VLC-PUFA	0.029 (–0.03, 0.09)	0.36	0.05 (–0.016, 0.12)	0.13	0.05 (–0.02, 0.11)	0.16	1.26 (1.04, 1.51)	0.02
n-9 LC-MUFA	–0.04 (–0.10, 0.02)	0.20	–0.10 (–0.16, –0.03)	0.005	–0.09 (–0.15, –0.02)	0.007	0.61 (0.5, 0.73)	< 0.0001
n-3 EFA	–0.06 (–0.13, 0.001)	0.05.	–0.060 (–0.13, 0.010)	0.09	–0.05 (–0.12, 0.011)	0.10	0.84 (0.69, 1.01)	0.07
R^2 (%)		30.78		16.73		25.76		29.74
Fully adjusted model[e]								
High-Satfat	0.27 (0.20, 0.34)	< 0.0001	0.22 (0.15, 0.30)	< 0.0001	0.20 (0.13, 0.27)	< 0.0001	1.54 (1.21, 1.95)	0.0004
n-3 VLC-PUFA	0.14 (0.08, 0.20)	< 0.0001	0.16 (0.087, 0.23)	< 0.0001	0.15 (0.08, 0.21)	< 0.0001	1.72 (1.38, 2.16)	< 0.0001
High-LA	–0.004 (–0.070, 0.06)	0.90	–0.06 (–0.13, 0.01)	0.11	–0.06 (–0.13, 0.01)	0.07	1.14 (0.93, 1.4)	0.22
n-6 VLC-PUFA	0.029 (–0.04, 0.09)	0.37	0.05 (–0.02, 0.12)	0.14	0.05 (–0.02, 0.11)	0.15	1.25 (1.02, 1.54)	0.03
n-9 LC-MUFA	0.002 (–0.06, 0.07)	0.957	–0.06 (–0.13, 0.02)	0.13	–0.05 (–0.11, 0.02)	0.17	0.61 (0.50, 0.75)	< 0.0001
n-3 EFA	–0.06 (–0.13, 0.005)	0.07	–0.06 (–0.13, 0.014)	0.12	–0.05 (–0.12, 0.02)	0.17	0.81 (0.66, 0.99)	0.04
R^2 (%)		33.69		20.38		28.38		31.09

[a]Standardised betas and standardised 95% confidence intervals (CI). [b]Crude model; consisted of plasma phospholipid fatty acid patterns only. [c]Adjusted model$_1$; crude model and additionally adjusted for age and gender. [d]Adjusted model$_2$; adjusted model$_1$, additionally adjusted for lifestyle confounders (physical activity, self-reported smoking, total dietary energy and alcohol intake (KJ) and level of education). [e]Fully adjusted model; adjusted model$_1$, additionally adjusted for contraceptive use. High-Satfat, saturated fatty acid pattern; n-3 VLC-PUFA, n-3 very-long-chain polyunsaturated fatty acid pattern; high-LA, high linoleic acid pattern; n-6 VLC-PUFA, n-6 very-long-chain polyunsaturated fatty acid pattern; n-9 LC-MUFA, long-chain mono-unsaturated fatty acid pattern; n-3 EFA, n-3 essential fatty acid pattern.

higher in lean than in overweight women. In women, small effect sizes (~ 0.35–0.44) were found for most FAs, except for C24:0, which had a medium effect size of 0.45.

The factor analysis identified two dietary FA and six plasma phospholipid FA patterns according to the Kaiser criterion and scree-plot visual inspection. Results are shown in Table 3. Eleven dietary FAs and 26 phospholipid FAs were entered into the analysis. The factors generated explained 89% of the cumulative variance in dietary FA patterns and 73% in plasma phospholipid FA patterns. The Kaiser's measure of sampling adequacy was 0.84 and 0.78 for the dietary FA and plasma phospholipid FA patterns, respectively. Loadings with absolute values higher than 0.5 were considered relevant for the contribution to each FA pattern. The patterns are characterised and named according to the highest loadings of the specific FAs present in a given pattern.

Among dietary FAs, the first extracted pattern presented with high positive loadings of saturated FAs, MUFAs, α-linolenic acid (C18:3n-3) and n-6 FAs, and therefore was named the

'non-marine' FA pattern. The second pattern was named the 'marine' FA pattern because it was characterised by high positive loadings of eicosapentaenoic acid (C20:5n-3) and C22:6n-3.

The six plasma phospholipid FA patterns are discussed in the order in which they were derived. The first pattern presented with positive loadings of LC-SFAs, C18:0, C20:0, C22:0 and C24:0 and very high negative loadings of C16:1n-7, C18:1n-7 and C18:1n-9; we named it the 'high-Satfat' pattern. The second pattern was named 'n-3 VLC-PUFA' and presented with high positive loadings of docosapentaenoic acid (C22:5n-3), C22:6n-3 and C20:5n-3, as well as C20:4n-6. The third pattern presented the highest positive loadings of C18:2n-6 and eicosadienoic acid (C20:2n-6) and was named accordingly as the 'high-LA' pattern. The fourth pattern was named 'n-6 VLC-PUFA' since it was characterised with high positive loadings of adrenic acid (C22:4n-6), C22:2-n6 and C20:3n-6. The fifth pattern extracted was named the 'n-9 LC-MUFA' pattern and presented with positive loadings of C24:1n-9 and gondoic acid (C20:1n-9). The sixth and last pattern had a positive loading of one FA, i.e. C18:3n-3, and we named it 'n-3 EFA' pattern.

Dietary FA patterns were weakly associated with measured outcomes (Table 4). The non-marine FA pattern showed marginal positive associations with WC in the crude model and the association remained marginal after adjusting for age and gender ($\beta = 0.06$, 95% CI = –0.01–0.13, $p = 0.09$). The association was lost after adjustment for lifestyle variables and energy intake. On the other hand, we did not find any associations with the marine FA pattern (Table 4). Neither pattern revealed any association with BMI, WHtR or the MetS. Further adjustment to the regressions for total fat, fibre, carbohydrates and added sugar did not result in any significant associations. The variables in the adjusted models explained 0.02 to 27% of the variation in measures of adiposity and 0.4 to 20% of the variation in the MetS.

Plasma phospholipid FA patterns resulted in stronger associations with measures of adiposity and the MetS (Table 5). The high-Satfat and n-3 VLC-PUFA patterns were positively associated with all measures of adiposity and the MetS. The associations remained significant in the fully adjusted model. The omega-6 VLC-PUFA pattern showed marginal and positive associations with WC and WHtR in the crude model, but associations were lost after further adjustments. This pattern also showed higher odds for having the MetS and remained significantly associated in the fully adjusted model (odds ratio, OR = 1.25, 95% CI = 1.02–1.54, $p = 0.03$).

The n-9 LC-MUFA pattern was inversely associated with WC and WHtR in the crude model as well as after adjustment for age and gender. The associations were, however, lost after adjustments for lifestyle variables and energy intake. This pattern also showed lower odds for having the MetS and remained significantly associated in the fully adjusted model (OR = 0.61, 95% CI = 0.50–0.75, $p \leq 0.0001$).

The omega-3 EFA pattern showed an inverse association with BMI, WC and WHtR, but in the fully adjusted model marginal significance remained for BMI only. This pattern also showed lower odds for having the MetS and remained significantly associated in the fully adjusted model (OR = 0.81, 95% CI = 0.66–0.99, $p = 0.04$). The variables in all the adjusted models explained 14 to 34% of the variation in measures of adiposity, and 18 to 31% of the variation in the MetS.

We further adjusted all regression models for use of contraceptives and intakes of total fat, fibre, carbohydrates, and energy from added sugar in association with plasma phospholipid FAs. Additional adjustment for these variables did not result in different associations with anthropometric indices. The association between high-LA pattern and the MetS remained marginally significant after adjusting for additional variables, whereas the associations with the n-6 VLC-PUFA and n-3 EFA patterns were lost.

Discussion

The results of this study add new information about identified FA patterns both in diet and plasma phospholipids among a selected group of black South Africans from the North West Province. We identified for the first time two dietary FA patterns and six plasma phospholipid FA patterns (Table 3) by means of factor analysis in this group of black adults. The dietary non-marine FA pattern showed a weak positive association with WC, whereas the marine pattern did not show any associations with outcomes measured.

On the other hand, two plasma phospholipid FA patterns (high-Satfat and n-3 VLC-PUFA) were positively associated with all measures of adiposity and the MetS. The omega-6 VLC-PUFA pattern showed a positive association with the MetS, but not with measures of adiposity. The n-9 LC-MUFA and the n-3 EFA patterns showed an inverse association with the MetS in fully adjusted models and tended to be negatively associated with some measures of adiposity. The high-LA pattern was neither associated with measures of adiposity nor the MetS. Our findings indicate that dietary FA patterns were weakly associated, whereas plasma phospholipid FA patterns were more strongly associated with measures of adiposity and the MetS.

Previous studies have reported FA patterns, derived from different components of blood and tissue in association with obesity[29] and the MetS,[22,30] but not with dietary patterns. These patterns were generated by varying numbers of FAs ranging from nine to 34 FAs,[22,29,30] and some included estimated desaturase activities,[30] by means of use of factor[29,30] and cluster[22] analysis. Consequently, these derived patterns differed from that obtained in our study.

A dietary pattern, consisting of SFAs, PUFAs, MUFAs and other nutrients, was not associated with obesity among Iranian adults.[45] On the contrary, a multiracial study in the USA reported a positive association of intakes of total fat, total saturated fat, LC-SFAs, myristic acid (C14:0), C16:0 and C18:0, and MUFAs with BMI.[46] Furthermore, a study investigating the association of dietary patterns with the MetS concluded that a pattern high in meat products was associated with a higher prevalence of the MetS.[47]

In our study, the dietary non-marine FA pattern showed marginal and positive associations with WC, but not with other measures of adiposity or the MetS. The non-marine FA pattern had positive loadings of FAs from SFAs, MUFAs and PUFAs, specifically from two SFAs (C16:0 and C18:0), two MUFAs (C16:1n-7, C18:1n-9) and two PUFAs (C18:2n-6 and C18:3n-3). The dietary marine FA pattern showed no association with outcomes measured.

Our results are in agreement with a study in the USA that also found no associations of n-3 LC-PUFAs with BMI due to low intakes of these FAs in their participants.[46] In our study and

the study in the USA, lower intakes of n-3 PUFA compared to the FAO/WHO recommendation of 0.25–2 g/day were found.[48] Under-reporting of dietary intake may significantly influence nutrient pattern investigation and association with disease,[49] however, in the PURE study, over- and under-reporters of dietary intake (subjects with reported energy intakes ≥ 30 000 or ≤ 3 000 KJ) were excluded prior to analyses.[50] Apart from the marine FA pattern, we did not derive other clear dietary FA patterns, likely due to the homogenous nature of food intake in this group of adults. Therefore, factor analysis may not be the most appropriate method to investigate dietary FAs in this population and the associations observed should be interpreted with caution.

The first plasma phospholipid FA pattern, high-Satfat, was positively associated with all measures of adiposity and the MetS. This pattern had high positive loadings of SFAs C18:0, C20:0, C22:0 and C24:0, as well as negative loadings of MUFAs. In our study, the plasma phospholipid levels of these saturated FAs were also higher in overweight men and women compared to their leaner counterparts, although effect sizes tended to be small.

Plasma phospholipid VLC-SFAs, such as C20:0, C22:0 and C24:0 have previously been reported to be inversely associated with the MetS among adults in Taiwan.[15] In a study in Japan, serum VLC-SFAs were also inversely associated with the MetS and positively associated with HDL-C.[16] The authors concluded that these VLC-SFAs may be indicative of healthier metabolic health.[15,16] Li and colleagues[22] derived a cluster that consisted of the same VLC-SFAs mentioned above. This cluster was also associated with the healthier metabolic profile,[22] but was not identical to the high-Satfat pattern identified in this current study, as it did not have negative loadings of MUFAs.

High intakes of MUFAs are generally considered the driving force behind the protective effect of the Mediterranean diet on cardiovascular diseases.[51] The combined presence of high loadings of some SFAs, particularly C18:0 and low loadings on MUFAs may therefore explain the association with obesity and the MetS found in our study. Plasma C18:0 levels were higher and plasma C18:1n-9 levels were lower in the overweight/obese groups than among their leaner counterparts in the current study, and the same FAs had positive and negative loadings, respectively, in the high-Satfat pattern. These two FAs made up a considerable proportion of the FAs in the plasma phospholipid profile and may be the driving force behind the positive association of the high-Satfat pattern with all measures of adiposity and the MetS in the current study.

The second pattern, n-3 VLC-PUFA, had high positive loadings of C20:5n-3, C22:5n-3 and C22:6n-3, as well as the n-6 PUFA arachidonic acid (C20:4n-6). This pattern was positively associated with all measures of adiposity and the MetS. In line with our findings, an n-3 FA pattern (with positive loading of C20:5n-3, and estimated delta 5 desaturase activity and negative loading of C20:3n-6) in the study by Warensjo *et al.*[30] predicted the development of the MetS in Swedish men, independent of lifestyle factors. The main difference between our study and that of Warensjo and colleagues[30] is that they included estimated desaturase activity in their patterns and measured FAs in serum.

Omega-3 PUFAs, especially C22:6n-3 and C20:5n-3, have multiple beneficial effects and are generally inversely associated with obesity and related risk factors, as detailed in a recent review.[52] Other studies have also reported the inverse association of circulating n-3 PUFAs with measures of adiposity and the MetS.[20,21] It should be kept in mind that the PURE-SA study population reported very low intakes of n-3 FAs; however, despite these low intakes, their plasma levels were considered sufficient.[43] Continuous low intake of n-3 LC-PUFAs, as reported in the present study, can result in up-regulation of the endogenous synthesis of n-3 LC-PUFAs from C18:3n-3. The possibility therefore exists that this upregulated conversion is a response to the cardiovascular risk milieu, reflecting reverse causality, rather than being the other way around. Further research is needed to elucidate the endogenous conversion of dietary n-3 PUFAs in black African populations.

It is also possible that the positive association of this pattern with adiposity and the MetS could have been driven by the C20:4n-6, which formed part of this pattern. Omega-3 and n-6 FAs compete for incorporation into target tissues and metabolism by common enzymes, which may lead to opposing health effects.[53] The eicosanoid metabolic products from C20:4n-6 promote inflammatory responses. There is some evidence that a higher ratio of n-6 PUFAs to n-3 PUFAs is associated with a higher prevalence of obesity and the MetS.[54]

The fourth plasma phospholipid pattern, n-6 VLC-PUFA, had positive loadings of n-6 VLC-PUFAS, C20:3n-6, C22:4n-6 and osbond acid (C22:5n-6) and was positively associated with the MetS. Mayneris-Perxachs *et al.*[18] also reported a positive association between plasma phospholipid C20:3n-6 PUFAs and the MetS among older adults in Spain.

Higher concentrations of plasma phospholipid C20:3n-6 were observed in both overweight men and women compared to their leaner counterparts in our study, but the n-6 VLC-PUFA pattern was not associated with BMI in the fully adjusted model. Plasma phospholipid levels of C20:3n-6 were also positively associated with BMI in participants from the USA and Mexico.[13,17] There was, however, also a longitudinal study that found higher total circulating n-6 PUFAs, in particular linoleic acid and arachidonic acid, to be protective of risk factors for the MetS, including both systolic and diastolic BP and plasma triglycerides in men,[24] indicating that different n-6 FAs showed opposite associations with the MetS. The association of C20:3n-6 with the MetS requires further investigation.[18]

The fifth pattern, n-9 LC-MUFA, loaded positively with C20:1n-9 and C24:1n-9, and negatively with myristic acid (C14:0). This pattern showed an inverse association with WC and WHtR, but lost association when adjusted for lifestyle variables and energy intake. However, lower odds for having the MetS remained after adjustment for covariates. In our study, levels of C20:1n-9 were significantly higher in lean men and women compared to their overweight counterparts, whereas C24:1n-9 was higher in overweight compared to lean women only. Nervonic acid (C24:1n-9) and C20:1n-9 are both products of endogenous metabolism by elongation from oleic acid,[55] but plasma C24:1n-9 may also be related to fish intake.[56] Since fish consumption was very low in our study population, this pattern could therefore reflect an upregulated metabolism of oleic acid in our lean study participants.

The sixth pattern, n-3 EFA, was positively loaded with C18:3n-3 and tended to be inversely associated with all measures of adiposity and showed lower odds for the MetS. This is in agreement with a study that found C18:3n-3 in serum cholesteryl

esters to be inversely associated with abdominal obesity in a recent cross-sectional study of 60-year-old men and women.[57] Alpha-linolenic acid (C18:3n-3) is an essential FA and a precursor from which n-3 LC-PUFAs are synthesised. Increased consumption of C18:3n-3-rich foods elevates its tissue levels as well as levels of C22:6n-3 and C20:5n-3 in the liver lipids.[58] Alpha-linolenic acid can be beneficial to health. Firstly, C18:3n-3 intake was associated with a moderately lower risk of cardiovascular disease in randomised, controlled studies as outlined in reviews.[59,60] Secondly, as explained above, C18:3n-3 competes for the same metabolic enzymes, as does C18:2n-6, and increased dietary intake may be a worthy approach to decrease elongation of n-6 FAs leading to reduced plasma C20:4n-6 levels and increased plasma levels of C22:6n-3 and C20:5n-3.[58] As C18:3n-3 is an essential FA, this pattern, identified in our study participants, is probably related to food intake and therefore indicative of a higher intake of vegetable oils, legumes, nuts and seeds.[61]

Strengths and limitations

A rigorous methodological approach of sequential regression modelling enabled us to investigate the associations between dietary FA and plasma phospholipid FA patterns, respectively, and measures of adiposity and the MetS. Another strength of our study is the use of both dietary FA and plasma phospholipid FA patterns,[27] which is a preferred method to investigate the association between diet and diseases.[27]

Our work is not free of limitations. Firstly, inaccuracies associated with collecting dietary intake data may have influenced the dietary FA results; however, in our population, fieldworkers collecting dietary data were intensively trained and supervised, and both under- and over-reporters of dietary intake were excluded.[50] In addition, repeatability of the QFFQ was also demonstrated.[10] Secondly, the cross-sectional design does not account for possible reverse causation between measures of adiposity and dietary FA intake or plasma phospholipid FA concentration, nor can causality be inferred. Thirdly, a possible limitation of the study is incomplete information on FA composition in the food composition databases. This limitation was compensated for by our study design that also considered plasma phospholipid FAs. Fourthly, we assessed the associations with indirect measurements of adiposity, including BMI, WHtR and WC, as secondary markers of total and central adiposity, whereas imaging methods would better differentiate between lean and fat mass.

Conclusion

To our knowledge, this is the first study to investigate and document novel data on dietary FA and plasma phospholipid FA patterns and their association with measures of adiposity and the MetS in a selected group of black South African adults. This study presents evidence that although marginal association was found with dietary FA patterns, some circulating plasma phospholipid FA patterns were more strongly and significantly associated with BMI, WC, WHtR and the MetS. The high-Satfat and n-3 VLC-PUFA patterns were positively associated with adiposity and the MetS, whereas the n-9 LC-MUFA and n-3 EFA patterns were inversely associated with adiposity. These patterns may suggest possible differences in FA metabolism between lean and overweight/obese individuals. It should also be considered that, in a study population with low-fat intakes, such as the PURE participants, plasma FA levels may reflect endogenous FA generation rather than dietary intakes, which could result in different findings than those reported in other studies from affluent communities.

Our results are not sufficiently conclusive to make recommendations on dietary FA intakes in this population. Further prospective cohort studies that explain possible differences in characteristics of FA metabolism among black South African men and women are needed. More studies that apply the use of dietary FA and plasma or tissue FA patterns are required to determine whether the results from the current study can be generalised to the black population of African descent.

References

1. Vorster HH, Kruger A, Margetts BM. The nutrition transition in Africa: can it be steered into a more positive direction? *Nutrients* 2011; **3**(4): 429–441.
2. Shisana O, Labadarios D, Rehle T, Simbayi L, Zuma K, Dhansay A, *et al*. The South African National Health and Nutrition Examination Survey, 2012: SANHANES-1: the health and nutritional status of the nation. Cape Town: HSRC Press, 2014. Report No.: 0796924767.
3. National Department of Health. South Africa Demographic and Health Survey 2016: Key Indicators. Pretoria, South Africa and Rockville, Maryland, USA: NDoH, Stats SA, South African Medical Research Council and ICF, 2017.
4. Kruger HS, Venter CS, Vorster HH. Obesity in African women in the North West Province, South Africa is associated with an increased risk of non-communicable diseases: the THUSA study. *Br J Nutr* 2001; **86**(06): 733–740.
5. Lim SS, Vos T, Flaxman AD, Danaei G, Shibuya K, Adair-Rohani H, *et al*. A comparative risk assessment of burden of disease and injury attributable to 67 risk factors and risk factor clusters in 21 regions, 1990–2010: a systematic analysis for the Global Burden of Disease Study 2010. *Lancet* 2013; **380**(9859): 2224–2260.
6. Micha R, Khatibzadeh S, Shi P, Fahimi S, Lim S, Andrews KG, *et al*. Global, regional, and national consumption levels of dietary fats and oils in 1990 and 2010: a systematic analysis including 266 country-specific nutrition surveys. *Br Med J* 2014; **348**: 2272.
7. Bourne LT, Lambert EV, Steyn K. Where does the black population of South Africa stand on the nutrition transition? *Public Health Nutr* 2002; **5**(1A): 157–162.
8. Patterson EWR, Fitzgerald GF, Ross RP, Stanton C. Health implications of high dietary omega-6 polyunsaturated fatty acids. *Nutr Metab Cardiovasc Dis* 2012; **539426**: 1–6.
9. MacIntyre U, Kruger H, Venter C, Vorster H. Dietary intakes of an African population in different stages of transition in the North West Province, South Africa: the THUSA study. *Nutr Res* 2002; **22**(3): 239–256.
10. Wentzel-Viljoen E, Lee S, Laubscher R, Vorster HH. Accelerated nutrition transition in the North West Province of South Africa: results from the Prospective Urban and Rural Epidemiology (PURE-NWP-SA) cohort study, 2005 to 2010. *Public Health Nutr* 2018; **21**: 1–12.
11. Smuts CM, Wolmarans P. The importance of the quality or type of fat in the diet: a food-based dietary guideline for South Africa. *Sth Afr J Clin Nutr* 2013; **26**(3): S87–S99.
12. Dehghan MMA, Zhang X, Swaminathan S, Li W, Mohan V, Iqbal R, *et al*, Prospective Urban Rural Epidemiology study investigators.

Associations of fats and carbohydrate intake with cardiovascular disease and mortality in 18 countries from five continents (PURE): a prospective cohort study. *Lancet* 2017; **390**(10107): 2050–2062.
13. Pickens CA, Sordillo LM, Comstock SS, Harris WS, Hortos K, Kovan B, *et al*. Plasma phospholipids, non-esterified plasma polyunsaturated fatty acids and oxylipids are associated with BMI. *Prostaglandins, Leukotrienes Essential Fatty Acids* 2015; **95**: 31–40.
14. Fretts AMMD, Siscovick DS, King IB, McKnight B, Psaty BM, Rimm EB, *et al*. Associations of plasma phospholipid SFAs with total and cause-specific mortality in older adults differ according to SFA chain length. *J Nutr* 2016; **146**(2): 298–305.
15. Yang WS, Chen PC, Hsu HC, Su TC, Lin HJ, Chen MF, *et al*. Differential effects of saturated fatty acids on the risk of metabolic syndrome: a matched case-control and meta-analysis study. *Metabolism* 2018; **83**: 42–49.
16. Yamazaki Y, Kondo K, Maeba R, Nishimukai M, Nezu T, Hara H. The proportion of nervonic acid in serum lipids is associated with serum plasmalogen levels and metabolic syndrome. *J Oleo Sci* 2014; **63**(5): 527–537.
17. Aglago EKBC, Torres-Mejía G, Angeles-Llerenas A, Gunter MJ, Romieu I, Chajès V. Association between serum phospholipid fatty acids levels and adiposity in Mexican women. *J Lipid Res* 2017: P73643–P73677.
18. Mayneris-Perxachs J, Guerendiain M, Castellote AI, Estruch R, Covas MI, Fito M, *et al*. Plasma fatty acid composition, estimated desaturase activities, and their relation with the metabolic syndrome in a population at high risk of cardiovascular disease. *Clin Nutr* 2013; **33**(1): 90–97.
19. Mozaffarian D, Cao H, King IB *et al.* Circulating palmitoleic acid and risk of metabolic abnormalities and new-onset diabetes. *Am J Clin Nutr* 2010; **92**(6): 1350–1358.
20. Micallef MMI, Phang M, Garg M. Plasma n-3 polyunsaturated fatty acids are negatively associated with obesity. *Br J Nutr* 2009; **102**(09): 1370–1374.
21. Huang T, Bhulaidok S, Cai Z, Xu T, Xu F, Wahlqvist ML, *et al*. Plasma phospholipids n-3 polyunsaturated fatty acid is associated with metabolic syndrome. *Mol Nutr Food Res* 2010; **54**(11): 1628–1635.
22. Li K, Brennan L, McNulty BA, Bloomfield JF, Duff DJ, Devlin NF, *et al*. Plasma fatty acid patterns reflect dietary habits and metabolic health: A cross-sectional study. *Mol Nutr Food Res* 2016; **60**(9): 2043–2052.
23. Kabagambe EK, Tsai MY, Hopkins PN, Ordovas JM, Peacock JM, Borecki IB, *et al*. Erythrocyte fatty acid composition and the metabolic syndrome: a National Heart, Lung, and Blood Institute GOLDN study. *Clin Chem* 2008; **54**(1): 154–162.
24. Yary T, Voutilainen S, Tuomainen TP, Ruusunen A, Nurmi T, Virtanen J. Omega-6 polyunsaturated fatty acids, serum zinc, delta-5-and delta-6-desaturase activities and incident metabolic syndrome. *J Hum Nutr Diet* 2016; **30**(4): 506–514.
25. Fekete KGE, Lohner S, Verduci E, Agostoni C, Decsi T. Long-chain polyunsaturated fatty acid status in obesity: a systematic review and meta-analysis. *Obes Rev* 2015; **16**(6): 488–497.
26. Michels KB, Schulze MB. Can dietary patterns help us detect diet-disease associations? *Nutr Res Rev* 2005; **18**(02): 241–248.
27. Kant AK. Dietary patterns and health outcomes. *J Am Diet Assoc* 2004; **104**(4): 615–635.
28. Newby P, Tucker KL. Empirically derived eating patterns using factor or cluster analysis: a review. *Nutr Rev* 2004; **62**(5): 177–203.
29. Dahm CCG-RA, Jakobsen MU, Schmidt EB, Tjonneland A, Sorensen TI, Overvad K. Adipose tissue fatty acid patterns and changes in anthropometry: a cohort study. *PLoS One* 2011; **6**(7): e22587–e22594.
30. Warensjo E, Sundstrom J, Lind L, Vessby B. Factor analysis of fatty acids in serum lipids as a measure of dietary fat quality in relation to the metabolic syndrome in men. *Am J Clin Nutr* 2006; **84**(2): 442–448.
31. Teo K, Chow CK, Vaz M, Rangarajan S, Yusuf S, Group PI-W. The Prospective Urban Rural Epidemiology (PURE) study: examining the impact of societal influences on chronic noncommunicable diseases in low-, middle-, and high-income countries. *Am Heart J* 2009; **158**(1): 1–7.
32. Kruger H, Venter C, Steyn H. A standardised physical activity questionnaire for a population in transition: the THUSA study. *Afr J Phys Health Educ Rec Dance* 2000; **6**: 54–64.
33. MacIntyre U, Venter C, Vorster H. A culture-sensitive quantitative food frequency questionnaire used in an African population: 1. Development and reproducibility. *Public Health Nutr* 2001; **4**(01): 53–62.
34. MacIntyre U, Venter C, Vorster H. A culture-sensitive quantitative food frequency questionnaire used in an African population: 2. Relative validation by 7-day weighed records and biomarkers. *Public Health Nutr* 2001; **4**(01): 63–71.
35. Venter C, MacIntyre U, Vorster H. The development and testing of a food portion photograph book for use in an African population. *J Hum Nutr Diet* 2000; **13**(3): 205–218.
36. Wolmarans P, Danster N, Dalton A, Rossouw K, Schönfeldt H. Condensed food composition tables for South Africa. Medical Research Council, Cape Town, South Africa, 2010.
37. Marfell-Jones MJ, Stewart A, de Ridder J. International standards for anthropometric assessment. Australia: National Library of Australia, 2012.
38. Friedewald WT, Levy RI, Fredrickson DS. Estimation of the concentration of low-density lipoprotein cholesterol in plasma, without use of the preparative ultracentrifuge. *Clin Chem* 1972; **18**(6): 499–502.
39. Folch J, Lees M, Sloane-Stanley G. A simple method for the isolation and purification of total lipids from animal tissues. *J Biol Chem* 1957; **226**(1): 497–509.
40. Baumgartner J, Smuts CM, Malan L, Kvalsvig J, van Stuijvenberg ME, Hurrell RF, *et al*. Effects of iron and n-3 fatty acid supplementation, alone and in combination, on cognition in school children: a randomized, double-blind, placebo-controlled intervention in South Africa. *Am J Clin Nutr* 2012; **96**(6): 1327–1338.
41. Alberti KG, Eckel RH, Grundy SM, Zimmet PZ, Cleeman JI, Donato KA, *et al*. Harmonizing the metabolic syndrome: a joint interim statement of the International Diabetes Federation Task Force on Epidemiology and Prevention; National Heart, Lung, and Blood Institute; American Heart Association; World Heart Federation; International Atherosclerosis Society; and International Association for the Study of Obesity. *Circulation* 2009; **120**(16): 1640–1645.
42. Pautz N, Olivier B, Steyn F. The use of parametric effect sizes in single study musculoskeletal physiotherapy research: A practical primer. *Phys Ther Sport* 2018; **32**: 87–97.
43. Richter M, Baumgartner J, Wentzel-Viljoen E, Smuts CM. Different dietary fatty acids are associated with blood lipids in healthy South African men and women: the PURE study. *Int J Cardiol* 2014; **172**(2): 368–374.
44. SAS II, inventor. The SAS System for Windows Release 9.4 TS Level 1M3 Copyright© by SAS Institute Inc, Cary, NC, USA2016.
45. Salehi-Abargouei A, Esmaillzadeh A, Azadbakht L, Keshteli AH, Feizi A, Feinle-Bisset C, *et al*. Nutrient patterns and their relation to general and abdominal obesity in Iranian adults: findings from the SEPAHAN study. *Eur J Nutr* 2016; **55**(2): 505–518.
46. Raatz SK, Conrad Z, Johnson LK, Picklo MJ, Jahns L. Relationship of the reported intakes of fat and fatty acids to body weight in US adults. *Nutrients* 2017; **9**(5): 438–450.
47. Xia Y, Gu Y, Yu F, Zhang Q, Liu L, Meng G, *et al*. Association between

dietary patterns and metabolic syndrome in Chinese adults: a propensity score-matched case-control study. *Sci Rep* 2016; **6**: 34748.
48. Food and Agriculture Organization of the United Nations (FAO). Fats and fatty acids in human nutrition: report of an expert consultation. Rome, IT: FAO, 2010.
49. Markussen MS, Veierød MB, Ursin G, Andersen LF. The effect of under-reporting of energy intake on dietary patterns and on the associations between dietary patterns and self-reported chronic disease in women aged 50-69 years. *Br J Nutr* 2016; **116**(3): 547–558.
50. Vorster HH, Kruger A, Wentzel-Viljoen E, Kruger HS, Margetts BM. Added sugar intake in South Africa: findings from the Adult Prospective Urban and Rural Epidemiology cohort study. *Am J Clin Nutr* 2014; **99**(6): 1479–1486.
51. Covas M-I, Konstantinidou V, Fitó M. Olive oil and cardiovascular health. *J Cardiovasc Pharmacol* 2009; **54**(6): 477–482.
52. Huang CWC, Chen YJ, Ajuwon KM, Mersmann HM, Ding ST. Role of n-3 polyunsaturated fatty acids in ameliorating the obesity-induced metabolic syndrome in animal models and humans. *Int J Mol Sci* 2016; **17**(10): 1689–1717.
53. Simopoulos AP. Essential fatty acids in health and chronic disease. *Am J Clin Nutr* 1999; **70**(3): 560s–569s.
54. Albracht-Schulte K, Kalupahana NS, Ramalingam L, Wang S, Rahman SM, Robert-McComb J, *et al*. Omega-3 fatty acids in obesity and metabolic syndrome: a mechanistic update. *J Nutr Biochem* 2018; **58**: 1–16.
55. Tvrzicka E, Kremmyda L-S, Stankova B, Zak A. Fatty acids as biocompounds: their role in human metabolism, health and disease: a review. Part 1: classification, dietary sources and biological functions. *Biomed Pap Med Fac Univ Palacky Olomouc Czech Repub* 2011; **155**(2): 117–130.
56. Ando Y, Sasaki T. GC separation of cis-eicosenoic acid positional isomers on an ionic liquid SLB-IL100 stationary phase. *J Am Oil Chem Soc* 2011; **88**(6): 743–748.
57. Alsharari ZD, Riserus U, Leander K, Sjogren P, Carlsson AC, Vikstrom M, *et al*. Serum fatty acids, desaturase activities and abdominal obesity: a population-based study of 60-year old men and women. *PLoS One* 2017; **12**(1): e0170684–e0170698.
58. Holman RT. The slow discovery of the importance of n-3 essential fatty acids in human health. *J Nutr Health Aging* 1998; **128**(2): 427S–4233S.
59. Pan A, Chen M, Chowdhury R, Wu JH, Sun Q, Campos H, *et al*. α-Linolenic acid and risk of cardiovascular disease: a systematic review and meta-analysis. *Am J Clin Nutr* 2012; **96**(6): 1262–1273.
60. Fleming JA, Kris-Etherton PM. The evidence for alpha-linolenic acid and cardiovascular disease benefits: Comparisons with eicosapentaenoic acid and docosahexaenoic acid. *Adv Nutr* 2014; **5**(6): 863S–8676S.
61. Ollis TE, Meyer BJ, Howe PR. Australian food sources and intakes of omega–6 and omega–3 polyunsaturated fatty acids. *Ann Nutr Metab* 1999; **43**(6): 346–355.

Exercise test predicts CVD mortality risk

Performance on a simple exercise test predicts the risk of death from cardiovascular disease, cancer, and other causes, reports a large study presented at EuroEcho-Imaging 2018. Good performance on the test equates to climbing three floors of stairs very fast, or four floors fast, without stopping. The findings underline the importance of fitness for longevity.

The study included 12 615 participants with known or suspected coronary artery disease. Participants underwent treadmill exercise echocardiography, in which they were asked to walk or run, gradually increasing the intensity, and continue until exhaustion. The test also generates images of the heart to check its function.

During a median 4.7-year follow up, there were 1 253 cardiovascular deaths, 670 cancer deaths and 650 deaths from other causes. After adjusting for age, gender and other factors that could potentially influence the relationship, each MET (metabolic equivalent) achieved was independently associated with 9, 9 and 4% lower risks of cardiovascular death, cancer death and other causes of death during follow up.

The death rate from cardiovascular disease was nearly three times higher in participants with poor compared to good functional capacity (3.2 vs 1.2%, $p < 0.001$). Non-cardiovascular and non-cancer deaths were also nearly three-fold higher in those with poor compared to good functional capacity (1.7 vs 0.6%, $p < 0.001$). Cancer deaths were almost double in participants with poor compared to good functional capacity (1.5 vs 0.8%, $p < 0.001$).

As expected, the imaging part of the examination was predictive of cardiovascular death but not of deaths caused by cancer or other conditions.

Study author Dr Jesús Peteiro, a cardiologist at the University Hospital A Coruña, A Coruña, Spain, said: 'Our results provide further evidence of the benefits of exercise and being fit on health and longevity. In addition to keeping body weight down, physical activity has positive effects on blood pressure and lipids, reduces inflammation, and improves the body's immune response to tumours.'

Peteiro said people do not need to undergo exercise echocardiography to check their fitness level. 'There are much cheaper ways to estimate if you could achieve 10 METs on the treadmill test,' he said. 'If you can walk very fast up three floors of stairs without stopping, or fast up four floors without stopping, you have good functional capacity. If not, it's a good indication that you need more exercise.'

ESC guidelines recommend at least 150 minutes a week of moderate aerobic physical activity or 75 minutes a week of vigorous aerobic physical activity, or a combination of the two intensities.

Source: Medical Brief 2019

Review Article

The role of echocardiography in acute viral myocarditis

Mamotabo R Matshela

Abstract

The diagnosis of acute viral myocarditis can be very challenging during the initial evaluation, warranting multiple diagnostic tests to be performed, including a full echocardiographic evaluation to exclude other aetiologies that might present similarly. Acute myocarditis may masquerade as acute myocardial infarction in older patients or as any form of cardiomyopathy in young patients. As a result, all these patients need a thorough evaluation and to be managed at a high cardiac-care setting from the very outset. A wide range of diagnostic tests may be warranted, including conventional echocardiography, to exclude other underlying cardiac diseases, to evaluate cardiac chamber size, wall thickness, ventricular function and the presence of pericardial collections, and to assist in guiding further management. Although left ventricular dysfunction tends to be described more often, right ventricular dysfunction has been reported as the most likely cause of unfavourable outcomes, compared with left ventricular dysfunction. Therefore it is important to thoroughly evaluate and report all echocardiographic parameters for both ventricles and to determine the prognosis.

Keywords: acute viral myocarditis, echocardiography, speckle-tracking echocardiography

Submitted 26/6/17, accepted 16/11/18
Published online 11/4/19
Cardiovasc J Afr 2019; **30**: 239–244 www.cvja.co.za

DOI: 10.5830/CVJA-2018-069

Diagnosis of acute viral myocarditis can be challenging as its clinical presentation may masquerade as other cardiac conditions, such as an acute myocardial infarction. As a result, all patients with suspected acute viral myocarditis should undergo thorough evaluation, including a full echocardiographic assessment to exclude other causes that could present in a similar fasion.[1-29] Most importantly, these patients need closer monitoring and should be managed in a high-care or cardiac-care setting.[1]

Diagnosis of acute viral myocarditis is based on the presenting symptoms, elevated cardiac markers suggestive of myocardial necrosis, and electrocardiographic and echocardiographic changes. Although a wide range of diagnostic tests may be warranted when initially evaluating these patients, conventional echocardiography remains a crucial imaging modality to exclude other underlying cardiac diseases, to evaluate cardiac chamber size, wall thickness, ventricular function and presence of pericardial collections, to differentiate fulminant from acute myocarditis, and to help guide the patient's management.

There is earlier information on the role of echocardiography in myocarditis, however data on new or advanced echocardiographic imaging modalities are limited; as a result, future research is warranted in this area. Hence, the main objective of this article was to review the role of different echocardiographic modalities that may be useful during suspicion of acute viral myocarditis, as well as to report on new or advanced echocardiographic modalities to be applied during echocardiographic assessment, including contrast and speckle-tracking echocardiography.

Two-dimensional transthoracic echocardiography

Conventional echocardiography forms a crucial component for diagnostic work up in patients suspected of acute myocarditis.[30] Two-dimensional transthoracic echocardiography (2D-TTE) plays a crucial role in evaluating ventricular function and excluding other causes of chest pain or heart failure, including valvular, congenital and ischaemic heart diseases, and pericardial diseases.

Previous data have extensively reported on acute myocarditis as an important masquerader of acute myocardial infarction, therefore regional wall-motion abnormalities should be looked for during TTE, particularly in elderly patients or those with traditional risk factors for coronary artery diseases, as opposed to young, healthy athletes.[2-29] Even though 2D-TTE features of acute myocarditis are non-specific, it is still useful to exclude potential differentials, assist in guiding further management, including follow ups, and for prognostic purposes.

Echocardiographic criteria for myocarditis

Despite the fact that echocardiographic diagnosis of acute myocarditis has been hampered by non-specific features at the time of examination, the diagnostic criteria were previously suggested and have been adopted.[31-34] These criteria focus mainly on distinguishing fulminant from acute myocarditis and are very important in assisting triaging patients for specialised care, depending on the disease stage.

Several studies have previously evaluated the role of echocardiography during initial and follow-up management of patients suspected of or confirmed with acute myocarditis. Therefore echocardiography plays a crucial role and should be implemented at the initial evaluation and during the follow up.[1-30,35]

University of KwaZulu-Natal, Durban, Mediclinic Heart Hospital, Pretoria, South Africa; London School of Economics and Political Science, London, UK
Mamotabo R Matshela, MB ChB, PhD, FESC, mamotabomatsh@gmail.com

Left ventricular function

Hsiao *et al*.[36] reported septal wall thickness, left ventricular dimensions and ejection fraction in acute myocarditis patients compared with healthy controls, and further implemented the role of two-dimensional speckle-tracking echocardiography (2D-STE). Here, the authors demonstrated that 2D-STE could be helpful when evaluating patients with acute myocarditis during initial presentation of the disease process, compared with 2D-TTE.

Traditionally, echocardiographic findings in patients with acute myocarditis include left ventricular (LV) regional/segmental or global dysfunction and overall LV dilatation, however normal LV function continues to be reported in biopsy-proven acute myocarditis.[37] Occasionally, myocardial interstitial oedema, which could be detected echocardiographically as increased ventricular wall thickness, has also been reported in acute myocarditis.[35,37,38] Additional echocardiographic measurements suggestive of myocarditis include depressed ventricular function, including systolic and diastolic dysfunction, and regional wall abnormalities; however there are other non-specific echocardiographic parameters characteristically associated with acute myocarditis.[39-43]

Right ventricular function

The LV is the most commonly assessed and reported cardiac chamber in acute myocarditis, however echocardiographic assessment of right ventricular (RV) function is also highly recommended in any form of myocarditis.[44,45] Pinamonti *et al*.[44] retrospectively reviewed echocardiographic images of 42 patients with biopsy-proven myocarditis and reported RV dysfunction to be fairly common, as 23% of their study patients had evidence of RV dysfunction.[44]

RV dysfunction in patients with acute viral myocarditis has been reported as the most likely cause of poorer outcomes in terms of death and increased need for cardiac transplantation compared with LV dysfunction.[44-47] The LV–RV interaction has also been reported to be crucial in patients with myocarditis, as significantly impaired LV function was reported more often in patients with depressed RV function than in those with normal RV function during the initial presentation.[44,45]

Speckle-tracking echocardiography

STE is a new echocardiographic technology with high sensitivity and reproducibility for detection of subclinical ventricular systolic and diastolic dysfunction. The invention of STE strain and strain rate indices are useful to evaluate intrinsic cardiac deformation. STE indices provide accurate measurements of both regional and global ventricular contractility enhanced by angle independency and fewer pitfalls throughout the motion plane, compared with convectional 2D echocardiography. STE has demonstrated its superior utility compared with conventional echocardiography in patients presenting with acute myocarditis or any form of inflammatory cardiomyopathy.[36,48-53]

The 2D-STE strain and strain rate parameters are useful prognostic measures, even in patients presumed to have preserved LV ejection fraction at baseline and during the follow-up periods of the acute myocarditis process.[36] In addition, strain parameters could be useful in predicting deterioration and overall event-free survival after an evidenced or recovery from acute viral myocarditis, and to differentiate myocarditis from other conditions including coronary artery disease.[36] An additional report indicated that STE should be recommended in daily clinical practice to evaluate multiple cardiac conditions, including inflammatory cardiomyopathies, as strain parameters could detect early ventricular dysfunction compared with conventional echocardiography, and it is also useful for long-term prognostic purposes.[52]

In the recent past, a case of acute viral myocarditis was reported where significantly impaired LV longitudinal, circumferential and radial systolic strain parameters were demonstrated.[54] The authors also reported significantly attenuated inferior, inferolateral and apical segmental strain values, with the inferolateral segment demonstrating a paradoxical circumferential strain.[54]

In a larger study of 28 consecutive patients with cardiac magnetic resonance (CMR) imaging-verified diagnosis of acute myocarditis based on the Lake Louise criteria, Løgstrup *et al*.[55] indicated that 2D-STE was useful during the initial evaluation, as global longitudinal systolic strain added supportive information to clinical and conventional echocardiography.[56] Furthermore the authors also reported that global longitudinal systolic myocardial strain (including epicardial and endocardial longitudinal systolic strain) correlated strongly with the degree of myocardial oedema. The same study highlighted that 2D-STE was undoubtedly useful for the diagnosis and to evaluate the degree of myocardial dysfunction in acute myocarditis.[55]

Even though three-dimensional (3D) STE is still evolving, Caspar *et al*.[57] demonstrated significantly lower 3D global longitudinal, circumferential, area and radial strain values in acute viral myocarditis cohorts compared with normal healthy controls, despite documented preserved baseline LV ejection fraction on standard echocardiography in both groups.

Tissue Doppler imaging

Tissue Doppler imaging (TDI) indices are important and more specific when evaluating patients with acute myocarditis. Despite limited reports on the detection of myocarditis by novel echocardiographic modalities, such as tissue Doppler, studies have demonstrated impaired longitudinal segmental myocardial strain on Doppler echocardiography due to myocardial oedema.[55-58] Furthermore, tissue Doppler parameters and contrast-enhanced CMR could synergistically help in confirming the diagnosis and guide further management.

Smedema *et al*.[58] reported a case where the authors demonstrated the importance of TDI as part of the diagnostic work-up and management of acute myocarditis. In the same report, the authors further highlighted TDI indices, which were indicative of abnormalities suggestive of myocardial scarring.[56] Here the echocardiographic parameters were better suited to characterise acute myocardial tissue changes and changes over time in patients with acute myocarditis.

Contrast echocardiography

Generally, the clinical applications of contrast echocardiography include LV quantification and Doppler enhancement, which are useful during the evaluation of ventricular function, particularly in patients with a poor echocardiographic window.[38,59-61]

Although the clinical utility of contrast echocardiography in acute myocarditis is yet to be demonstrated and is controversial, contrast echocardiography is used routinely to exclude LV apical thrombus in patients with acute myocardial infarction and could also be useful in acute myocarditis, particularly in patients with impaired LV systolic function.

The presence of LV thrombus may be difficult to confidently image using standard TTE and, as recommended by national guidelines, contrast echocardiography can be useful to aid in the diagnosis in difficult situations.[59] A LV mural thrombus is a common complication, particularly in patients with LV dilatation and significantly impaired contractility, so contrast echocardiography could be used in those patients in guiding further management to prevent peripheral emobilisation.[38,59-61] Other imaging modalities, including CMR or 3D echocardiography, should be considered for confirmatory purposes.

Three-dimensional echocardiography

The real-time 3D-TTE is an advanced and important echocardiographic imaging modality used to evaluate cardiac patients; however its role in acute myocarditis is yet to be elucidated as larger data on its utility are limited. Despite this pitfall, a case was previously reported using real-time 3D echocardiography in acute myocarditis.[35] Thuny *et al*.[35] reported the role of both 2D and 3D echocardiography in a 43-year-old male with acute myocarditis, where the authors demonstrated the presence of hypokinetic and impaired LV contractility and biventricular thromboses, which were better delineated by 3D compared with 2D echocardiography.[35]

Differentiating acute from fulminant myocarditis

Echocardiography in patients with myocarditis allows for serial assessment of LV dysfunction and is useful to distinguish fulminant from acute myocarditis.[61-64] Fulminant myocarditis is characterised by the presence of a normal cavity and hypocontractile LV with increased septal thickness, compared with acute myocarditis. Acute myocarditis is characterised by marked LV dilation, normal septal thickness and ventricular dysfunction. In any form of myocarditis or inflammatory cardiomyopathy, cardiac function should be monitored using serial echocardiograms to demonstrate any change over time.[37,62-64] In general, LV function improves over a period of approximately six months in fulminant myocarditis, compared with acute myocarditis.[37,62-64]

An athlete with myocarditis

Responding to increased cardiac output demanded during exercise, both ventricles must increase stroke volume, which imposes high stress on myocardial structures, more so on the RV, which normally works at low pressures compared with the LV. Previously, studies on athletes' hearts were more focused on the LV; however recently, due to the evolution of advanced echocardiographic techniques and CMR, RV exercise-induced remodelling has been demonstrated.

Echocardiography is a widely available imaging modality that could provide useful information in sports cardiology, particularly in areas of pre-participation screening and to evaluate exercise-induced cardiac remodelling. Based on current guidelines, it is recommended resuming competitive sport once there are no biomarkers or evidence of inflammation and no concerns regarding arrhythmias, and after the LV has assumed normality.[65] Prior to clearance, the athlete should demonstrate a normal work-up based on an echocardiogram, exercise electrocardiogram and Holter monitor. If the athlete wishes to return to competitive sporting activity, recommendations are provided on how best to do so in a safe manner and should be followed closely, using intermittent repeated rhythm monitors, imaging and stress testing, depending on the sporting activity and degree of delayed gadolinium enhancement.

Since several reports have indicated a strong prognostic role for residual myocardial scarring after myocarditis, athletes should be prohibited from participating in competitive sport if there is evidence or concern regarding either ventricular arrhythmias or progressive LV dysfunction, which could be associated with the presence of residual myocardial scarring.[66,67] Furthermore, CMR has added prognostic implications, as evidence of late gadolinium enhancement was significantly associated with major adverse cardiac events in athletes.[68,69] Despite current advancements in imaging, including echocardiography, for young athletes wishing to return to sport after an acute episode of myocarditis, more data on advanced echocardiography, including STE, are warranted.

Discussion

Even though only standard echocardiography has been used, reports indicate that echocardiography plays some part during the initial evaluation and subsequently in diagnosing possible myocarditis. This limitation, compared with normal healthy individuals, is mostly due to normal reported evaluations in those with less severe forms of myocarditis. Despite these negatives, multiple abnormalities have been reported, namely segmental and global ventricular wall-motion abnormalities, and different patterns of cardiomyopathies, such as dilated, hypertrophic or even restrictive forms of cardiomyopathy in patients with histology-proven myocarditis. In addition, areas of necrosis and inflammation have been reported, which are associated with or lead to myocardial perfusion defects on further imaging.

Despite the lack of prior larger reports, studies or broader knowledge of myocardial contrast echocardiography in acute myocarditis, contrast echocardiography is useful to rule out ventricular mural thrombus. It is also useful in guiding further management and to prevent embolisation, which could lead to devastating outcomes, particularly in severely impaired ventricular contractility.[58-61]

Two-dimensional STE strain echocardiography is useful in evaluating regional contractile function and assisting with detecting subclinical myocardial dysfunction, despite presumed normal ventricular function, based on conventional echocardiography.[36,57] 2D-STE has a favourable signal-to-noise ratio, angle independence and the ability to differentiate active from passive myocardial motion, compared with standard echocardiography.

Despite limited information about the sensitivity and specificity of some of these newer echocardiographic techniques, their availability allows a window of opportunity to prospectively address important questions in myocarditis. Furthermore, since

there are no well-established echocardiographic criteria to predict outcomes in patients with any form of myocarditis, it is a good opportunity to develop new criteria to guide management and for prognostic purposes in future. Despite this premise, systolic and diastolic dysfunction, the presence of regional wall-motion abnormalities, and changes in echocardiographic image texture have previously been reported, which may be modified with larger studies in the future. Echocardiography may further assist with classification of myocarditis patients into clinically relevant subgroups, with prognostic implications.

Conclusion

The presentation of acute myocarditis may masquerade as other cardiac conditions, making the diagnosis even more challenging. A wide range of diagnostic tests may be warranted when initially evaluating patients with suspected acute myocarditis, where conventional echocardiography could assist in excluding other cardiac diseases. Conventional echocardiography could be useful to evaluate cardiac chamber size and function, exclude complications, and help guide further management in terms of optimising heart failure and thromboprophylaxis therapies accordingly.

New and advanced echocardiographic modalities, including STE, should be considered for future daily clinical practice for early detection of subclinical ventricular dysfunction, to help develop criteria to predict outcomes, and for prognostic purposes. Most clinicians are concerned with LV dysfunction, however echocardiographic exclusion of RV dysfunction is crucial because RV dysfunction in acute myocarditis is common and predicts poorer outcomes and an increased need for cardiac transplantation, compared with LV dysfunction.

References

1. Zheng XZ, Wu J, Zheng Q, Zha WZ. Coronary sinus flow is reduced and recovered with time in viral myocarditis mimicking acute coronary syndrome. A transthoracic Doppler echocardiographic study. *J Ultras Med* 2016; **35**: 63–69.
2. Thambidorai SK, Korlakunta HL, Arouni AJ, Hunter WJ, Holmberg MJ. Acute eosinophilic myocarditis mimicking myocardial infarction. *Tex Heart Inst J* 2009; **36**: 355–357.
3. Widyawati DG and Rina K. Acute fulminant myocarditis mimicking ST-elevation myocardial infarction. *Eur Heart J Suppl* 2016; **18**: B51–B51.
4. Arslan Z, Tavlasoglu M, Unlu M, Aparci M, Demirkol S. Acute myocarditis mimicking acute inferior myocardial infarction. *Int J Cardiol* 2013; **163**: S181–S181.
5. Erden I, Erden EC, Ozhan H, Basar C. Acute myocarditis mimicking acute myocardial infarction associated with pandemic 2009 (H1N1) influenza A virus. *Cardiol J* 2011; **18**: 552–555.
6. Pomara C, Villani A, D'Errico S, Riezzo I, Turillazzi E, Fineschi V. Acute myocarditis mimicking acute myocardial infarction: A clinical nightmare with forensic implications. *Int J Cardiol* 2006; **112**: 119–121.
7. Mottard N, Mewton N, Bonnefoy E, Abdellaoui M, Revel D, Kirkorian G. Acute myocarditis mimicking lateral myocardial infarction. *Anaesth Intens Care* 2008; **36**: 739–742.
8. Monsuez JJ, Ferchal F, Evans J, Lachurie ML, Passeron J. Acute myocarditis mimicking myocardial infarction in an HIV infected patient. *Eur Heart J* 1996; **17**: 1449–1449.
9. Zhang T, Miao W, Wang SX, Wei M, Su GH, Li ZH. Acute myocarditis mimicking ST-elevation myocardial infarction: A case report and review of the literature. *Exp Ther Med* 2015; **10**: 459–464.
10. Nucifora G, Di Chiara A, Miani D, Piccoli G, Puppato M, Slavich G, *et al*. Acute myocarditis mimicking ST-segment elevation myocardial infarction: relation between electrocardiographic changes and myocardial damage as assessed by cardiac magnetic resonance. *Eur Heart J* 2012; **33**: 48–49.
11. Paillard F, Deplace C, Lebreton H, Mabo P, Almange C, Daubert C. Acute myocarditis with favorable outcome mimicking acute myocardial-infarction. *Circulation* 1990; **82**: 118–118.
12. Yorgun H, Hazirolan T, Kaya EB, Canpolat U, Taher A, Ates AH, *et al*. Acute regional myocarditis mimicking acute myocardial infarction: discordant findings on positron emission tomography and cardiac magnetic resonance imaging. *Int J Cardiol* 2010; **140**: S76–S76.
13. Li YD, Hsiao FT, Lai CP, Chen CW. Acute viral myocarditis mimicking st elevation myocardial infarction: manifestation on cardiac magnetic resonance. *Acta Cardiol Sin* 2010; **26**: 44–47.
14. Danti M, Sbarbati S, Alsadi N, Di Filippo A, Gangitano G, Giglio L, *et al*. Cardiac magnetic resonance imaging: diagnostic value and utility in the follow-up of patients with acute myocarditis mimicking myocardial infarction. *Radiol Med* 2009; **114**: 229–238.
15. Kontogianni DD, Kouris NT, Papoulia EP, Goranitou GS, Grassos HA, Babalis DK. Discordance between echocardiographic and MRI findings in two cases of acute myocarditis mimicking myocardial infarction. *Int J Cardiol* 2007; **114**: E21–E23.
16. Chen TC, Lu PL, Lin CY, Lin WR, Chen YH. *Escherichia coli* urosepsis complicated with myocarditis mimicking acute myocardial infarction. *Am J Med Sci* 2010; **340**: 332–334.
17. Satiroglu O, Vural M, Uyar I, Meric M. Focal myocarditis mimicking acute st-elevation myocardial infarction. *Nobel Med* 2011; **7**: 119–123.
18. Testani JM, Kolansky DM, Litt H, Gerstenfeld ER. Focal myocarditis mimicking acute ST-elevation myocardial infarction – Diagnosis using cardiac magnetic resonance Imaging. *Tex Heart Inst J* 2006; **33**: 256–259.
19. Camastra GS, Cacciotti L, Marconi F, Sbarbati S, Pironi B, Ansalone G. Late enhancement detected by cardiac magnetic resonance imaging in acute myocarditis mimicking acute myocardial infarction: location patterns and lack of correlation with systolic function. *J Cardiovasc Med* 2007; **8**: 1029–1033.
20. Karthikesan D, Kang HY, Saad AS, Liew KS, Tob NHM, Khoo SW, *et al*. Leptospiral myocarditis mimicking acute st-elevation myocardial infarction. *J Am Coll Cardiol* 2016; **67**: 1074–1074.
21. Van Nierop J, Limburg A, van Ofwegen-Hanekamp CEE. Myocarditis mimicking acute myocardial infarction. *Neth Heart J* 2015; **23**: 502–503.
22. Sarda L, Peter AS, Nguyen C, Vilain D, Delahaye N, Lebtahi R, *et al*. Myocarditis mimicking acute myocardial infarction assessed by indium-111-antimyosin-antibody (AM) and rest thallium imaging. *J Nucl Med* 1998; **39**: 140.
23. Angelini A, Calzolari V, Calabrese F, Boffa GM, Maddalena F, Chioin R, Thiene G. Myocarditis mimicking acute myocardial infarction: role of endomyocardial biopsy in the differential diagnosis. *Heart* 2000; **84**: 245–250.
24. Basic D, Gupta S, Kwong RY. Parvovirus B19-induced myocarditis mimicking acute myocardial infarction clarification of diagnosis by cardiac magnetic resonance imaging. *Circulation* 2010; **121**: E40–E42.
25. Dinckal MH, Davutoglu V, Soydinc S, Kirilmaz A. Phaeochromocytoma-induced myocarditis mimicking acute myocardial infarction. *Int J Clin Pract* 2003; **57**: 842–843.
26. Zou YH, Lin L, Xiao H, Xiang DC. A Rare case of toxic myocarditis

caused by bacterial liver abscess mimicking acute myocardial infarction. *Am J Case Rep* 2016; **17**: 1–5.
27. Antonio RS, Lopez MP, Perea RJ, Sabate M. ST-segment elevation mimicking myocardial infarction after hydrochloric acid ingestion: Acute caustic myocarditis. *J Cardiovasc Comput* 2017; **11**: 70–71.
28. Goland S, Luthringer D, Shirvani V, Trento A, Czer LSC. An unusual case of allograft neutrophilic myocarditis mimicking acute myocardial infarction in a post-heart transplant patient. *J Heart Lung Transpl* 2009; **28**: 843–846.
29. Dec GW, Waldman H, Southern J, Fallon JT, Hutter AM, Palacios I. Viral myocarditis mimicking acute myocardial-infarction. *J Am Coll Cardiol* 1992; **20**: 85–89.
30. Eppenberger M, Hack D, Ammann P, Rickli H, Maeder MT. Acute eosinophilic myocarditis with dramatic response to steroid therapy the central role of echocardiography in diagnosis and follow-up. *Tex Heart Inst J* 2013; **40**: 326–330.
31. Calabrese F, Milanesi O, Boffa GM, Angelini A, Valente M, Thiene G, Rigo E. Molecular detection of viral genome in paediatric patients with myocarditis and dilated cardiomyopathy: clinico-pathologic correlates. *Eur Heart J* 2001; **22**: 143–143.
32. Stiller B. Management of myocarditis in children: The current situation. *Adv Exp Med Biol* 2008; **609**: 196–215.
33. Fairweather D, Stafford KA, Sung YK. Update on coxsackievirus B3 myocarditis. *Curr Opin Rheumatol* 2012; **24**: 401–407.
34. Kindermann I, Barth C, Mahfoud F, Ukena C, Lenski M, Yilmaz A, *et al*. Update on myocarditis. *J Am Coll Cardiol* 2012; **59**: 779–792.
35. Thuny F, Avierinos JF, Jop B, Tafanelli L, Renard S, Riberi A, *et al*. Massive biventricular thrombosis as a consequence of myocarditis – Findings from 2-dimensional and real-time 3-dimensional echocardiography. *Circulation* 2006; **113**: E932–E933.
36. Hsiao JF, Koshino Y, Bonnichsen CR, Yu Y, Miller FA, Pellikka PA, *et al*. Speckle tracking echocardiography in acute myocarditis. *Int J Cardiovas Imag* 2013; **29**: 275–284.
37. Felker GM, Boehmer JP, Hruban RH, Hutchins GM, Kasper EK, Baughman KL, Hare JM. Echocardiographic findings in fulminant and acute myocarditis. *J Am Coll Cardiol* 2000; **36**(1): 227–232.
38. Rakhit DJ, Becher H, Monaghan M, Nihoyannopoulis P, Senior R. The clinical applications of myocardial contrast echocardiography. *Eur J Echocardiogr* 2007; **8**: S24–S29.
39. Ammirati E, Lilliu M, Cipriani M, Garascia A, Brambatti M, Nonnini S, *et al*. Short and mid-term survival and left ventricular function changes in fulminant versus non-fulminant acute myocarditis. *Eur Heart J* 2015; **36**: 622–623.
40. Brown C and Budhram G. Evaluation of Left Ventricular Function by Bedside Ultrasound in Acute Toxic Myocarditis. *J Emerg Med* 2013; **45**: 588–591.
41. Cocker MS, Abdel-Aty H, Friedrich MG. In acute myocarditis, myocardial edema is related to left ventricular function. *Can J Cardiol* 2007; **23**: 231c–231c.
42. Pauschinger M, Rutschow S, Chandrasekharan K, Westermann D, Weitz A, Schwimmbeck LP, *et al*. Carvedilol improves left ventricular function in murine coxsackievirus-induced acute myocarditis – Association with reduced myocardial interleukin-1 beta and MMP-8 expression and a modulated immune response. *Eur J Heart Fail* 2005; **7**: 444–452.
43. Rutschow S, Leschka S, Westermann D, Schwimmbeck LR, Tschoepe C, Noutsias M, *et al*. Carvedilol improves left ventricular function in murine Coxsackievirus-induced acute myocarditis with reduced myocardial inflammation and a modulated immunresponse. *Eur Heart J* 2004; **25**: 109–109.
44. Pinamonti B, Alberti E, Cigalotto A, Dreas L, Salvi A, Silvestri F, Camerini F. Echocardiographic findings in myocarditis. *Am J Cardiol* 1988; **62**: 285–291.
45. Mendes LA, Dec GW, Picard MH, Palacios IF, Newell J, Davidoff R. Right-ventricular dysfunction – an independent predictor of adverse outcome in patients with myocarditis. *Am Heart J* 1994; **128**: 301–307.
46. Caforio AL, Angelini A, Calabrese F, Paccagnella O, Bagato F, Loddo I, *et al*. Biopsy-proven myocarditis: young age, female gender and right ventricular dysfunction at diagnosis are independent predictors of death or transplantation in a contemporary prospective series. *Circulation* 2010; **122**: A17976.
47. Caforio ALP, Angelini A, Bagato F, Loddo I, Bottaro S, Daliento L, *et al*. Young age, female gender and right ventricular dysfunction at diagnosis, but not viral genome are independent predictors of dismal prognosis in biopsy-proven myocarditis. *Eur Heart J* 2011; **32**: 486–487.
48. Nesukay E, Kovalenko V, Cherniuk S, Danilenko A. The diagnostic value of speckle-tracking echocardiography in myocarditis and dilated cardiomyopathy. *Eur Heart J* 2013; **34**: 689–689.
49. Hyafll F, Serfaty JM, Ducrocq G, Messika-Zeitoun D, Stag PG, Laissy JP, *et al*. Speckle tracking echocardiography can identify the location of myocardial injury in acute myocarditis. *Circulation* 2008; **118**: S851–S851.
50. Ten Cate FEAU, Schmidt BE, Sudholt H, Wilmes C, Sreeram N. Speckle tracking echocardiography in childhood myocarditis: Spontaneous reversal of severe left ventricular rotational abnormalities during follow-up. *Int J Cardiol* 2011; **151**: 257–260.
51. Prasad A, Klugman D, Gierdalski M, Cross R. Utilizing speckle tracking echocardiography to analyze strain patterns in pediatric patients with suspected myocarditis. *Circulation* 2011; **124**: Am Heart Assoc scientific session (poster), Orlando, FL, 16/11/2011.
52. Fine NM, Shah AA, Han IY, Yu Y, Hsiao JF, Koshino Y, *et al*. Left and right ventricular strain and strain rate measurement in normal adults using velocity vector imaging: an assessment of reference values and intersystem agreement. *Int J Cardiovas Imag* 2013; **29**: 571–580.
53. Paiva M, Goncalves A, Melao F, Sousa C, Rangel I, Martins E, *et al*. Global assessment of left ventricle longitudinal strain in patients after acute myocarditis: going further in left ventricular function. *Eur Heart J* 2013; **34**: 690.
54. Luisada AA. Prognosis of acute myocarditis. *Trans Am Coll Cardiol* 1955; **4**: 106–109.
55. Logstrup BB, Nielsen JM, Kim WY, Poulsen SH. Myocardial oedema in acute myocarditis detected by echocardiographic 2D myocardial deformation analysis. *Eur Heart J Cardiovasc Imag* 2016; **17**: 1018–1026.
56. Friedrich MG, Sechtem U, Schulz-Menger J. Cardiovascular magnetic resonance in myocarditis. *J Am Coll Cardiol* 2009; **53**(17): 1475–1487.
57. Caspar T, Fichot M, Ohana M, El Ghannudi S, Morel O, Ohlmann P. Late detection of left ventricular dysfunction using two-dimensional and three-dimensional speckle-tracking echocardiography in patients with history of non-severe acute myocarditis. *J Am Soc Echocardiogr* 2017; **30**(8): 756–762. doi: 10.1016/j.echo.2017.04.002. Epub 2017 Jun 7.
58. Smedema JP. Images in cardiovascular medicine: myocardial inflammation in viral peri-myocarditis detected by tissue Doppler echocardiography and magnetic resonance imaging. *Cardiovasc J Afr* 2007; **18**: 238–240.
59. Mulvagh SL, Rakowski H, Vannan MA, Abdelmoneim SS, Becher H, Bierig SM, *et al*. American Society of Echocardiography consensus statement on the clinical applications of ultrasonic contrast agents in echocardiography. *J Am Soc Echocardiogr* 2008; **21**: 1179–1201.
60. Belcik JT, Bierig SM, Chadwell K, Roberts B. Clinical application of harmonic power Doppler imaging in the assessment of myocardial

perfusion by contrast echocardiography. *J Am Soc Echocardiogr* 2005; **18**: 1083–1092.
61. Olszewski R, Timperley J, Cezary S, Monaghan M, Nihoyannopoulis P, Senior R, Becher H. The clinical applications of contrast echocardiography. *Eur J Echocardiogr* 2007; **8**: S13–S23.
62. Shauer A, Gotsman I, Keren A, Zwas DR, Hellman Y, Durst R, Admon D. Acute viral myocarditis: current concepts in diagnosis and treatment. *Isr Med Assoc J* 2013; **15**(3): 180–185.
63. Morimoto S, Kato S, Hiramitsu S, Uemura A, Ohtsuki M, Kato Y, *et al*. Narrowing of the left ventricular cavity associated with transient ventricular wall thickening reduces stroke volume in patients with acute myocarditis. *Circ J* 2003; **67**(6): 490–494.
64. Jeserich M, Konstantinides S, Pavlik G, Bode C, Geibel A. Non-invasive imaging in the diagnosis of acute viral myocarditis. *Clin Res Cardiol* 2009; **98**(12): 753–763. doi: 10.1007/s00392-009-0069-2. Epub 2009 Sep 11.
65. Ljungqvist A, Jenoure P, Engebretsen L, et al.: The International Olympic Committee (IOC) Consensus Statement on periodic health evaluation of elite athletes' March 2009. *Br J Sports Med* 2009; **43**(9): 631–643.
66. Grani C, Eichhorn C, Biere L, Murthy VL, Agarwal V, Kaneko K, *et al*. Prognostic value of cardiac magnetic resonance tissue characterization in risk stratifying patients with suspected myocarditis. *J Am Coll Cardiol* 2017; **70**(16): 1964–1976.
67. Aquaro GD, Perfetti M, Camastra G, Monti L, Dellegrottaglie S, Moro C, *et al*. Cardiac MR with late gadolinium enhancement in acute myocarditis with preserved systolic function: ITAMY study. *J Am Coll Cardiol* 2017; **70**: 1977–1987.
68. Zorzi A, Perazzolo Marra M, Rigato I, De Lazzari M, Susana A, *et al*. Nonischemic left ventricular scar as a substrate of life-threatening ventricular arrhythmias and sudden cardiac death in competitive athletes. *Circ Arrhythm Electrophysiol* 2016; **9**(7): e004229.
69. Schnell F, Claessen G, La Gerche A, Bogaert J, Lentz PA, Claus P, *et al.* Subepicardial delayed gadolinium enhancement in asymptomatic athletes: let sleeping dogs lie? *Br J Sports Med* 2016; **50**: 111–117.

Losing weight can reverse atrial fibrillation in obese patients

Australian research shows for the first time that obese people who are suffering from atrial fibrillation can reduce or reverse the effects of the condition by losing weight. The researchers found that a 10% loss in weight along with management of associated risk factors can reverse the progression of the disease. They studied 355 overweight or obese people who lost varying amounts of weight.

The research was led by the Centre for Heart Rhythm Disorders at the University of Adelaide and the South Australian Health and Medical Research Institute (SAHMRI). 'This is the first time that evidence has been found that if people who are obese and are suffering from atrial fibrillation the disease can be alleviated by losing weight and treating lifestyle factors,' says lead author Dr Melissa Middeldorp, researcher from the University of Adelaide's Centre for Heart Rhythm Disorders.

Atrial fibrillation (AF), Australia's most common heart rhythm disorder, is a leading cause of stroke and can lead to heart failure. Millions of people around the world are diagnosed with this condition every year. Chest pain, a 'racing' or unusual heart beat and shortness of breath are all symptoms of AF.

'AF is a progressive disease in which initial short, intermittent symptoms develop into more sustained forms of the condition. Obesity and lifestyle factors are associated with its progression,' says Middeldorp.

The number of overweight and obese adults has doubled over the past two decades, with Australia now being ranked as one of the fattest developed nations. 'The study showed that if obese people lose more than 10% of their weight and subsequent management of other risks to their lifestyle, they can reverse the progression of the disease. People who lost weight experienced fewer symptoms, required less treatment and had better outcomes. Those who previously had sustained symptoms experienced only intermittent symptoms or indeed stopped experiencing AF entirely,' says Middeldorp.

'Progression of the disease is shown to have a direct link with the degree of weight loss. Without weight loss, there is a progression of AF to more persistent forms of AF.'

The Centre for Heart Rhythm Disorders is led by Professor Prash Sanders, world leader in atrial fibrillation research. 'This study shows that weight loss and treating lifestyle factors is an essential component for effectively managing AF, in many instances being an alternative to surgery or drug intervention. Melissa's work has widespread implications for the management of this disease globally and is good news for people with the condition,' says Sanders.

'With record levels of obesity in Australia and in most high-income countries, this study gives hope that obese people can have a better quality of life as well as reducing their dependence on health-care services if they lose weight.'

Source: Medical Brief 2019

Case Report

Wellens' syndrome: a life-saving diagnosis

Yan ming Chen, Kang xing Song

Abstract

Wellens' syndrome is a relatively common clinical entity; however, it is often missed, especially in young patients. Without prompt diagnosis and aggressive intervention, patients with Wellens' syndrome may rapidly go on to develop extensive anterior wall myocardial infarction and possibly sudden death. In this case report, we present a 33-year-old male patient with atypical chest pain, and discuss the significance of a prompt recognition of Wellens' syndrome.

Keywords: Wellens' syndrome, ECG, electrocardiogram, young patient, medical education

Submitted 19/1/19, accepted 22/2/19
Published online 24/5/19
Cardiovasc J Afr 2019; **30**: e1–e3 www.cvja.co.za

DOI: 10.5830/CVJA-2019-010

Wellens' syndrome is a pattern of electrocardiographic T-wave changes associated with severe stenosis of the left anterior descending artery (LAD). The risk factors for Wellens' syndrome are the same as for acute coronary syndrome, such as diabetes mellitus, hypertension, hyperlipidaemia, advanced age, and family history of premature coronary heart disease. However, it is different from other acute coronary syndromes in that an electrocardiogram (ECG) obtained during episodes of pain demonstrates normalisation, and T-wave changes are found during pain-free periods. Therefore it is inclined to be missed in young patients without obvious cardiovascular risk factors.

Without prompt diagnosis and aggressive intervention, patients with Wellens' syndrome may rapidly go on to develop extensive anterior wall myocardial infarction and possibly sudden death. Immediate repetitive ECG evaluation after the chest pain subsides and timely recognition of this diagnostic ECG pattern are crucial to decrease cardiovascular risk. Here we report on a fortunate young man with Wellens' syndrome who was correctly diagnosed and treated.

Department of Cardiology, General Hospital of Chinese PLA, Beijing, China
Yan ming Chen MD, chenyanmingabcd0@sina.com
Kang xing Song, MD

Case report

A 33-year old man was admitted to the hospital because of intermittent chest pain for seven days. The chest pain was substernal and 'prickling'. It occurred in the morning and at night, and lasted for 10 minutes to a few hours. He had no history of diabetes, hypertension, hyperlipidaemia, drug abuse or family history of premature coronary heart disease. He had a sedentary lifestyle.

The physical examination was unremarkable. The initial ECG obtained after admission was normal. At 07:40 the next morning, his pain recurred. An immediate ECG was obtained and there were no obvious T-wave changes (Fig. 1A). Twenty minutes later, the pain was relieved with 0.5 mg sublingual nitroglycerin, and then a pain-free ECG was performed (Fig. 1B), which showed biphasic T waves in leads V2–V4.

The dynamic T-wave changes raised concerns about Wellens' syndrome, which is associated with severe stenosis of the LAD. The patient underwent immediate coronary angiography, and the procedure showed 95% stenosis of the proximal LAD (Fig. 2A); the stenosis was treated with a drug-eluting stent (Fig. 2B). The troponin T level rose to a peak of 0.195 ng/ml (normal value < 0.1 ng/ml).

The patient was discharged home symptom free and referred to a cardiac rehabilitation programme. He has been in constant follow up and has not experienced angina again.

Discussion

Wellens' syndrome is a pre-infarction stage of coronary artery disease. It comprises 10 to 15% of all acute coronary syndromes in the USA. However, it is often missed, especially in young patients.[1-3]

Khan reported Wellens' syndrome in a 24-year-old woman with atypical chest pain and characteristic ECG changes. This was initially unrecognised and the young patient subsequently progressed to an anterior non-ST elevation myocardial infarction.[4] Wang reported another Wellens' syndrome in a 22-year-old man.[5] Both young patients in these two cases had cardiovascular risk factors, namely diabetes and familial hypercholesterolaemia, respectively.[4,5] Our case was different, as the young patient has no obvious cardiovascular risk factors or family history of premature coronary heart disease.

Wellens' syndrome is prone to misdiagnosis. However the characteristic ECG pattern is specific for a differential diagnosis.

Wellens' syndrome, first reported by de Zwaan in 1982, is a pattern of electrocardiographic T-wave changes associated with severe stenosis of the LAD.[6] More specifically, Wellens' syndrome can be classified into two types. Type 1 Wellens constitutes 24% of cases, is less common, poorly recognised, and

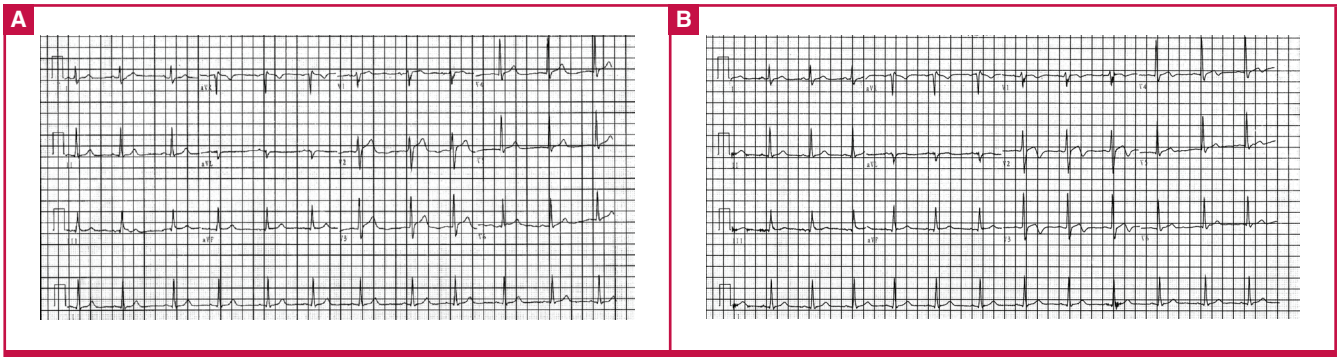

Fig. 1. A. ECG obtained during onset of pain, showing no obvious T-wave changes. B. Pain-free ECG was then performed, which showed biphasic T waves in leads V2–V4.

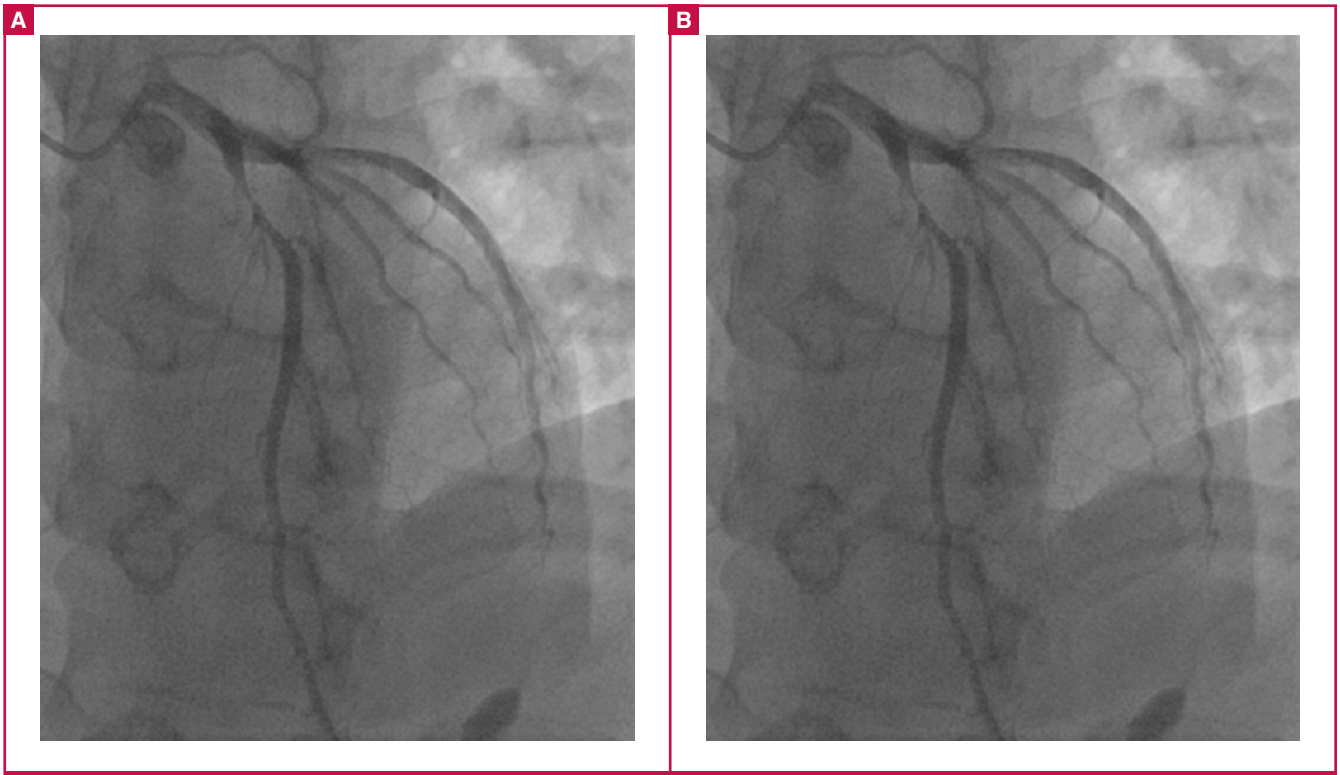

Fig. 2. A. After coronary angiography, 95% stenosis of the proximal left anterior descending coronary artery was seen. B. After the stenosis was treated with a drug-eluting stent.

described as biphasic T waves in V2–V3, which was the finding in our patient (Fig. 1B). The more common type 2 Wellens' accounts for the remaining 76% of cases and is identified by deep, symmetrically inverted T waves in V1–V4. This T-wave pattern is well recognised by junior doctors. It is important to emphasise that the T-wave changes of Wellens' syndrome occur during pain-free periods, while during an episode of chest pain, the T waves normalise.

The criteria for Wellens' syndrome are as follows: previous history of chest pain, no Q waves or loss of R waves, no significant ST-segment elevation, normal or minimally elevated cardiac markers, and biphasic/inverted T-wave changes in the precordial leads. Without prompt diagnosis and aggressive intervention, patients with Wellens' syndrome may rapidly go on to develop extensive anterior wall myocardial infarction, with a mean time of 8.5 days. As a result, patients with Wellens' syndrome should undergo immediate or rapid invasive coronary strategy.[7]

Conclusion

We highlight three learning points about this case: (1) immediate repetitive ECG evaluation after the chest pain subsides, even in young patients without significant risk factors; (2) timely recognition of the diagnostic ECG pattern of Wellens' syndrome; (3) emergency coronary angiography should be conducted if diagnosed.

References

1. Coutinho Cruz M, Luiz I, Ferreira L, Cruz Ferreira R. Wellens' syndrome: A bad omen. *Cardiology* 2017; **137**(2): 100–103.

2. Jaiswal D, Boudreau D. An incidental case of Wellens' syndrome in a community emergency department. *World J Emerg Med* 2016; **7**(2): 153–156.
3. Zhao YT, Huang YS. ECG pattern associated with left anterior descending coronary artery occlusion. *N Engl J Med* 2018; **378**(16): e22.
4. Khan B, Alexander J, Rathod KS, Farooqi F. Wellens' syndrome in a 24-year-old woman. *Br Med J Case Rep* 2013; 2013. pii: bcr2013009323. doi: 10.1136/bcr-2013-009323.
5. Wang JY, Chen H, Su X, Zhang ZP. Wellens' syndrome in a 22-year-old man. *Am J Emerg Med* 2016; **34**(5): 937.e3–4.
6. De Zwaan C, Bär FW, Wellens HJ. Characteristic electrocardiographic pattern indicating a critical stenosis high in left anterior descending coronary artery in patients admitted because of impending myocardial infarction. *Am Heart J* 1982; **103**: 730–736.
7. Roffi M, Patrono C, Collet JP, *et al*. 2015 ESC guidelines for the management of acute coronary syndromes in patients presenting without persistent ST-segment elevation: task force for the management of acute coronary syndromes in patients presenting without persistent ST-segment elevation of the European Society of Cardiology (ESC). *Eur Heart J* 2016; **37**: 267–315.

CVJ AFRICA

www.cvja.co.za | CardioVascular Journal of Africa (official journal for PASCAR)

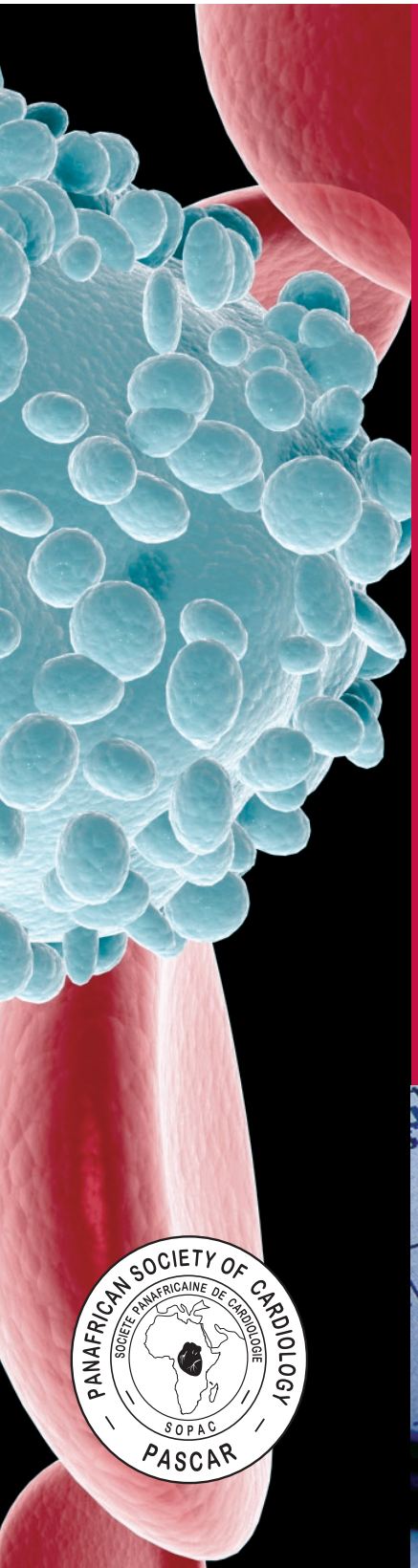

Why you should publish with CVJA

- Increased international exposure (indexed in PubMed, Medline, PubMed Central, Scopus, Embase and Thompson Reuters/ISI)
- Quick return on submissions
- Changing patterns of heart disease in Africa get more exposure than in other journals
- Acceptance of diabetes studies as vascular studies in CVJA
- African studies are given preference
- Well-illustrated interventional studies are needed for CME in Africa (full website support capability)
- Instructions for authors on www.cvja.co.za
- A PowerPoint presentation for new authors: 'How to write a scientific paper'
- Submit your manuscript online at www.cvja.co.za

Contact us on info@clinicscardive.com

CVJA has the capability of publishing on PubMed Central

Call for Abstracts and Cases Registration is Now Open

PASCAR, SA Heart® & AfricaPCR Join forces for the 2019 Congress

31 October – 3 November 2019
Sandton Convention Centre
Johannesburg, South Africa

Cardiovascular Care – Meeting the Needs of Africa

Featuring scientific sessions from ESC

www.saheart.org/congress2019

The Congress is proudly organised by europa organisation africa

+27 (0)11 325 0020 claire@eoafrica.co.za www.eoafrica.co.za

pharma dynamics
EFFECTIVE AFFORDABLE HEALTHCARE
A Lupin Group Company.

bilocor

BISOPROLOL FUMARATE
5 mg / 10 mg

bilocor co

BISOPROLOL FUMARATE 2,5 mg / 5 mg / 10 mg
HYDROCHLOROTHIAZIDE 6,25 mg

For further product information contact **PHARMA DYNAMICS** P O Box 30958 Tokai Cape Town 7966 **Fax** +27 21 701 5898
Email info@pharmadynamics.co.za **CUSTOMER CARE LINE** 0860 PHARMA (742 762) / +27 21 707 7000 **www.pharmadynamics.co.za**

BILOCOR 5, 10. Each tablet contains 5, 10 mg bisoprolol fumarate respectively. S3 A38/5.2/0053, 0051. NAM NS2 06/5.2/0061, 0062. For full prescribing information, refer to the professional information approved by SAHPRA, 23 July 2010. **BILOCOR CO 2,5/6,25, 5/6,25, 10/6,25.** Each tablet contains 2,5, 5, 10 mg bisoprolol fumarate respectively and 6,25 mg hydrochlorothiazide. S3 A44/7.1.3/1010, 1011, 1012. NAM NS2 13/7.1.3/0260, 0261, 0262. For full prescribing information, refer to the professional information approved by SAHPRA, 2 November 2012. **1)** IMS MAT UNITS March 2018. **BRG478/06/2018.**